Leg 189 Preliminary Report

The Tasmanian Gateway between Australia and Antarctica—Paleoclimate and Paleoceanography

Shipboard Scientific Party

Ocean Drilling Program
Texas A&M University
1000 Discovery Drive
College Station TX 77845-9547
USA

June 2000

This report was prepared from shipboard files by scientists who participated in the cruise. The report was assembled under time constraints and does not contain all works and findings that will appear in the *Initial Reports* of the ODP *Proceedings.* Reference to the whole or to part of this report should be made as follows:

Shipboard Scientific Party, 2000. Leg 189 Preliminary Report: The Tasmanian Seaway Between Australia and Antarctica Paleoclimate and Paleoceanography. *ODP Prelim. Rpt.,* 89 [Online]. Available from World Wide Web: <http://www-odp.tamu.edu/publications/prelim/189_prel/189prel.pdf>. [Cited YYYY-MM-DD]

Distribution

Electronic copies of this series may be obtained from the Ocean Drilling Program's World Wide Web site at http://www-odp.tamu.edu/publications.

DISCLAIMER

This publication was prepared by the Ocean Drilling Program, Texas A&M University, as an account of work performed under the international Ocean Drilling Program, which is managed by Joint Oceanographic Institutions, Inc., under contract with the National Science Foundation. Funding for the program is provided by the following agencies:

Australia/Canada/Chinese Taipei/Korea Consortium for Ocean Drilling
Deutsche Forschungsgemeinschaft (Federal Republic of Germany)
Institut National des Sciences de l'Univers-Centre National de la Recherche Scientifique (France)
Ocean Research Institute of the University of Tokyo (Japan)
National Science Foundation (United States)
Natural Environment Research Council (United Kingdom)
European Science Foundation Consortium for the Ocean Drilling Program (Belgium, Denmark, Finland, Iceland, Ireland, Italy, The Netherlands, Norway, Spain, Sweden, and Switzerland)
Marine High-Technology Bureau of the State Science and Technology Commission of the People's Republic of China

The following scientists were aboard *JOIDES Resolution* for Leg 189 of the Ocean Drilling Program:

Neville F. Exon
Co-Chief Scientist
Petroleum and Marine Division
Australian Geological Survey Organisation
PO Box 378
Canberra, ACT 2601
Australia
Phone: (61) 2-6249-9347
Fax: (61) 2-6249-9920
E-mail: neville.exon@agso.gov.au

James P. Kennett
Co-Chief Scientist
Department of Geological Sciences and
Marine Science Institute
University of California, Santa Barbara
Santa Barbara CA 93106
USA
Phone: (805) 893-3103
Fax: (805) 893-2314
E-mail: kennett@magic.geol.ucsb.edu

Mitchell J. Malone
Staff Scientist/Inorganic Geochemist
Ocean Drilling Program
Texas A&M University
1000 Discovery Drive
College Station TX 77845
USA
Phone: (979) 845-5218
Fax: (979) 845-0876
E-mail: malone@odpemail.tamu.edu

Hendrik Brinkhuis
Palynologist
Laboratory of Palaeobotany and Palynology
Utrecht University
Budapestlaan 4
Utrecht 3584 CD
The Netherlands
Phone: (31) 30-253-7692
Fax: (31) 30-253-5096
E-mail: h.brinkhuis@bio.uu.nl

George C.H. Chaproniere
Paleontologist (foraminifers)
Department of Geology
The Australian National University
Canberra, ACT 0200
Australia
Phone: (61) 2-6249-0619
Fax: (61) 2-6249-5544
E-mail: george.chaproniere@anu.edu.au

Atsuhito Ennyu
Sedimentologist
Department of Geosciences
Pennsylvania State University
437 Deike Building
University Park PA 16802
Phone: (814) 865-3321
Fax: (814) 863-7823
E-mail: aennyu@psu.edu

Patrick Fothergill
LDEO Logging Staff Scientist
Department of Geology
Borehole Research
University of Leicester
University Road
Leicester LE1 7RH
United Kingdom
Phone: (44) 116-252-3921
Fax: (44) 116-252-3918
E-mail: paf10@leicester.ac.uk

Michael D. Fuller
Paleomagnetist
Hawaii Institute of Geophysics and
Planetology
University of Hawaii at Manoa
2525 Correa Road
Honolulu HI 96822
USA
Phone: (808-956-4038
Fax: (808) 956-3188
E-mail: mfuller@soest.hawaii.edu

Marianne Grauert
Sedimentologist
Geological Institute Institut
University of Copenhagen
Øster Voldgade 10
Copenhagen 1350K
Denmark
Home: (45) 35840107
Fax: (45) 35322499
E-mail: marianne@grauert.dk (or gm040573@geo.geol.ke.dk)

Peter J. Hill
Stratigraphic Correlator
Petroleum and Marine Division
Australian Geological Survey Organisation
GPO Box 378
Canberra, ACT 2601
Australia
Phone: (61) 2-6249-9292
Fax: (61) 2-6249-9956
E-mail: peter.hill@agso.gov.au

Thomas R. Janecek
Stratigraphic Correlator
Antarctic Research Facility
Florida State University
108 Carraway Building
Tallahassee FL 32306-4100
USA
Phone: (850) 644-2407
Fax: (850) 644-4214
E-mail: janecek@gly.fsu.edu

Daniel C. Kelly
Paleontologist (foraminifers)
Department of Geology and Geophysics
Woods Hole Oceanographic Institution
266 Woods Hole Road
MailStop #23, Clark Building
Woods Hole MA 02543
USA
Phone: (508)288-2577
Fax: (508) 289-2175
E-mail: dkelly@whoi.edu

Jennifer C. Latimer
Physical Properties Specialist
Department of Geology
Indiana University/Purdue University, Indianapolis
723 West Michigan Street
Indianapolis IN 46202
Phone: (317) 274-7484
Fax: (317) 274-7966
E-mail: jclatime@iupui.edu

Stefan Nees
Sedimentologist
GEOMAR
Christian-Albrechts-Universität zu Kiel
Wischhofstrasse 1-3
Kiel 24148
Germany
Phone: (49) 431-600-2823
Fax: (49) 431-600-2941
E-mail: snees@geomar.de

Ulysses S. Ninnemann
LDEO Logging Staff Scientist
Borehole Research Group
Lamont-Doherty Earth Observatory
PO Box 1000
Route 9
Columbia University
Palisades NY 10964
USA
Phone: (914) 365-8695
Fax: (914) 365-3182
E-mail: ulysses@ldeo.columbia.edu

Dirk Nürnberg
Inorganic Geochemist
GEOMAR
Department of Paleoceanography
Christian-Albrechts-Universität zu Kiel
Wischhofstrasse 1-3
Kiel 24148
Germany
Phone: (49) 431-600-2313
Fax: (49) 431-600-2925
E-mail: dnuernberg@geomar.de

Stephen F. Pekar
Sedimentologist
Department of Geological Sciences
Rutgers, The State University of New Jersey
Wright Labs
Piscataway NJ 08854
USA
Phone: (732) 445-6989
Fax: (212) 888-3168
E-mail: spekar@rci.rutgers.edu

Caroline C. Pellaton
Sedimentologist
Département de Géologie et de Paléontologie
Université de Genève
13 rue des Maraîchers
Genève 4 1211
Switzerland
Phone: (41) 22-702-6644
Fax: (41) 22-320-5732
E-mail: pellato2@sc2a.unige.ch

Helen A. Pfuhl
Paleontologist (foraminifers)
Godwin Laboratory
University of Cambridge
Pembroke Street/NMS
Cambridge CB2 3SA
United Kingdom
Phone: 44-(0)-1223-334870
Fax: 44-(0)-1223-334871
E-mail: hap21@cus.cam.ac.uk

Christian M. Robert
Sedimentologist
Centre d'Océanologie de Marseille
Luminy case 901
13288 Marseille Cedex 09
France
Phone: (33) 4-91-82-94-02
E-mail: robert@com.univ-mrs.fr

Kristeen L. McGonigal
Paleontologist (nannofossils)
Department of Geology
Florida State University
108 Carraway Building
Tallahassee FL 32306-4100
USA
Phone: (850) 644-5860
Fax: (850) 644-4214
E-mail: roessig@gly.fsu.edu

Ursula Röhl
Physical Properties Specialist
Fachbereich Geowissenschaften
Universität Bremen
Postfach 33 04 40
Bremen 28334
Germany
Phone: (49) 421-218-24-82
Fax: (49) 421-218-31-16
E-mail: uroehl@allgeo.uni-bremen.de

Stephen A. Schellenberg
Sedimentologist
Department of Earth Sciences
University of California, Santa Cruz
EMS-A232
1156 High Street
Santa Cruz CA 95064
USA
Phone: (831) 459-4089
Fax: (831) 459-3074
E-mail: schellen@es.ucsc.edu

Amelia E. Shevenell
Sedimentologist
Department of Geological Sciences
University of California, Santa Barbara
Santa Barbara CA 93106
USA
Phone: 805) 893-4817
Fax: (805) 893-2314
E-mail: amelia@magic.geol.ucsb.edu

Catherine E. Stickley
Paleontologist (diatoms)
Environmental Change Research Centre
Department of Geography
University College London
26 Bedford Way
London WC1H 0AP
United Kingdom
Phone: (44)-(0)20-7679-5562
Fax: (44)-(0)20-7679-7565
E-mail: c.stickley@ucl.ac.uk

Noritoshi Suzuki
Paleontologist (radiolarians)
Institute of Geology and Paleontology
Tohoku University
Aoba, Aramaki
Sendai, Miyagi 980-8578
Japan
Phone: (81) 22-217-6623
Fax: (81) 22-217-6634
E-mail: suzuki.noritoshi@nifty.ne.jp

Yannick Touchard
Paleomagnetist
CNRS
CEREGE, Domaine de L'Arbois
Europole Mediterranean L'Arbois, BP 80
13545 Aix-en-Provence Cedex 4
France
Phone: (33) 4-42-97-15-79
Fax: (33) 4-62-97-15-49
E-mail: touchard@cerege.fr

Wuchang Wei
Paleontologist (nannofossils)
Scripps Institution of Oceanography
Geoscience Research Division
University of California, San Diego
La Jolla CA 92093-0244
Phone: (858) 534-5844
Fax: (858) 558-2081
E-mail: wwei@ucsd.edu

Timothy S. White
Organic Geochemist
EMS-Earth Institute
2217 Earth-Engineering Science Building
The Pennsylvania State University
University Park PA 16802
USA
Phone: (814) 865-2213
Fax: (814) 865-3191
E-mail: tswhite@essc.psu.edu

SCIENTIFIC REPORT

ABSTRACT

The Cenozoic Era is unusual in its development of major ice sheets. Progressive cooling at high latitudes during the Cenozoic eventually formed major ice sheets, initially on Antarctica and later in the Northern Hemisphere. In the early 1970s, a hypothesis was proposed that climatic cooling and an Antarctic cryosphere developed as the Antarctic Circumpolar Current progressively thermally isolated the Antarctic continent. This current resulted from the opening of the Tasmanian Gateway south of Tasmania during the Paleogene and the Drake Passage during the earliest Neogene.

The five Leg 189 drill sites, in 2463 to 3568 m water depths, tested the above hypothesis and refined and extended it, greatly improving understanding of Southern Ocean evolution and its relation with Antarctic climatic development. The relatively shallow region off Tasmania is one of the few places where well-preserved and almost-complete marine Cenozoic carbonate-rich sequences can be drilled in present-day latitudes of 40°–50°S, and paleolatitudes of up to 70°S. The broad geological history of all the sites was comparable, although there are important differences among the three sites in the Indian Ocean and the two sites in the Pacific Ocean, as well as from north to south.

In all, 4539 m of core was recovered with an excellent overall recovery of 89%, with the deepest core hole penetrating 960 m beneath the seafloor. The entire sedimentary sequence cored is marine and contains a wealth of microfossil assemblages that record marine conditions from the Late Cretaceous (Maastrichtian) to the late Quaternary and terrestrial conditions until the earliest Oligocene. The drill sites are on submerged continental blocks extending as far as 600 km south of Tasmania. These continental blocks were at polar latitudes in the Late Cretaceous when Australia and Antarctica were still united, although rifts had developed as slow separation and northward movement of Australia commenced. The cores indicate that the Tasmanian land bridge, at polar latitudes, completely blocked the eastern end of the widening Australo-Antarctic Gulf, during both the slow-spreading phase and the fast-spreading phase (starting at 43 Ma), until the late Eocene.

Prior to the late Eocene, marine siliciclastic sediments, largely silty claystone, were deposited in a relatively warm sea on broad, shallow tranquil shelves. Sediment supply was rapid and despite the rifting, drifting, and compaction, largely deltaic deposition kept up with subsidence. Calcareous and siliceous microfossils are sporadic, and dinocysts, spores, and pollen are ever present. The spores and pollen are compatible with, throughout this time, this part of Antarctica being relatively warm with little ice and supporting temperate rain forests with southern beeches and ferns—part of the “Greenhouse” world. Differences in the claystones between east and west indicate that the eastern Australo-Antarctic Gulf was more poorly ventilated than the gradually

widening Pacific Ocean with its western boundary current, the East Australian Current. However, currents from low latitudes warmed both sides of the land bridge.

In the late Eocene (37 Ma), the Tasmanian land bridge had separated from Antarctica, the bridge and its broad shelves began to subside, and cool surface currents started to circulate around Antarctica from the west. These swept the still-shallow offshore areas, and glauconitic siltstones were deposited very slowly as condensed sequences. Palynological and other evidence suggests that there were considerable fluctuations in temperature superimposed on a general cooling and that the amount of upwelling also fluctuated in response to the changing oceanic circulation. Calcareous microfossils are rare, but diatoms and foraminifers indicate that some sites began to reach bathyal depths in the latest Eocene (34 Ma).

By the early Oligocene, warm currents from the tropics were cut off by the developing Antarctic Circumpolar Current from some parts of Antarctica, leading to cooling and some ice sheet formation. This contributed to global cooling. Conditions were significantly cooler in the Tasmanian offshore region, and there is no positive evidence of land vegetation although this organic matter could have been oxidized during deposition in well-ventilated waters. Much of the land bridge had subsided beneath the ocean, so there was a smaller hinterland to supply sediment. Furthermore, the colder ocean provided less moisture, decreasing precipitation, and erosion. Altogether, far less siliciclastic sediment was transported from the land and generally slow deposition of deep-water pelagic sediments set in. However, the East Australian Current and currents moving down the western Australian margin continued to keep the Tasmanian region relatively warm, resulting in carbonate deposition rather than the siliceous biogenic deposition that marks much of the Antarctic margin. Furthermore, in the Tasmanian region, and even in the Cape Adare region on the conjugate Antarctic margin, there is no sign of glaciation during the early Oligocene.

The Drake Passage opened early in the Neogene, and the Tasmanian Seaway continued to open, strengthening and widening the Antarctic Circumpolar Current and strongly isolating Antarctica from warm-water influences from lower latitudes. At ~15 Ma, the east Antarctic cryosphere evolved into ice sheets comparable to those of present day. This intensified global cooling and thermohaline circulation. The “Icehouse” world had arrived. However, temperatures and current activity fluctuated, and dissolution and erosion varied over time. The Tasmanian region had been moving steadily northward so that its sediments were never south of the Polar Front, and pelagic carbonate continued to accumulate in deep waters at average rates of 1–2 cm/k.y. The upper Neogene sequences contain windblown dust from Australia, which was moving progressively northward into the drier midlatitudes. Along with global climate change associated with high-latitude ice sheet expansion, this led to the massive aridity of Australia and an increase in dust abundance in some sequences after 5 Ma.

Comparisons with sequences drilled elsewhere on the Antarctic margin will further improve our understanding of these momentous changes in Earth’s history and some of the constraints on modern climates. If Australia had not broken away from Antarctica and moved northward, global

climate may well have remained warm. We can now document in some detail the changes related to that tectonic movement. Tectonic information indicates that there were three critical tectonic events during the Cenozoic in the Tasmanian region: Paleocene strike-slip movement, terminating at 55 Ma by seafloor spreading south of the South Tasman Rise (STR); Eocene strike-slip movement along the western boundary between the STR and Antarctica, terminating in the latest Eocene around 34 Ma; and early Oligocene subsidence of the STR and collapse of the continental margin around Tasmania. The early Oligocene subsidence and collapse also occurred in the Victoria Land Basin east of the rising Transantarctic Mountains (Cape Roberts Scientific Team, 2000) and along the Otway coast on mainland Australia, northwest of Tasmania.

Postcruise studies and comparisons will better define and explain regional similarities and differences in tectonism, sedimentation, and climate. Initial studies of physical properties, wireline logs, and microfossils all show that climatic cycles of varying length are present throughout the entire sequence, and postcruise studies will better define Milankovitch and other cycles. In the Neogene pelagic carbonates, the excellent preservation and high depositional rates will allow detailed isotope studies of surface- and bottom-water temperatures through time. There is a unique opportunity to build Southern Ocean correlations between various microfossil groups—calcareous nannofossils, planktonic foraminifers, diatoms and radiolarians, and dinocysts, spores, and pollen. Geochemical studies have identified some unusual trends in the sequences, and the Paleogene sequence contains thin, almost-mature hydrocarbon source rocks at most sites.

Leg 189 results essentially encapsulate the evolution during the Cenozoic of the Antarctic system from “Greenhouse” to “Icehouse.” The changes recorded in the cored sequences clearly reflect evolution of a tightly integrated, and at times dynamically evolving, system involving the lithosphere, hydrosphere, atmosphere, cryosphere, and biosphere.

INTRODUCTION

The area between Australia’s southernmost prolongation (Tasmania and the South Tasman Rise [STR]) and Antarctica is a key to understanding global Cenozoic changes in climate and current patterns, involving

1. The breakup of Gondwana between 130 and 30 Ma (Fig. 1);
2. The drifting of Australia northward from Antarctica;
3. Initiation in the Paleogene to early Neogene of the Antarctic Circumpolar Current and the meridional expansion of the Southern Ocean with concomitant thermal isolation of the Antarctic continent and development of its cryosphere during the Paleogene and Neogene (Kennett, Houtz, et al., 1975); and

4. The effects these processes have had on global cooling (Fig. 2), climatic variability, and biotic evolution.

The opening of the Tasmanian Gateway between Australia and Antarctica and the only other important constriction in the establishment of the Antarctic Circumpolar Current, the Drake Passage, had enormous consequences for global climate. These consequences came in part by isolating Antarctica from warm gyral surface circulation of the Southern Hemisphere oceans and also by providing the necessary conduits that eventually led to ocean conveyor circulation between the Atlantic and Pacific Oceans. Both factors, in conjunction with positive feedbacks and other changes in the global system, have been crucial in the development of the polar cryosphere, initially in Antarctica during the Paleogene and early Neogene and later in the Northern Hemisphere during the late Neogene. Furthermore, the continued expansion of the Southern Ocean during the Cenozoic, because of the northward flight of Australia from Antarctica, has clearly led to further evolution of Earth's environmental system and of oceanic biogeographic patterns.

The geographic position of the Tasmanian offshore region makes this a crucial location to study the effects of Eocene–Oligocene Australia-Antarctic separation on global paleoceanography. Australia and Antarctica were still locked together in the Tasmanian area during the middle Eocene, preventing the establishment of circum-Antarctic circulation (Fig. 1). At that time, and earlier, the water masses were separated on either side of the barrier in the southern Indian and Pacific Oceans and most likely exhibited distinct physical, chemical, and biological properties. The Tasmanian region is also well suited for the study of post-Eocene development of Southern Ocean climate development, feedbacks that contribute to ice sheet development and increased stability, and formation and variation of high-latitude climate zones. This region is one of the few ideally located in the Pacific sector of the Southern Ocean for comparison with the models of Cenozoic climate development and variation in the Indian Ocean and the South Atlantic. Therefore, an outstanding question is whether paleoceanographic variability, known from the Atlantic and Indian sectors, is characteristic of the entire circum-Antarctic ocean or whether there are zonal asymmetries in the Southern Ocean and, if so, when these developed.

The meridional spread of the sites on the STR (Fig. 3) is well suited for monitoring the migration of frontal zones through time, analogous to transects on the Southeast Indian Ridge (SEIR) (Howard and Prell, 1992). The total meridional displacement of fronts on the STR is expected to be somewhat less than on the SEIR because the STR is a shallower topographical barrier to the Antarctic Circumpolar Current. The East Tasman Plateau (ETP) site is ideally located to monitor paleoceanographic changes at the interface between the East Australian Current and the Antarctic Circumpolar Current because the East Australian Current transports heat into the Southern Ocean, an important "gateway" objective.

The sites cored during Leg 189 also provide high-quality paleoclimatic and paleoceanographic records of Neogene age, including the Quaternary, from the southern temperate and subantarctic regions. These sequences are being employed to examine the development of surface-water productivity, oscillations in subtropical and polar fronts, changing strength of the East Australian Current, and changes related to further expansions of the Antarctic cryosphere during the middle and late Miocene.

Previous investigations have demonstrated that the Southern Ocean late Quaternary paleoceanographic record, manifested in its temperature response (Howard and Prell, 1992) and carbon cycling (Howard and Prell, 1994; Oppo et al., 1990), mirrors that of the Northern Hemisphere. This suggests similar cryospheric, atmospheric, and oceanographic variability in Southern Ocean climate during the past 500 k.y. compared with that of the Northern Hemisphere (Imbrie et al., 1992; Imbrie et al., 1993). However, on the Milankovitch band there appears to be a lead in the Southern Ocean, perhaps reflecting the importance of this region. For example, the potential role of Southern Ocean paleoproductivity changes on global climate remains a topic of significant interest. Despite the excellent documentation of Southern Ocean paleoclimate history of the latest Pleistocene, where variability is dominated by 100-k.y. cycles, there is a lack of fully cored sections to address the mid-Pleistocene (900 ka) transition from obliquity-dominated cycles (40-k.y. periodicity) to eccentricity-dominated (100-k.y. periodicity) cycles (Ruddiman et al., 1989) in this region. A documented Southern Ocean section over this "transitional" period was based on poor recovery (Hodell and Venz, 1992), so this important transition in global climate remains to be properly documented. However, two giant piston cores taken on the STR (*Marion Dufresne,* 1997) provide excellent records back to 900 ka including this transition. Sedimentation rates were up to 2.2 cm/ky. The STR Ocean Drilling Program (ODP) sites will add to this record and complement subantarctic South Atlantic transect sites (Leg 177) in documenting this transition.

Major questions addressed during Leg 189 include the following:

1. How did the Antarctic Circumpolar Current develop, and what were the roles of the opening of the Tasmanian Gateway (~34 Ma) and Drake Passage (~20 Ma)?
2. When did the Tasmanian Seaway open to shallow water, and how did this affect east-west biogeographic differences, isotopic differences relating to changing climatic regimes, and geochemical differences?
3. When did the seaway open to deep waters, and how did this affect surface- and deep-water circulation?
4. How is circum-Antarctic circulation related to changes in Antarctic climate?
5. How did the East Antarctic cryosphere develop in this part of Antarctica, and how does it compare to other sectors?
6. What was the nature of the adjacent Antarctic climate in the Greenhouse period during the middle to late Eocene?

7. How did sedimentary facies change as the Tasmanian region moved northward, circum-Antarctic circulation became important, and upwelling commenced?
8. How did Antarctic surface waters develop in terms of temperature, the thermocline, and oceanic fronts?
9. How did intermediate waters evolve during the Neogene, and how was this evolution tied to Antarctic cryosphere development?
10. How did Australia's climate change as the continent moved northward?
11. How were changes in the marine biota tied to changes in the oceanographic system?

An understanding of Cenozoic climate evolution has required better knowledge of the timing, nature, and responses of the opening of the Tasmanian Seaway during the Paleogene (Figs. 1, 2). Early ocean drilling in the Tasmanian Seaway (Deep Sea Drilling Project [DSDP] Leg 29) provided a basic framework of paleoenvironmental changes associated with its opening but was of insufficient quality and resolution to fully test the hypothesis of potential relationships among the development of plate tectonics, circumpolar circulation and global climate. Until now, the timing of events has remained insufficiently constrained.

The relatively shallow region off Tasmania (mostly above the present carbonate compensation depth [CCD]) is strategically well located for studies of the opening and later expansion of the Tasmanian Seaway. It is also one of the few places where almost-complete marine Eocene to Holocene carbonate-rich sequences can be drilled in present-day latitudes of 40°–50°S and paleolatitudes of up to 70°S (Fig. 4).

Geological Setting

Broad Phases of Cretaceous and Cenozoic Deposition

The Tasmanian region lay within the continent of Gondwana until breakup started during the Late Cretaceous (Fig. 5). Rifting related to the separation of Antarctica and Australia may have started as early as the Late Jurassic, and by the Early Cretaceous there was a well-developed east-west rift system along the southern margin of Australia that passed north of Tasmania through the Bass Strait (Willcox and Stagg, 1990). The rift sequences in outcrop and petroleum exploration wells are volcaniclastic fluviatile and lacustrine sediments thousands of meters thick in places. The volcanism was basic to andesitic, and the Lower Cretaceous sediments are dominantly immature lithic conglomerates, sandstones, and mudstones, with some better sorted quartz-rich sandstone bodies. They were probably derived from volcanism along what is now the east coast of Australia.

During the beginning of the Late Cretaceous, the early rifting in the Bass Strait failed and a NW–SE zone of strike-slip faulting, west of Tasmania, absorbed motion related to the continuing east-west rifting (Fig. 5). This motion eventually separated Australia and Antarctica (Figs. 6, 7). During the Late Cretaceous, the sea intruded into the rift from the west, along the gulf between Australia and Antarctica, here named the Australo-Antarctic Gulf (Fig. 1). Data from petroleum

exploration wells show that coastal plain to shallow-marine detrital sediments were deposited along the east-west rift (Smith, 1986; Lavin, 1997; McKerron et al., 1998) and also along the northernmost part of the zone of strike-slip faulting (Moore et al., 1992). In depocenters near Tasmania, these sediments are relatively mature, quartz-rich and 1000–2000 m thick (Moore et al., 1992). However, southwest of Tasmania, dredging has recovered immature, shallow-marine lithic sandstones and mudstones (Hinz et al., 1985; Exon et al., 1992) of Late Cretaceous age that are reminiscent of the Lower Cretaceous rocks farther north. Seismic reflection profiles show that these sequences are frequently prograded and deltaic (Hill et al., 1997b).

Australia's Eastern Highlands were uplifted at the end of the Early Cretaceous at ~95 Ma (O'Sullivan et al., 1995), and rifting commenced between Australia to the west and the Lord Howe Rise and the Campbell Plateau to the east. During the Campanian (75 Ma, Chron 33), drifting of the latter elements to the east-northeast was well established (Royer and Rollet, 1997), and the eastern margin of Australia/Tasmania/STR started to collapse.

In the latest Cretaceous to Eocene, the east-west rift continued to fill with prograding shallow-marine detrital sediments and coal-bearing strata. The depression along the strike-slip zone also filled with prograding sediments, and seismic interpretation suggests the depocenter moved southward with time relative to Tasmania, with Paleocene sedimentation dominating in the north and Eocene in the south (Hill et al., 1997b). Paleogene sediments are as thick as 1500 m in places. In the Oligocene, Australia cleared Antarctica, its margins subsided, and deposition of relatively thin hemipelagic, pelagic, and shallow-water carbonate predominated thereafter.

The Tasmanian Offshore Region

Today, the Tasmanian offshore region consists of continental crust of the Tasmanian margin (Moore et al., 1992; Hill et al., 1997b), the STR (Hinz et al., 1985; Exon, et al., 1997b), and the ETP (Exon et al., 1997a) and is bounded on all sides by oceanic abyssal plains (Fig. 3). Oceanic crust to the east was created by the seafloor spreading that formed the Tasman Sea in the Late Cretaceous and Paleogene. The crust to the south and west was formed during the Cenozoic, and perhaps the latest Cretaceous, by the seafloor spreading that led to the separation of Australia and Antarctica.

The continental shelf around Tasmania (Fig. 3) is mostly nondepositional at present. The continental slope west of Tasmania slopes fairly regularly, at ~4°, from 200 to 4000 m. The continental rise lies at 4000–4500 m, and the abyssal plain is generally 4500–5000 m deep. Sampling cruises have shown that the slope is underlain by continental basement and that Upper Cretaceous and Paleogene shallow-marine sandstone, siltstone, and mudstone are widespread in deep water west of Tasmania, overlain by Oligocene to Holocene pelagic carbonates. Seismic interpretation shows that basement is generally overlain by several kilometers of sediments (Fig. 8A).

The current-swept STR is a large, north-northwest–trending bathymetric high that rises to <1000 m below sea level (mbsl) and is separated from Tasmania by the west-northwest–trending

South Tasman Saddle >3000 m deep (Fig. 3). The STR is a continental block, and seismic profiles show it is cut into basement highs and deep basins with several kilometers of sedimentary section (Fig. 8B, 8C). The overlying sequences in faulted basins include known Oligocene to Holocene pelagic carbonates and Paleogene marine mudstones, and seismic evidence suggests they also contain Cretaceous sediments. The top of the rise is a gentle dome with low slopes, but slopes are generally steeper between 2000 and 4000 m. The western slope is more gentle to 3000 m, but below that there is a very steep scarp trending 350°, which drops away to 4500 m as part of the Tasman Fracture Zone.

The ETP is a nearly circular feature, 2500–3000 m deep, separated from southeast Tasmania by the 3200-m-deep East Tasman Saddle (Fig. 3). Slopes are generally low, but considerably greater on the plateau's flanks. Atop the plateau is the Cascade Seamount guyot, which formed as the result of hot spot volcanism and has yielded Eocene and younger shallow-water sandstone and volcanics. Seismic profiles show that the plateau has as much as 3 s two-way traveltime (TWT) of sediment cover (Fig. 8D), which are believed to comprise mainly Oligocene to Holocene pelagic carbonates and Cretaceous to Eocene siliciclastic sediments. These are underlain by continental basement rocks.

The structural setting of Sites 1168–1172 is shown in Figure 9. The west Tasmanian margin is cut by strike-slip faults, trending north-northwest or northwest, that were most active in the latest Cretaceous to mid-Paleocene (Hill et al., 1997b). They were generated by the northwest movement of Australia away from Antarctica. The STR is cut by these early faults, and also by younger, middle Eocene- to late Oligocene-age faults. These younger faults are strike-slip faults trending north-south, and on the northwestern STR, related normal faults trending east-west (Exon et al., 1997b). The three sets of faults all have throws reaching as much as 3 km. Sites 1168–1172 were all located in depocenters to ensure that thick Cenozoic sections with high sedimentation rates would be cored.

Plate Tectonics

Early extension between Australia and Antarctica began in a northwest–southeast direction during the Late Jurassic (Willcox and Stagg, 1990), and this motion created much of the western margin off Tasmania. Subsidence studies along the southern Australian margin, as well as the conjugate pattern of magnetic anomalies off Australia and Antarctica, suggest that the breakup between Australia and Antarctica propagated toward Tasmania from the Great Australian Bight (Mutter et al., 1985). Seafloor spreading may have started west of Tasmania during the Late Cretaceous and continued at a slow rate until the early Eocene, when fast spreading began. The trajectory of the central STR since Australia–Antarctic separation, and its paleolatitudes since the Campanian, are shown in Figure 4. Royer and Rollet (1997) reexamined the seafloor magnetic anomaly data and satellite-derived gravity data in the region along with plate tectonic reconstructions and concluded the following about the region south of Tasmania (Fig. 10):

1. The STR is composed of two distinct domains of different origin: a western terrane, lying between the Tasman Fracture Zone and a N170°E oriented boundary at 146.5°E, was initially part of the continental shelf of north Victoria Land, Antarctica (and adjacent to west Tasmania), whereas an eastern terrane, east of the 146.5°E boundary, rifted from Tasmania and the ETP.
2. The western terrane rifted from Antarctica during the late Paleocene to early Eocene and was welded to the eastern terrane. Then, until the early Oligocene (Chron 13), when the STR cleared the Antarctic margin, the western domain underwent severe wrenching and left-lateral shearing between the Antarctic shelf break and the 146.5°E boundary. Deformation continued, but perhaps to a lesser extent, along the transform margin until the early Miocene.
3. The western margin of the STR became active as a transform in the late Paleocene to early Eocene; the SEIR axis was in contact with the margin rim from the early Eocene (~Chron 24) until the early Miocene (~Chron 6B, 23 Ma), after which the transform margin became passive.
4. Seafloor spreading initiated in the Tasman Sea in the Campanian (Chron 34), north of the ETP. A spreading center also probably initiated between the STR and the ETP during the Campanian (Chron 33) and failed shortly afterward during the Maastrichtian (~Chron 30).

Earlier Drilling (DSDP) Results

During DSDP Leg 29, four partially cored sites were drilled in the Tasmanian region (Kennett, Houtz, et al., 1975) (Fig. 3; Table 1). The three sites most relevant to the goals of Leg 189 are Site 282 on the west Tasmanian margin, Site 281 on the STR, and Site 280 on the abyssal plain immediately south of the STR (Fig. 3). The Leg 29 sites were generally located on regional highs to minimize the depth of penetration necessary to reach older strata, and hence much of the succession was cut out by hiatuses. Furthermore, during the first scientific drilling in the area, core recovery was relatively poor. Total sediment recovery for the three critical sites was fairly low (Table 1).

Site 282 was drilled to 310 mbsf on a basement high in deep water west of Tasmania. This sequence includes much of the Cenozoic but contains four major unconformities. The sequence consists of a veneer of Pleistocene ooze, underlain by upper Miocene ooze, lower Miocene marl, lower to mid-Oligocene mudstone, and upper Eocene mudstone. The sediments rest on a pillow basalt of presumed Tertiary age. There is little in the sediments to suggest that the site was located in deep water until the margin began to subside during the Oligocene. Calcareous microfossils are present throughout, and total core recovery was 20%.

Site 281 was drilled to 169 mbsf on a basement high of quartz-mica schist of latest Carboniferous age southwest of the crest of the STR. The sequence consists of Pliocene–Pleistocene foraminifer-nannofossil ooze, Miocene foraminifer-nannofossil ooze, upper

Oligocene glauconite-rich detrital sand, and upper Eocene basement conglomerate and glauconitic sandy mudstone. Evidence from the recovered intervals suggests that the site subsided into deep water after the Miocene. Calcareous microfossils are present throughout, and total core recovery was relatively high (62%).

Site 280 was drilled to 524 mbsf, on a basement high in deep water southwest of the STR (Fig. 3), and bottomed in an "intrusive basalt," almost certainly associated with oceanic crust. The site penetrated a veneer of upper Miocene to upper Pleistocene clay and ooze, underlain (beneath a sampling gap) by 55 m of siliceous lower Oligocene sandy silt, and 428 m of middle Eocene to lower Oligocene sandy silt, containing chert in the upper 100 m and glauconite and manganese micronodules in the lower succession. The lower 200 m is rich in organic carbon (0.6%–2.2%). The younger part of the lower Oligocene to upper Eocene sequence contains abundant diatoms, but the lower part is almost completely devoid of pelagic microfossils. All sediments were probably deposited in abyssal depths. A brown organic staining suggests that reducing conditions were present in parts of the upper Oligocene and lower Miocene. Total core recovery was only 19%.

Site 281, in particular, assisted with the development of a broad, globally significant history of Cenozoic paleoceanographic events. Shackleton and Kennett (1975) produced composite foraminiferal oxygen and carbon isotope curves from the late Paleocene to the Pleistocene from Sites 277, 279, and 281. This record, although of relatively low resolution, exhibits the now classically known general increase in oxygen isotopic values, reflecting a decrease in bottom- and surface-water temperatures and/or ice buildup during the Cenozoic. A general increase occurred in isotopic values following the early Eocene, with a rapid increase during the early Oligocene reflecting major cryosphere expansion and cooling. Average oxygen isotopic values remained steady but oscillatory until the middle Miocene, when there was another rapid oxygen isotopic increase as the Antarctic cryosphere expanded farther. This was followed by further increase in oxygen isotopic values reflecting the development of the West Antarctic ice sheet during the late Miocene and the Northern Hemisphere cryosphere during the late Pliocene (Fig. 2). Isotopic studies were conducted at Site 281 (STR) for the interval from the early Miocene to the Pliocene. In contrast, at Site 277 (Campbell Plateau) isotopic analyses were conducted on the earliest Miocene to late Paleocene.

Modern Hydrography

The two northernmost sites drilled during Leg 189 are located in temperate (cool subtropical) waters north of the present-day position of the Subtropical Front or Subtropical Convergence (Fig. 11). The southern sites are located in subantarctic waters between the Subtropical Front and the Subantarctic Front. The area drilled during Leg 189 therefore lies north of and straddling the Subtropical Front and south to the region near the Subantarctic Front. The Polar Front lies farther to the south of our southernmost site. Rintoul and Bullister (1999) showed that the Subtropical Front is centered on 46°S and lies just south of the saddle between Tasmania and the STR. The

Subantarctic Front is centered on 51°S and lies ~200 km south of the STR. The Polar Front is centered on 53°S, ~200 km south of the Subantarctic Front. The Subtropical Front is marked by a zone of rapid north-south decrease in temperature and salinity and an increase in dissolved nutrients (Barrows et al., 2000) and is approximated by the 34.8–35.1 isohalines and the ~10°C winter and the ~15°C summer isotherms in the southern Tasman Sea (Garner, 1959). During summer, sea surface temperatures are >15°C north of the Subtropical Front, ~10°C between the Subtropical Front and the Subantarctic Front, ~8°C between the Subantarctic Front and the Polar Front, and <6°C south of the Polar Front. During midwinter, sea surface temperatures are several degrees lower. The sedimentary sequences drilled during Leg 189 should record migrations of these fronts as a result of climatic change. Furthermore, as a result of plate tectonic motion, the Tasmanian continental block migrated northward in relation to these fronts during the Cenozoic, leaving records in the marine sediments.

Subantarctic surface water south of the Subtropical Front is driven eastward across the STR by the prevailing westerly winds as the northern part of the Antarctic Circumpolar Current. These surface currents extend to great depths, sweeping the seabed as deep as 2000 m in places. The East Australian Current is a western boundary current that flows southward along the east coast of Tasmania to the vicinity of the ETP. Here subtropical surface water converges with cooler, less saline subantarctic surface water at the Subtropical Front (Orsi et al., 1995).

SCIENTIFIC OBJECTIVES

Paleogene History

Previous sampling has shown that basinal Paleocene history was probably similar in two areas, the west Tasmanian margin and the STR. Clearly, there were differences in shallow-marine deltaic deposition during the Eocene, when the northern area experienced more carbonaceous sedimentation while the southern area experienced the deposition of siliceous radiolarian-bearing glauconitic mudstones. Overall, results are summarized by Hill et al. (1997b), Exon et al. (1997a), and Exon et al. (1997b). As Australia cleared Antarctica, submarine erosion in both areas formed an Oligocene unconformity, and both areas subsided steadily. However, the southern area sank vertically as a block, whereas the west Tasmanian margin rotated downward from a hingeline near the coast, increasing water depths with increasing distance from Tasmania. In many southern areas, the Antarctic Circumpolar Current removed most Neogene sediments, but thick late Oligocene to Holocene carbonate sediments are present in depocenters off west Tasmania and on the STR.

The stratigraphy of petroleum exploration wells on the west Tasmanian continental shelf was summarized by Moore et al. (1992). The detrital Upper Cretaceous sequence is probably disconformably overlain by the Cenozoic. Nonmarine to shallow-marine, Paleocene to early Eocene fining-upward sequences are always present. The middle Eocene to lower Oligocene sequence is more calcareous, consisting of shallow-marine sandstone, marl, and limestone.

Above a major unconformity, the late Oligocene-age and younger sediments are dominantly shelfal marl and limestone. All of the Late Cretaceous, Paleocene, and Eocene siliciclastic sediments sampled are interpreted as shallow or restricted marine and are commonly deltaic (prograding is marked in seismic profiles).

Existing stratigraphic and sedimentologic information indicates that middle Eocene sequences are different in the northern sites west of Tasmania (DSDP Site 282; Hill et al., 1997b) and in the south in the STR (DSDP Site 281; Exon et al., 1997b), although shallow-marine and deltaic facies are found in both areas. Northern sequences contain abundant organic matter and calcareous temperate microfossil assemblages. Southern sequences contain more siliceous microfossils of colder water character. One occurrence of varves (Exon, et al., 1997b) suggests strong seasonality of the Antarctic climate. The middle Eocene to upper Oligocene sequences are crucial to understanding the opening of the Tasmanian Seaway, initially in shallow and later in deep water. Before the Oligocene, sequences on either side of the STR should have distinctive biogeographic characters.

Study of the uppermost Eocene through Oligocene sequences will be of special importance in examining the timing of the development of the circumpolar circulation both across and south of the STR (~65°S at that time). The opening of this gateway was such a profound event that biotic, sedimentologic, and geochemical parameters would almost certainly have undergone distinct changes. When studied in detail and in unison, changes in these parameters are expected to provide the crucially needed evolutionary information on the gateway. The dating of unconformities or hiatuses will provide critical information on major current activity during the Oligocene, especially in the shallow sequences, although sites have been selected to minimize the effects of sediment erosion. We are especially interested in the timing of initial shallow-water linkage across the STR and deep-water linkage south of the STR.

Sites 1168 and 1170 will provide data about the Indian Ocean paleoenvironment before the opening of the Tasmanian Gateway (middle to late Eocene), whereas Sites 1171 and 1172 will provide information about South Pacific paleoenvironments before the opening. All sites will address the initial shallow-water breakthrough (late Eocene), and most will address the deep-water breakthrough to some extent (early–mid-Oligocene?).

Results from DSDP Leg 29 suggested that a sequential appearance of marine microfossils, from dinocysts and arenaceous foraminifers (early Eocene) to calcareous nannofossils (middle Eocene) to calcareous benthic foraminifers (early late Eocene) and to planktonic foraminifers (late late Eocene), might well be revealed at most of the sites. The order of appearance of major groups is paleoenvironmentally significant and is expected to provide crucial insights about the evolution of the Southern Ocean biota. The upper middle Eocene to the lower Oligocene sequence, where calcareous microfossils are present and sedimentation rates were expected to be 1.5 to 3 cm/k.y., should provide excellent documentation of tectonic, climatic, and oceanographic changes. Planktonic foraminiferal and calcareous nannofossil biostratigraphy, in conjunction with strontium and oxygen isotope stratigraphies should provide a chronology of sufficient

resolution. Specific stratigraphic boundary events (e.g., Eocene/Oligocene and Miocene/Pliocene) will be analyzed at high resolution.

Neogene and Quaternary History

Data from the coring in the Tasmanian region will assist in evaluation of the dynamic oceanographic and climate evolution that continued in the Southern Ocean during the Neogene and Quaternary. Information gained will include that related to climate and ocean evolution, oscillations in ocean temperatures, migration of ocean fronts, paleoproductivity, and biotic evolution. This leg is complementary to three recent ODP Neogene paleoceanographic legs: Leg 182 in the Great Australian Bight to the northwest, Leg 177 in the subantarctic South Atlantic, and Leg 181 east of New Zealand. Leg 189 fills a key geographic gap. For example, the sites provide temperate and subantarctic Neogene biostratigraphy of foraminifers and calcareous nannofossils.

In particular, the history of water-mass formation and mixing among Antarctic, Indian, and Pacific sources can be monitored in this area through isotopic and trace metal proxies measured in the abundant planktonic and benthic foraminifers. These sites will complement the Leg 177 South Atlantic subantarctic transect sites in answering questions about the circum-Antarctic symmetry of Southern Ocean paleoclimate change and interbasin circulation patterns that influence the ocean's dissolved carbon and alkalinity budgets.

Most knowledge of Southern Ocean paleoceanography has been derived from the Atlantic and Indian sectors (Legs 113, 114, 119, 120, and 177). It is usually assumed that the history from an individual site or region represents the "zonal" behavior of the Southern Ocean, but differences among the sectors may have been significant, especially for the Paleogene and early Neogene. Even in the late Pleistocene, when there is no doubt that circum-Antarctic flow was fully established, there is some evidence that the Atlantic and Indian Ocean sectors may have had important differences in paleoceanographic variability (Wright et al., 1991; Miller et al., 1991). These differences not only provide useful insights about paleocirculation, but also about meridional heat transport (driving zonal thermal anomalies), in the Pliocene–Pleistocene as well as in the Miocene and Oligocene (Hodell and Venz, 1992).

Intersector differences in heat transport could have important implications for the possible melting history of different sectors of the Antarctic ice sheets. For example, if meridional heat transport was greater in the southwest Pacific, the West Antarctic Ice Sheet may have been more vulnerable to melting. Did this ice sheet maintain its present mass balance in the face of such circulation changes? Much work related to the cooling of Earth during the late Neogene ice ages is now focused on the role of oceanic and atmospheric polar heat transport.

Sites cored during Leg 189 will also provide records of the interaction of the Antarctic Circumpolar Current and the Western Boundary Current (East Australian Current). Areas of Western Boundary Current "injection" into the Southern Ocean (the Brazil-Malvinas Confluence and the Agulhas Retroflection) are regions of large-scale heat and carbon dioxide exchange

between ocean current systems, and between the ocean and atmosphere that ventilate the main ocean thermocline, and will be one of the key components of the ocean to respond to global warming. Understanding the dynamics of such confluences on a geologic time scale is vital to anticipating their possible response to future climate change (e.g., Trenberth and Solomon, 1994).

The Neogene sites also continue global biostratigraphic transects in middle to upper bathyal water depths toward the south. West of the STR, the results from the mid-latitude Great Australian Bight Cenozoic carbonates drilled during Leg 182 will be extended southward almost to a present latitude of 50°S by four of our holes. East of the STR, the results of the Lord Howe Rise Leg 90 will be extended south to the same latitude by two of our holes. An additional advantage of the northern Sites 1168 and 1172 is that these sites may contain pollen from nearby Tasmania, allowing direct terrestrial-marine climate comparisons for the Neogene. So far the only mid-latitude Southern Hemisphere drill site that has yielded such a record is Site 594 east of New Zealand (Heusser and van de Geer, 1994).

PRINCIPAL RESULTS

Site 1168

Site 1168 is located in middle bathyal water depths (2463 m) on the 4° slope of the western margin of Tasmania (50 km from coast) in a 25-km-wide strike-slip basin between upthrown northwest-trending ridges of Cretaceous rocks. The site is 80 km southeast of DSDP Site 282, which is located in deeper water and on a structural high. It lies north of the oceanographic Subtropical Front. Site 1168 was planned to penetrate marine rift to open-margin sediments deposited from the Eocene onward as Australia moved northward from Antarctica. Initially, the site was at the far eastern end of the restricted Australo-Antarctic Gulf and separated from the Pacific Ocean by the Tasmanian land bridge. Plate movements and related margin subsidence led to its Neogene location in open water facing a broad Southern Ocean. The primary objectives were to core and log (1) a prograding detrital sequence, formed during Eocene opening of the ocean south of Australia, for its paleoceanographic, paleoclimatic, and biotic history, (2) an Oligocene to present-day pelagic carbonate sequence for better understanding of the evolution of the Southern Ocean during its expansion in the Cenozoic and for high-resolution paleoclimatic studies, and (3) a Cenozoic sequence for high-resolution biostratigraphic studies.

Seismic profiles suggest that the site was subject to downslope sediment movement to the northwest in the Paleogene but was protected from downslope movement from the east in much of the Neogene by the upslope high (Fig. 12). The Paleocene and Eocene sediments prograde to the northwest, and the drilled late Eocene is hummocky in the southwest–northeast section, with ridges and troughs 0.5–1 km across, suggesting deltaic lobes. Younger sequences are poorly parallel bedded and almost transparent seismically.

We cored two advanced hydraulic piston corer/extended core barrel corer (APC/XCB) holes, and a third hole with just the APC, at Site 1168. Hole 1168A reached 883.5 mbsf with 98% recovery (Table 2). Hole 1168B was APC cored to 108.4 mbsf with 98.3% recovery, and Hole 1168C reached 290.5 mbsf with 85.4% recovery. Wireline logging was conducted in Hole 1168A with the triple-combination (triple-combo) tool string (877 to 101 mbsf) and the geological high-sensitivity magnetic tool (GHMT)-Sonic tool string (730 to 102 mbsf). A bridge prevented running the GHMT-sonic tool string to the base of the cored interval, and we chose not to run the Formation MicroScanner (FMS) because of the poor hole conditions.

Construction of a composite section of the triple-cored portion of the sedimentary sequence (~110 mbsf) indicates that there are no stratigraphic gaps to that depth. Beyond that, there are limited gaps, but overall core recovery averaged 93%, producing an excellent record of near-continuous deposition since the early late Eocene. Biostratigraphy indicates no major time breaks. Sedimentation rates were relatively low throughout (6.9–1.5 cm/k.y.) for a margin setting close to land. The drilled sequence broadly consists of 260 m of nannofossil ooze of middle Miocene and younger age (lithostratigraphic Unit I); 400 m of clayey chalk, nannofossil siltstone, and sandstone of early Miocene and Oligocene age (Unit II); and 220 m of shallow-marine late Eocene carbonaceous mudstone and sandstone (Units III–V).

Lithostratigraphic Unit I (0–260 mbsf) was subdivided into two subunits: Subunit IA to 45 mbsf and Subunit IB to 260 mbsf. Subunit IA is light greenish gray foraminifer-bearing nannofossil ooze with minor calcareous turbidite sands, and Subunit IB is white nannofossil ooze. Carbonate content averages 90 wt%, and magnetic susceptibility and organic carbon content are both very low. Calcareous microfossils are abundant and little altered, benthic foraminifers are always present, dinoflagellate cysts are absent only in the middle Miocene, and radiolarians and diatoms are common in the upper Miocene. Microfossil ages (early middle Miocene to Pleistocene) show that average sedimentation rates were low at 1.65 cm/k.y. Deposition was in middle bathyal depths in well-oxygenated bottom waters.

Lithostratigraphic Unit II (260–660 mbsf) has three subunits: Subunit IIA to 410 mbsf, Subunit IIB to 540 mbsf, and Subunit IIC to 660 mbsf. These three olive-gray subunits become darker and more clayey and silty downward. Calcareous microfossils are abundant and little altered in the Miocene and moderately preserved in the upper Oligocene. Dinoflagellates and benthic foraminifers are pervasive, and radiolarians are uncommon. Microfossil ages (late Oligocene to early middle Eocene) show that sedimentation rates are higher, averaging 4.3 cm/k.y. through the Miocene and late Oligocene. Deposition was bathyal with variation in the oxygenation of bottom waters. Visible bubbling in the cores and high methane content in headspace and vacutainer samples indicate production of biogenic gas in the upper part of the unit. An association with reduced pore-water chlorinity initially suggested the presence of gas hydrates; however, a lack of a well-log resistivity shift suggests that this may not be the case. Nevertheless, the presence of fluid escape structures (soft-sediment deformation) in Subunit IIA suggests that hydrates may indeed have been present in the past.

Subunit IIA consists of clay-bearing nannofossil chalk to nannofossil claystone. Carbonate content averages 40 wt%, magnetic susceptibility is moderate, and the organic carbon content is low. Subunit IIB consists of nannofossil claystone and nannofossil-bearing claystone. Carbonate content averages 30 wt%, magnetic susceptibility is moderate, and the organic carbon content is low. Subunit IIC consists of silty nannofossil chalk to nannofossil siltstone. Carbonate content averages 40 wt%, magnetic susceptibility is fairly low, and organic carbon content is low.

Lithostratigraphic Unit III (660–748.6 mbsf) has two subunits: Subunit IIIA to 725 mbsf and Subunit IIIB to 748.6 mbsf. These two olive-gray units become darker downward. They contain calcareous microfossils that are abundant but only moderately preserved. Dinoflagellates and benthic foraminifers are persistent and radiolarians are uncommon. Microfossil ages (early Oligocene) indicate very low sedimentation rates. The environment of deposition was bathyal marine in a relatively tranquil environment. Carbonate content is variable but averages 20–30 wt%, magnetic susceptibility is moderate, and organic carbon content is low. Subunit IIIA consists of clayey nannofossil chalk to nannofossil-bearing organic clayey siltstone. Subunit IIIB consists of organic-bearing silty claystone and organic clayey siltstone.

Lithostratigraphic Units IV and V (748.6–883.5 mbsf) form a late Eocene package of related sediments. These two units are dark gray to black. Carbonate content is low, magnetic susceptibility is moderate but variable, and the organic carbon content is as high as 5 wt%. Dinoflagellates are rare but spores and pollen are abundant, and the abundant dispersed organic matter is dominantly from land plants. Geochemical and micropaleontological evidence suggests a presence of brackish conditions in part, with normal marine salinities at other times. Characterization of the organic matter indicates that it is largely terrigenous in origin and is immature, but with increasing maturity toward the base of the hole (approaching the oil window).

Two nannofossil datums give average sedimentation rates of 6.9 cm/k.y. Calcareous microfossils are sporadic, rarer downward, and moderately to poorly preserved. Agglutinating benthic foraminifers are sporadic. The environment of deposition was reducing, shelfal to bathyal marine, and protected from currents and waves. Evidence from palynology suggests a subtropical to temperate climate, with a terrestrial plant assemblage containing abundant ferns. Calcareous nannofossils are represented by a warm-water assemblage containing warmer water elements than those previously found elsewhere at equivalent latitudes in the Southern Ocean. Plate reconstructions suggest that the Kerguelen Plateau may have been shielding the Australo-Antarctic Gulf from cold water from the west so that the only water entering the gulf came from warmer areas north of western Australia.

Lithostratigraphic Unit IV (748.6–762 mbsf) consists of dark gray glauconitic, quartzose sandstone, and clayey siltstone, with interbedded black carbonaceous silty claystone. Thin calcareous stringers contain microfossils. Both glauconite and quartz are fine to very coarse grained, and the quartz is subangular. Microfossil ages within this Eocene–Oligocene transition indicate very low sedimentation rates during deposition of glauconite layers because of

intensified bottom-water activity leading to winnowing. A condensed section with possible hiatuses is indicated.

Lithostratigraphic Unit V (762–883.5 mbsf) consists of black carbonaceous silty claystone and clayey siltstone and is finely laminated in part. Pyritic replacements of burrows and fossils are common. There are rare, thin lenses of rippled fine sand, and thin calcareous stringers contain microfossils.

In summary, the sediment sequence records paleoenvironmental changes, beginning with a shallow-water, nearshore, restricted basinal setting with poor ventilation and siliciclastic sedimentation, low oxygenation, and high organic carbon deposition. Site 1168 Eocene sediments, similar to those at DSDP Site 282 to the northwest and DSDP Site 280 just south of the STR, suggest widespread late Eocene anoxic conditions in the eastern Australo-Antarctic Gulf. Following a transitional phase during the Oligocene, by the Neogene these conditions had been replaced by deposition of carbonate ooze in a well-oxygenated, open ocean on a passive margin at middle bathyal depths.

The succession of sediment, climatic, and biotic changes recorded at Site 1168 reflect three major steps in the state of Cenozoic climate: “greenhouse” in the late Eocene; “doubthouse” of intermediate mode in the Oligocene through early Miocene; and “icehouse” since the middle Miocene. Relatively rapid changes mark the boundaries at the Eocene–Oligocene transition and during the middle Miocene at ~14 Ma. The most conspicuous change in the sediment and biotic sequence occurred during the transition from the Eocene to the early Oligocene with conspicuous reduction in sedimentation rates and deposition of glauconite sands. This transition reflects a transient event associated with temporary increased bottom-water activity in the basin. The timing of this episode is consistent with the hypothesis of linkage with initial opening of the Tasmanian Gateway and/or major cooling of Antarctica and associated cryospheric development. The changes are documented in part by excellent microfossil sequences of calcareous nannofossils, planktonic and benthic foraminifers throughout, and dinoflagellates after the late Eocene. Spores and pollen are abundant in the upper Eocene, fewer in the lower Oligocene, and intermittently present in younger sequences. Major biostratigraphic achievements will be the first comprehensive Cenozoic zonations for the cool temperate region south of Australia for planktonic foraminifers, calcareous nannofossils, and dinoflagellates.

Site 1169

Site 1169 is located in deep water (3568 m) in a flat plain on the western part of the STR, 400 km south of Tasmania. It lies 15 km east of the ridge of the Tasman Fracture Zone (TFZ) that rises 400 m above the plain. The site is 100–200 km south of the Subtropical Front (Subtropical Convergence). At Site 1169 we planned to penetrate open-ocean carbonate oozes deposited from the Miocene onward as Australia moved northward from Antarctica. In the early Miocene (20 Ma), the site was at 55°S compared to its present latitude of 47°S. The primary objective was to

core a complete late Neogene sequence with high sedimentation rates in northern subantarctic waters for high-resolution biostratigraphic and paleoclimate investigations.

Seismic profiles indicate that the site is in a westerly thickening wedge of transparent young Neogene ooze, ~200 m thick at the site, that onlaps a prominent reflector and unconformity below, which is more transparent ooze or chalk. This wedge of ooze appears to have been deposited in the lee of the western ridge (TFZ), which provided protection from scouring by the easterly flowing Antarctic Circumpolar Current. The results from Site 1170, where a comparable section was drilled in shallower water to the east, show that the transparent wedge results from facies change rather than younging westward.

We had planned to core three APC/XCB holes, but poor weather conditions and large heaves greatly degraded the quality of the cores, and only Hole 1169A was cored to 246.3 mbsf with 91.4% recovery (Table 2). Although recovery was high in the APC cores, flow-in and other disturbances meant that both core structure and age reliability were severely compromised. This will preclude future high-resolution paleoclimatic investigations.

The drilled sequence consists of 246.3 m of nannofossil ooze with a total age range from the late Miocene (12.2 Ma) to the late Quaternary, although much of the record is missing in two disconformities. The upper ~200 mbsf of the sequence represents the last ~4 m.y. and disconformably overlies a thin (~200 to 220 mbsf) sequence of late Miocene age (6.5 to 6.8 Ma). This, in turn, is underlain by sediments with possible 12.2 Ma age, although strong sediment disturbance makes for difficult dating in this part of the sequence. This level is correlated with a seismic unconformity. Sediments are dominated throughout by nannofossil ooze with rare to common foraminifers and siliceous microfossils that include diatoms and radiolarians. Siliciclastic sediment components are largely absent in this open-ocean location. One lithostratigaphic unit is recognized, which is subdivided into two subunits: Subunit IA (0–170.1 mbsf) is a nannofossil ooze with common to abundant siliceous microfossils. Subunit IIB (170.1–246.3 mbsf) is a nannofossil ooze with rare to few siliceous microfossils. Sedimentation rates were low (1.6 cm/k.y.) during the Quaternary through late Pliocene, very high (20 cm/k.y.) during the early Pliocene, and moderately high (10.9 cm/k.y.) during the brief late Miocene interval represented. The nannofossil oozes were deposited in upper abyssal water depths under well-oxygenated bottom-water conditions.

Although the primary objective, high-resolution climatic history, could not be met, Site 1169 provides a number of highlights. We were able to develop a useful, although relatively broad, integrated subantarctic biostratigraphy for the Pliocene and Quaternary involving planktonic foraminifers, calcareous nannofossils, diatoms, radiolarians, and organic dinocysts. Ostracods are also persistently present throughout. Few previous sites from the subantarctic region have allowed the development of such an integrated stratigraphy, particularly from the Australian sector of the Southern Ocean. This site also contains the southernmost late Neogene dinocyst record ever found. A conspicuous level of microtektites were discovered in association with the latest Miocene/earliest Pliocene disconformity, the first of this age to be reported from the

Southern Ocean. Conspicuous late Miocene unconformities suggests intensification during that time of bottom-water circulation and associated carbonate dissolution on the STR at depths close to 3.5 km.

Planktonic microfossil assemblages reflect the influence of both subantarctic and temperate water masses in this northern subantarctic location. These mixed assemblages may indicate shifts in position of the Subtropical Convergence over the region. Antarctic elements are also present in some planktonic microfossil groups, reflecting influence of more highly productive Antarctic surface waters to the south. The very high sedimentation rates of the early Pliocene at this site have previously been observed over broad areas of the South Pacific and elsewhere. These high rates have previously been considered to represent a significant increase in calcareous biogenic productivity associated with fundamental paleoceanographic changes affecting surface waters during early Pliocene warmth. Rates of early Pliocene biogenic sedimentation at Site 1169 may have been even further amplified by winnowing of calcareous nannofossils from the STR into the local catchment basin in which Site 1169 is located. Site 1169 extends observations for the first time to the subantarctic region of this remarkably high early Pliocene biogenic productivity.

Site 1170

Site 1170 is located in deep water (2704 m) on the flat western part of the STR, 400 km south of Tasmania and 60 km east of Site 1169. It is 10 km west of a fault scarp, ~500 m high and trending north-south, that separates the lower western and higher central blocks of the STR. The site lies within present-day northern subantarctic surface waters, ~150 km south of the Subtropical Front and well north of the Subantarctic Front. The primary objectives of Site 1170 were to core and log (1) an Eocene detrital section deposited during early rifting between the STR and Antarctica to ascertain marine paleoenvironmental conditions before and leading into the initial marine connection that developed between the southern Indian and Pacific Oceans as the Tasmanian gateway opened during the mid-Paleogene, (2) an Oligocene to Holocene pelagic carbonate sequence to document the paleoceanographic and paleoclimatic responses to the opening of the Tasmanian gateway and subsequent expansion of the Southern Ocean, and (3) a late Neogene sequence to construct a high-resolution subantarctic biostratigraphy and a high-resolution record of paleoclimatic change.

Plate tectonic reconstructions show the site as being in a northwest–southeast rift between Antarctica and Tasmania during the Cretaceous and moving south with Antarctica until the latest Cretaceous, when it became welded to the remainder of the STR and became part of the Australian Plate. From the earliest Paleogene, the site was close to the active rift. A shallow sea associated with Paleogene rifting and east-west spreading between Australia and Antarctica placed the site in the far southeastern corner of the restricted Australo-Antarctic Gulf, on the Indian Ocean side of the Tasmanian land bridge. Marine magnetic lineations show that in the late Oligocene (26–27 Ma) the east-west spreading axis was 100 km west of the site at Chron 8. The passing of the axis probably caused nearby uplift followed by subsidence.

Seismic profiles and regional correlations suggest that the site was subject to steady deposition of prograded siliciclastic deltaic sediments through the Cretaceous into the Eocene, and hemipelagic sedimentation grading to pelagic sedimentation thereafter (Fig. 13). Much of the Cenozoic siliciclastic detritus must have come from the higher central block to the east, believed to consist largely of continental basement and Cretaceous to Eocene sedimentary rocks. Parts of the central block, which was initially the Tasmanian land bridge, may have remained subaerial and, hence, a source of siliciclastic sediments well into the Oligocene. Seismic profiles suggest that there was a period of current erosion against the fault scarp of the central block, probably during the Miocene. A wedge of sediments was deposited in the depression.

At Site 1170 we cored one APC/XCB hole, two more with the APC, and a rotary-cored hole (Table 2). Because the suboptimal weather conditions affected the APC coring, construction of a composite section of the triple-cored portion of the sedimentary sequence was possible only to 70 mbsf (early late Pliocene). Beyond that, there are limited gaps, but overall core recovery averaged 90.4%. Hole 1170A reached 464.3 mbsf with 81.8% recovery. Hole 1170B was APC cored to 175.8 mbsf with 102.2% recovery, and Hole 1170C reached 180.1 mbsf with 99.7% recovery. Hole 1170D was rotary cored from 425 to 779.8 mbsf with 81.1% recovery. Wireline logging was conducted over ~540–770 mbsf in Hole 1170D with the triple-combo string, the GHMT-sonic tool string, and the FMS-Sonic tool. Logging was terminated when the drill pipe became stuck in the hole, and the bottom-hole assembly had to be severed with explosives.

Site 1170, with a total sediment thickness of 780 m, ranges in age from the middle Eocene (43 Ma) to the Quaternary. The older sequence consists broadly of ~282 m of rapidly deposited, shallow-water silty claystones of middle and late Eocene age (lithostratigraphic Unit V, see below), overlain by 25 m of shallow-water, glauconite-rich clayey siltstone deposited slowly during the latest Eocene to earliest Oligocene (Unit IV). Unit IV is overlain by 472 m of slowly deposited, deep-water pelagic nannofossil chalk and ooze of early Oligocene through Quaternary age (Units III-I); limestone and siliceous limestone beds are low in the Oligocene section. There is a hiatus of ~4 m.y. in the mid-Oligocene between Units IV and III. The Neogene is almost completely continuous except for a hiatus of ~4 m.y. in the late Miocene.

The lithostratigraphic sequence has been divided into five units and a number of subunits. Lithostratigraphic Unit I (0–93 mbsf), of early Pliocene to Pleistocene age, is a nannofossil ooze with abundant siliceous microfossils. It is generally white with some darker laminations and bioturbation. Carbonate content averages 80%, and organic carbon content is <1%. Average sedimentation rates are low. Deposition was in an open, well-oxygenated ocean in upper abyssal water depths. The considerable kaolinite in the clay fraction may be ancient material derived by increased wind erosion from a more arid Australia.

Lithostratigraphic Unit II (93–373 mbsf) of early Miocene to early Pliocene age has three subunits: Subunit IIA to 181 mbsf, Subunit IIB to 290 mbsf, and Subunit IIC to 373 mbsf. The unit generally consists of white nannofossil ooze or chalk, with more calcium carbonate (average 95%) than Unit I. Organic carbon content is generally very low (<0.5%) between 220 and 270

mbsf. Average sedimentation rates are low. Deposition was in upper abyssal water depths in open-ocean conditions.

Subunit IIA is late early Pliocene to late middle Miocene. It is uniform white nannofossil ooze exhibiting laminations that are light bluish to greenish gray. Subunit IIB is late middle Miocene to early middle Miocene. It is also white nannofossil ooze, but lacks laminations. Subunit IIC is white nannofossil ooze to chalk, with some laminations that are light bluish to greenish gray. The presence of quartz grains in the early middle Miocene supports the evidence from the seismic profiles of a period of increased current activity and scouring (removing all the Oligocene) against the scarp 10 km to the east.

Lithostratigraphic Unit III (373–472 mbsf) is a light greenish gray nannofossil chalk of early early Miocene to earliest Oligocene age. The lower part of the unit (below 446.6 mbsf), which is more clay rich, also contains pale gray clay-bearing limestone with evidence of pressure solution and thin layers of hard siliceous limestone. Calcium carbonate percentages are lower (78 to 93%) than in Unit II. Both calcareous (foraminifers and calcareous nannofossils) and siliceous (diatoms and radiolarians) microfossils are abundant throughout the unit. Organic carbon content is very low, except in the lower part where it reaches ~0.5%. Sedimentation rates are moderate. Paleoenvironmental indicators suggest increasing water depths and more oxygenation from outermost shelf or upper bathyal depths in the lower part of the unit to perhaps lower bathyal depths in the upper part. Although the contact between the limestone and underlying siltstone is very sharp, the sediment character in the lowermost part of the limestone suggests a continued shallow-water influence.

Lithostratigraphic Unit IV (472–497 mbsf) is a dark greenish gray, glauconitic-rich, sandy to clayey siltstone of earliest Oligocene to latest Eocene age. Crystalline quartz, diatoms, and glauconite are very abundant in the upper part of the unit, but decrease downward as it becomes more clayey. About 1.5 m below the top of the unit, there is a break between more sandy and harder sediments above and more muddy sediments below. Calcium carbonate content is very low (5% average, but as much as 10%) and calcareous fossils are rare, whereas organic carbon content is <1%. Carbonaceous fragments and bioturbation are ubiquitous. Sedimentation rates are low. Abundant palynomorphs (dinocysts, spores, and pollen) suggest a cool climate, and temperate forest was on the adjacent land. The clay minerals (illite/smectite) tend to support the evidence of cool climate. The lithologic transition to the underlying sequence is gradational.

Lithostratigraphic Unit V (497–779.8 mbsf) is a bioturbated, dark gray, glauconite-bearing silty claystone to clayey siltstone of late to middle Eocene age that has two subdivisions: Subunit VA to 534.9 mbsf and Subunit VB to 780 mbsf (total depth). Calcium carbonate content is low (<5% on average) and calcareous microfossils are rare. Organic carbon exhibits a steady downward increase from ~0.5% in its upper part to <3.5% in its lower part. Sedimentation rates are high. Palynology and clay minerals (smectite) both suggest that conditions were warm, and rainforests cloaked the nearby land. Dinocysts are present in massive concentrations.

Subunit VA is late Eocene in age. It consists of clayey quartzose siltstone with glauconite-rich intervals and some carbonate. Subunit VB is of late middle Eocene age and consists of silty claystone. Some levels contain abundant small (1 mm diameter) white siliceous tubes. There are occasional occurrences of volcanic glass, solitary corals, bivalves, and pyrite nodules. There are also some decimeter-thick beds of grayish or brownish limestone in the lower part.

Calcareous nannofossils are abundant except in the earliest Oligocene and the Eocene. Planktonic foraminifers and diatoms are abundant down to the middle Miocene, but generally decline below in older sediments. Benthic foraminifers are present, except in the late Eocene, and suggest that water depths were 50–100 m during the middle and late Eocene, and deepened rapidly during the early Oligocene. Dinoflagellate cysts are common down to the late Pliocene, are abundant in earliest Oligocene and late Eocene, and reach massive concentrations in the Eocene. During the middle Eocene, dinoflagellate cysts, diatoms, and nannoplankton show intriguing cycles, thought to be related to differing levels of nutrients (degree of eutrophication), perhaps related to fluctuations in sea level and/or ventilation. Calcareous nannofossils suggest the possibility of two long hiatuses, one in Unit IV (Eocene/Oligocene boundary) and the other in Subunit VB (middle/late Eocene boundary). However, the existence of such hiatuses is refuted by sedimentologic, diatom, and palynologic information.

Sedimentation rates determined from the fossil record were rapid (10 cm/k.y.) during the early rifting phase of the middle Eocene, followed by slow sedimentation and condensed sequences during the late Eocene, slow sedimentation during the early Oligocene (1 cm/k.y.), moderate sedimentation for a brief period during the late early Oligocene (5 cm/k.y.), slow sedimentation from the mid-Oligocene to the early middle Miocene (1 cm/k.y.), rapid sedimentation during the late middle Miocene (4 cm/k.y.), and slow sedimentation to the present day (2 cm/k.y.). There were periods of minimal sedimentation or erosion affecting the late Oligocene and late Miocene sequences.

The geochemistry data show a very sharp change at the base of the carbonates at the Eocene/Oligocene boundary. This sharp change is associated with a diffusion barrier for pore waters and dissolved gases (e.g., methane is abundant below the barrier but absent above). Organic carbon below the barrier averages 0.5% and is dominantly marine in origin. However organic carbon peaks up to 2% in the lower part of the Eocene and appears to have been caused by increased nonmarine input. A variety of evidence suggests that, despite an only slightly higher than normal present-day thermal gradient, the organic matter is nearing thermal maturity. Gases low in the hole are approaching the thermogenic range, and bitumen traces appear to be present. Similar to Site 1168, pore waters become fresher with depth. Determination of the source of the fresher (low Cl^-) waters awaits further work.

The wireline logs covered only Unit VB in the bottom of Hole 1170D because of hole stability problems. However, they show a very clear cyclicity of 4.1 m in the Th log, which awaits more paleontologic certainty before it can be converted into a time series.

Magnetostratigraphy gave better results than at Site 1168, but these were convincing only in the Pliocene-Pleistocene, the middle and late early Miocene, and the latest Oligocene intervals.

The sedimentary succession of Site 1170 records three major phases of paleoenvironmental development.

1. Middle to early late Eocene rapid deposition of shallow-water siliciclastic sediments during rifting between Antarctica and the STR, a time of minimal or no connection between the southern Indian and Pacific Oceans.
2. A transitional interval of slow sedimentation, with shallow-water late Eocene glauconitic siliciclastic sediments giving way suddenly to earliest Oligocene clayey biogenic carbonates, representing the activation of bottom currents as the Tasmanian Gateway opened and deepened during early drifting.
3. Oligocene through Quaternary deposition of biogenic carbonate sediments in increasingly deep waters and in increasingly open-ocean conditions, as the Southern Ocean developed and expanded with the northward flight of the STR and the Australian continent. The sedimentary sequence, in conjunction with information from earlier ODP results, seems to record an integrated history of interplay between decreasing continental influence, rifting and subsidence of the rise, Antarctic cooling, Antarctic Circumpolar Current development, and other related factors.

A question that is being addressed by this and the other nearby sites is why there was such a sharp change from siliciclastic to carbonate sedimentation at the Eocene/Oligocene boundary. A very broad, shallow Australian-Antarctic shelf had been supplied with siliciclastics for tens of millions of years, and, even though rifting, subsidence, and compaction had started early in the Cretaceous, sedimentation kept up, and shallow marine sediments were deposited. In the Tasmanian–STR area there was also subsidence related to the Late Cretaceous opening of the Tasman Sea. Rifting between Australia and Antarctica gave way to almost complete separation of the continents and fast spreading during the middle Eocene (43 Ma). This separation could be expected to increase the rate of subsidence, after a time lag before the thermal anomaly under the margin dissipated. At Site 1170, siliciclastic sedimentation kept up until the Eocene/Oligocene boundary (33 Ma), some 10 m.y. after the onset of fast spreading, even though the local sedimentation rate had declined in the late Eocene. Then, the climate changed quickly, the supply of siliciclastics dropped off further, slow deposition of pelagic carbonate took over, and the sea deepened rapidly. The most likely explanation is that the climatic cooling led to greatly reduced rainfall, weathering, and erosion, and hence to greatly reduced siliciclastic supply. Such changes, from siliciclastic to biogenic sedimentation, appear to be apparent and synchronous wherever ODP drilling has taken place on the Antarctic margin.

In summary, the Eocene siliciclastic sedimentary interval contains a remarkable sequence of abundant organic dinocysts, pollen, and spores in addition to sufficiently persistent calcareous

microfossils to assist with age control. The microfossils will provide an integrated record of terrestrial and shallow-marine paleoclimatic history of the Antarctic continental margin in the middle Eocene through early Oligocene. The Oligocene pelagic biogenic sediments provide a sequence of calcareous and siliceous microfossils for integrated studies of the early development of the Southern Ocean, as the STR both subsided and migrated toward the north. The younger Neogene succession generally contains a sequence of calcareous and siliceous microfossils that are abundant and well preserved throughout and will provide excellent paleoceanographic records.

Site 1171

Site 1171 is located in lower bathyal water depths of ~2150 m on a gentle southwesterly slope on the southernmost STR, ~550 km south of Tasmania and 270 km southeast of Site 1170. At 48°30′S, Site 1171 lies in subantarctic waters between the Subtropical Convergence and the Subantarctic Front. In this area, very strong surface and bottom currents are associated with the Antarctic Circumpolar Current. The major objectives were (1) to core and log an Oligocene to Holocene pelagic carbonate section to evaluate expected major paleoceanographic and paleoclimatic effects resulting from the opening of the Tasmanian Gateway near the time of the Eocene/Oligocene boundary and later development of deep Antarctic Circumpolar Current flow; (2) to core and log an expected underlying detrital sedimentary Eocene sequence to evaluate paleoenvironmental conditions during rifting of the STR from Antarctica; and (3) to obtain high-resolution sedimentary records from critical subantarctic latitudes to better understand the role of the Southern Ocean in climate changes during the Neogene.

Site 1171 is located on thinned continental crust, just west of the strike-slip boundary between the central and eastern STR blocks that moved with Antarctica until 66 Ma. The boundary is the Balleny Fracture Zone, which extends southward to Antarctica. Seismic and other data indicate that during the Late Cretaceous to Paleocene, the blocks themselves were cut by strike-slip faults that developed as Australia moved northwestward, and later northward, past Antarctica. Basins that formed in association with this tectonism are filled with ~1000 to 2000 m of Cretaceous through Eocene rift sediments deposited during steady subsidence.

Site 1171 is in a small north-south oriented rift basin, bounded to the east by the Balleny Fracture Zone. The middle Eocene fast seafloor spreading and opening to the south strengthened the basin's connection to the Pacific Ocean and its difference in setting to that of Site 1170 in the Australo-Antarctic Gulf. Seismic profiles and regional correlations suggest that the site was subject to steady deposition of prograded siliciclastic deltaic sediments through the Cretaceous into the Eocene and hemipelagic sedimentation grading to pelagic sedimentation thereafter (Fig. 14). Much of the siliciclastic detritus must have come from the high, subaerial bounding blocks of continental crust and also along the basin from the higher northern areas. The southwestern tip of the STR cleared Antarctica during the early Oligocene and deep circum-Antarctic circulation became established. Site 1171 was selected because of its extreme southern location on the STR,

in sufficiently shallow water to provide a carbonate sequence unaffected by dissolution. Thus, the site was designed to provide critical data about the subsidence of the STR and on the timing of the initial surface water, and later deep-water flow, through the opening of the Tasmanian Gateway between Australia and Antarctica.

At Site 1171 we cored two APC holes, one APC/XCB hole, and a rotary cored hole (Table 2). Because weather conditions were good during the APC drilling, construction of a composite section of the total triple-cored portion of the sedimentary sequence was possible to 118 mbsf (late Miocene). Beyond that, there are limited gaps, but core recovery averaged 81.8%. Hole 1171A was APC cored to 124 mbsf with 94.5% recovery, Hole 1171B was APC cored to 109 mbsf with 98.1% recovery, and Hole 1171C was APC/XCB cored to 275 mbsf with 89.4% recovery. Hole 1171D was rotary cored from 248 to 959 mbsf with 73.9% recovery. The interbedded hard and soft beds from 265 to 440 mbsf greatly reduced recovery of both XCB and RCB and stopped XCB coring earlier than desired. Because of operational problems, wireline logging was conducted only with the triple-combo string over most of Hole 1171D.

Site 1171, with a total sediment thickness of 959 m, ranges in age from the late Paleocene (58 Ma) to the Quaternary. The Neogene section is largely complete except for a hiatus in the latest Miocene. The Paleogene record from the early middle Eocene to the latest Oligocene is cut by five hiatuses, and the Oligocene is poorly represented. The older sequence consists broadly of ~616 m of rapidly deposited, shallow-water silty claystone of late Paleocene to late Eocene age (lithostratigraphic Units V and VI) overlain by 67 m of diatom-bearing claystone of late Eocene age (lithostratigraphic Unit IV) and 6 m of shallow water, glauconitic siltstone, deposited slowly during the latest Eocene (Unit III). Unit III is overlain by 67 m of slowly deposited, deep-water nannofossil chalk and ooze of early Oligocene to early Miocene age (Unit II); limestone and siliceous limestone beds are low in the Oligocene section. Unit I consists of 234 m of deep-water foraminifer-bearing nannofossil ooze and chalk of early Miocene to Holocene age.

The lithostratigraphic sequence has been divided into six units and a number of subunits. Lithostratigraphic Unit I (0–234 mbsf), of early Miocene to Pleistocene age, has been divided into two subunits: Subunit IA to 41 mbsf and Subunit IB to 234 mbsf. Subunit IA is a white to light gray foraminiferal nannofossil ooze and foraminifer-bearing nannofossil ooze, whereas Subunit IB is a nannofossil ooze and chalk, which is distinguished from Unit IA by decreasing content of foraminifers. Carbonate content averages 93% and organic carbon is very low (<0.2%) in Unit I. In general, calcareous and siliceous microfossils are abundant. Average sedimentation rates were low.

Lithostratigraphic Unit II (234–270 mbsf), of late Oligocene age, is a white to light greenish gray nannofossil chalk characterized by a downsection increase in the detrital components (e.g., glauconite, quartz, and mica) and a decrease in the biogenic fraction. Organic carbon content is low. Carbonate content decreases from 95% at the top to 75% at the base. Sedimentation rates were very low.

Lithostratigraphic Unit III (270–276 mbsf) is ~6 m of dark greenish gray to blackish green glauconitic sandy to clayey glauconitic siltstone of late Eocene age. Carbonate content decreases from 77% at the top of the unit to 0.4% at the base. Organic carbon content is extremely low, approaching zero.

Lithostratigraphic Unit IV (276–343.5 mbsf), of middle to late Eocene age, is a nannofossil-bearing, diatomaceous silty claystone that darkens downsection from olive gray to dark gray and bottoms in a black chert. Carbonate content is low (5%) and organic carbon averages 0.4 wt%.

Lithostratigraphic Unit V (343.5–692.5 mbsf) is composed of claystones and silty claystones of middle Eocene age and is divided into three subunits. Subunit VA consists of dark greenish gray or dark olive gray claystone and nannofossil-bearing claystone. Carbonate content averages 14%, and organic carbon is 0.5%. Subunit VB is a dark gray claystone, occasionally organic-matter–bearing, and is distinguished from Subunit VA by the lower nannofossil abundance, darker color and higher organic matter content (average = 1%). Carbonate content is very low (1%). Subunit VC is olive gray and dark olive gray silty claystone with higher nannofossil abundance and lower organic matter (0.5%) than the overlying subunit. Carbonate content averages 8%. Sedimentation rates fluctuated between 4–12 cm/k.y.

Lithostratigraphic Unit VI (692.4–958.8 mbsf) is early Eocene to late Paleocene in age and has been divided into two subunits. Subunit VIA is lower Eocene greenish gray nannofossil-bearing silty claystone in the upper part and silty claystone in the lower part. Carbonate nodules and pressure seams are sporadic through the interval. Carbonate content is low, averaging 2%, and organic carbon is 0.5%. Subunit VIB is lowermost Eocene to upper Paleocene silty claystones that gives way to dark grayish brown, organic matter-bearing clayey siltstones in the lower part. The bottom ~40 m of the subunit contains pervasive laminations. Carbonate content is <1% and organic carbon content (0.9%) is higher than in Sububit VIA. Sedimentation rates averaged 4 cm/k.y.

In general, calcareous nannofossils are abundant in the Neogene and Oligocene, highly variable in abundance in the Eocene (where they are also absent in many intervals), and rare in the Paleocene. The Neogene and Oligocene are marked by highly abundant and well-preserved calcareous nannofossils and planktonic foraminifers and relatively abundant radiolarians and diatoms. In contrast, the Eocene has many intervals barren of calcareous microfossils, especially planktonic foraminifers. Radiolarians and diatoms are rare to absent throughout much of the Eocene, although neritic planktonic and benthic diatoms are present in the late Eocene. The shallow-water Eocene siliciclastics are distinguished by a continuous record of abundant organic dinoflagellate cysts and pervasive pollen and spores, which are critical for biostratigraphic subdivision of this interval and provide a richness of paleoenvironmental information. The Paleocene sediments also contain abundant assemblages of organic palynomorphs, but only rare to few calcareous nannofossils. Planktonic foraminifers, radiolarians, and diatoms are absent. Benthic foraminifers, which have provided critical information on benthic environments, are largely present throughout the entire sequence and are noticeably more abundant in the Eocene.

Sedimentation rates determined from the fossil record were rapid (4–12 cm/k.y) during the Paleocene to middle Eocene. Biostratigraphic datums indicate four brief hiatuses (~2 m.y.) interspersed with brief periods of slow sedimentation (<1 cm/k.y.) through the late Oligocene to the middle Eocene. Sedimentation rates were low, fluctuating between 0.7–2.0 cm/k.y. in the early and middle Miocene, increased to 3.8 cm/k.y across the middle/late Miocene boundary, and decreased again to a very low 0.5 cm/k.y. in the late Miocene. The Miocene/Pliocene boundary is marked by a hiatus of at least 1.6 m.y., followed by slow sedimentation (1.3 cm/k.y.) in the Pliocene-Pleistocene.

A major result of the coring was the discovery that the unconformity separating flat-lying strata from gently dipping strata in seismic profiles corresponds to the Paleocene/Eocene boundary. This means that tectonism in this small basin, bounded by the major strike-slip fault system of the Balleny Fracture Zone, ended at ~55 Ma. This strongly suggests that the driving force for the strike-slip motion, the separation of Australia and Antarctica, no longer affected this part of the STR from that time, accurately defining the age of the onset of seafloor spreading to the south as 55 Ma.

Similar to Site 1168 on the west Tasmania margin, and Site 1170 on the eastern STR, pore-water freshening (13% decrease in Cl^- relative to seawater) is also observed at Site 1171 below ~320 mbsf, which is coincident with the onset of methanogenesis, but unexpectedly below the observed bottom-simulating reflector. Organic matter is immature through most of the cored interval, with maturity increasing with depth. However, toward the base of the cored interval organic matter is mature, and gases have a thermogenic signature, although gas quantities are low. Characterization of the organic matter (hydrogen index) indicates three intervals of upwardly increasing marine influence in the early to middle Eocene.

The wireline logs were confined to a single complete run of the triple-combo tool in Hole 1171D because of technical and hole stability problems. Logging data appear to be strongly cyclic, especially the Th spectrum of the natural gamma-ray log in the middle Eocene section. Variability in log data also may be recording alternating marine and terrestrial influences. Distinct spikes in resistivity and density are observed in middle Eocene sediments, which likely correlate with indurated carbonates and/or glauconite and tend to be directly above peaks of Th and K, indicating increased input of terrestrial clays.

The depositional history of the Paleogene (late Paleocene through Oligocene) is one of increasing ventilation and a major, rapid increase in water depths that began to occur near the Eocene/Oligocene boundary causing transformation from shallow (neritic) to deep open-ocean conditions. Late Paleocene sediments were deposited in near anoxic conditions in near-shore highly sheltered environments, with resulting high organic carbon content. Neritic environments of the early to middle Eocene show evidence of being less restricted as reflected by pervasive, well-developed sediment bioturbation and increasing abundance of calcareous nannofossils.

The Eocene–Oligocene transition at Site 1171 is marked by a series of distinct step-wise environmental changes, reflecting increasingly cool conditions and coeval rapid deepening of the

basin. By the earliest Eocene, a change had occurred from inner neritic environments with fresh-water influences and sluggish circulation, to outer neritic environments with increased ventilation and bottom-current activity. Concomitant cooling is indicated by episodic increases of endemic Antarctic dinocyst taxa, a trend that continues through the late Eocene to earliest Oligocene (~34.0–33.3 Ma). Sediments and biota indicate increasing bottom-water ventilation and more productive surface waters at slightly deeper depths (outer neritic to upper bathyal depths), with increasingly cold conditions. This trend culminates in the early Oligocene (33–30 Ma) with distinct increase in open-ocean upwelling and rigorous ventilation that precluded accumulation of organic matter, despite the overall higher surface water productivity. At this time, slow deposition of silica-rich calcareous sediments commenced in lower bathyal depths.

As at Site 1170, the sedimentary succession of Site 1171 records three major phases of paleoenvironmental development that are consistent with the hypothesis that initial development and evolution of the cryosphere during the middle and late Cenozoic resulted from thermal isolation of the Antarctic by the development of the Antarctic Circumpolar Current and the Southern Ocean.

1. Late Paleocene to early late Eocene rapid deposition of shallow-water (neritic) siliciclastic sediments during rifting between Antarctica and the STR. This was a time of minimal or no connection between the Pacific Ocean, in which these sediments were deposited, and the Australo-Antarctic Gulf in the southern Indian Ocean.
2. A relatively brief transitional interval of slow sedimentation with shallow-water late Eocene glauconitic siliciclastic sediments giving way suddenly to earliest Oligocene deeper water clayey biogenic carbonates. Deposition of the glauconitic sediments represents initiation of moderate current activity as the Tasmanian Gateway opened to shallow (neritic) waters. Deposition of the overlying carbonates heralds the development of open-ocean conditions in the Gateway and initiation of circumpolar circulation.
3. Oligocene through Quaternary deposition of pelagic carbonate sediments in increasingly deep waters and in increasingly open-ocean conditions as the Southern Ocean developed and expanded with the northward flight of the STR and the Australian continent.

Although the history of sedimentation at Sites 1171 and 1170 exhibits the same broad regional trends, strong evidence exists that, up until the late Eocene, they accumulated sediments in separate basins isolated by the Tasmanian land bridge. This is most clearly shown by the poorly ventilated environment of deposition at Site 1170 vs. the relatively more ventilated environment at Site 1171. This is consistent with the interpretation of more restricted environmental conditions in highly restricted marine conditions at the easternmost end of the

Australo-Antarctic Gulf, as is also suggested by the Eocene sediment record at Site 1168 off western Tasmania.

Climatic implications resulting from interpretations of data from Site 1170 and other locations on the STR include the following:

1. The rapid transformation from Eocene siliciclastic sediments to Oligocene pelagic carbonates near the Eocene/Oligocene boundary in the STR region seems to have resulted largely from major cooling of Antarctica that caused greatly reduced rainfall, weathering, and erosion and, hence, greatly reduced siliciclastic supply. Siliciclastic sediment starvation appears to have occurred broadly at this time around the Antarctic margin.
2. No evidence for glaciation has yet been observed in the Oligocene sediments of Sites 1171 and 1170, the two southernmost sites drilled during Leg 189. This and other supporting evidence suggests that this margin of the Antarctic was warmer than other sectors.
3. A strong meridional climatic gradient appears to have existed during the Oligocene between the STR margin of Antarctica and the Ross Sea at Cape Roberts (77°S), where early Oligocene diamictites were deposited (Cape Roberts Science Team, 2000).
4. Antarctica was clearly marked by strong regional climatic differences during the Oligocene, well before a unifying circumpolar influence had developed in the Neogene.
5. It is unlikely that continent-wide ice sheets of proportions typical of the Neogene developed in the Oligocene.

Site 1172

Site 1172 is located in a water depth of ~2620 m on the flat western side of the ETP, ~150 km southeast of Tasmania. At 44°S, the site lies in cool subtropical waters just north of the Subtropical Front in an area where both the Subtropical Front and the East Australian Current have had variable influence through time. The primary objectives of coring and logging at Site 1172 were to obtain in the far southwest Pacific (1) an Oligocene to Holocene pelagic carbonate section under long-term influence of the East Australian Current to construct moderate to high-resolution paleoceanographic and biostratigraphic histories, (2) an Eocene siliciclastic sediment sequence for better understanding of paleoceanographic and paleoclimatic conditions before Antarctic Circumpolar Current development, (3) an Eocene–Oligocene transitional sequence to determine effects of the initial opening of the Tasmanian Gateway on the paleoceanography of the Pacific Tasmanian margin, and (4) to compare and contrast changing paleoenvironmental and paleoceanographic conditions on each side of Tasmania as the Tasmanian Seaway opened and the Antarctic Circumpolar Current developed. This site was also expected to provide valuable

information about the tectonic history of the ETP, including evolution of an inferred volcanic hot spot in the Eocene.

Site 1172 is on thinned continental crust on the western side of the ETP. The plateau is roughly circular, 200 km across, lies in water depths of 2200–2800 m, has Late Cretaceous oceanic crust on three sides, and is attached to Tasmania to the northwest. During the middle Eocene, the ETP was at ~65°S when its fast movement (55 km/m.y.) north with Australia commenced. Continental basement rocks form its margins, and seismic profiles and other evidence suggest that at the site they are overlain by gently dipping Cretaceous sediments and flat-lying Cenozoic sediments. The late Eocene Cascade Seamount is a guyot in the middle of the plateau consisting of basaltic volcanics and volcaniclastics.

At Site 1172 we cored two APC holes, one APC/XCB hole, and a rotary cored hole. Because weather conditions were good during the APC drilling, construction of a composite section of the total triple-cored portion of the sedimentary sequence was possible to 146 m composite depth (mcd) (late Miocene) (Table 2). Beyond that, there are limited gaps, but core recovery averaged 92%. Hole 1172A was APC/XCB cored to 522.6 mbsf with 92.6% recovery. Hole 1172B was APC cored to 206.7 mbsf with 102.1% recovery. Hole 1171C was APC cored to 171 mbsf with 100.9% recovery. Hole 1172D was rotary cored from 344 to 373 mbsf, drilled to 497 mbsf, and cored to 766 mbsf with 80% recovery. Despite heave of up to 10 m, wireline logging was conducted over most of Hole 1172D with successful runs of the triple-combo tool string and the GHMT-sonic tool string. However, the heave was too great to run the FMS tool string.

The results significantly changed our precruise understanding of the history of the ETP, with much older sequences being cored at the site than expected. Site 1172 penetrated ~65 m of black shallow-marine mudstones of latest Cretaceous (Maastrichtian) age (Fig. 15). This was overlain by 335 m of Paleocene and Eocene brown, green, and gray shallow-marine mudstones and 364 m of Oligocene and Neogene pelagic carbonates. The pelagic carbonates were deposited in ever-increasing depths after rapid Oligocene subsidence, and much of the Oligocene and early Miocene sections are missing because of current action. A series of volcanic ash horizons of late Eocene to Oligocene age suggest that the volcanism that formed the Cascade Seamount continued for at least 5 m.y. The lithostratigraphic sequence has been divided into four units, with three subunits in Unit I and two subunits in Units III and IV.

Lithostratigraphic Unit I (0–355.8 mbsf), of early Miocene to Pleistocene age, is divided into three subunits: Subunit IA to 70 mbsf, Subunit IB to 271.2 mbsf, and Subunit IC to 355.8 mbsf. Subunit IA is a white foraminifer nannofossil ooze and foraminifer-bearing nannofossil ooze, whereas Subunit IB is a white and light greenish gray nannofossil ooze. The two subunits are distinguished mainly by a decrease in foraminifer content in Subunit IB. Subunit IC is a white, pale yellow, and light gray foraminifer-bearing nannofossil chalk characterized by an increase in the foraminifer content and increasing minor components of clay and volcanic glass. Calcium carbonate content increases from 80% in Subunit IA to 97% in Subunit IB and decreases in Subunit IC to 90%.

Lithostratigraphic Unit II (355.8–361.12 mbsf) is a thin transitional unit of latest Eocene to Oligocene age. The sediments are mainly characterized by increased glauconite and a decrease in nannofossils and consist of variations of greenish gray glauconite-bearing silty diatomaceous claystone and dark greenish gray glauconitic diatomaceous clayey siltstone. A distinct surface at 357.27 mbsf is characterized by abundant glauconite and rip-up clasts above and by angular clasts below. This transition may be a highly condensed section or a hiatus. Carbonate content decreases from 69% at the top to 0.3 % at the base.

Lithostratigraphic Unit III (361.12–503.4 mbsf), of late to middle Eocene age, has been divided into two subunits: Subunit IIIA to 433.89 mbsf and Subunit IIIB to 503.4 mbsf. Subunit IIIA is a greenish gray and dark brownish gray diatom- and nannofossil-bearing claystone and a very dark grayish brown diatomaceous claystone. Subunit IIIB is a dark gray to dark olive-gray diatomaceous silty claystone. The two subunits are distinguished by calcium carbonate content averaging 10% in Subunit IIIA and very low values, approaching zero, in Subunit IIIB.

Lithostratigraphic Unit IV (503.4–766.5 mbsf) is Late Cretaceous to early Eocene in age and is divided into two subunits: Subunit IVA to 695.99 mbsf and Subunit IVB to 766.5 mbsf. Subunit IVA is a middle Eocene to Paleocene olive-gray claystone with minor amounts of silty claystone, nannofossil-bearing claystone, and clayey siltstone. The subunit is distinguished from Unit III above by a lack of siliceous microfossils and an increase in opaque and accessory minerals, which reach a maximum of 15% at 542 mbsf. Subunit IVB is of Cretaceous (Maastrichtian) age and is a very dark olive-gray, very dark gray, and black claystone and silty claystone. It is distinguished from Subunit IVA by its darker color, less bioturbation, less glauconite grains, and more organic matter. Sedimentological studies suggest that the Cretaceous/Tertiary boundary is at 695.99 mbsf, where a distinct lithologic change occurs at the subunit boundary, from brown and highly bioturbated silty claystone above to black massive claystone below. Carbonate is generally very low with a maximum of 6.5 wt% at 762.9 mbsf.

Microfossils are present throughout the entire Cenozoic and upper Cretaceous sequence with dominance of different groups drastically changing with sedimentary environments. Siliceous microfossils are rare to absent in the Quaternary to Pliocene interval, but are common to abundant and well preserved in the Miocene. The thin Oligocene succession yielded few radiolarians, whereas diatoms remained abundant downhole. Both groups are common to locally abundant in the Eocene with good preservation. The upper Paleocene to upper Maastrichtian interval is virtually barren of siliceous microfossils. Planktonic foraminifers and calcareous nannofossils are generally abundant in the Neogene and Oligocene, with preservation ranging from moderate to good. Although less abundant, calcareous nannofossils remain consistently present until the middle Eocene, when abundance and preservation decrease dramatically. Below the middle Eocene, the Cenozoic succession is barren of calcareous nannofossils. Planktonic foraminifers are virtually absent below the middle/late Eocene boundary. Well-preserved and reasonably diversified calcareous microfossils are present in the upper Maastrichtian. Calcareous benthic foraminifers are consistently present throughout the Neogene–Oligocene carbonate

succession. The middle Eocene sequence yields only rare agglutinating species. However, calcareous and agglutinating taxa are present in the Paleocene to upper Maastrichtian succession. Well-preserved organic-walled dinoflagellate cysts (dinocysts) and few sporomorphs are present in the Quaternary. The remaining Neogene to lower Oligocene strata are devoid of acid-resistant organic matter. Moderate to well-preserved dinocysts are the dominant constituent of palynological associations in the upper Paleocene to lowermost Oligocene and are persistent below this interval. Well-preserved terrestrial palynomorphs dominate upper Maastrichtian to middle Paleocene sediments.

Changes in sedimentation rates exhibit three distinct phases in the sequence. In contrast to other Leg 189 sites, sedimentation rates were relatively low (between 2.6 and 1.04 cm/k.y.) in the Paleogene interval (and Maastrichtian) through the late Eocene. From the late Eocene through the middle Miocene (15 Ma) sedimentation rates decrease (0.16 to 3.2 cm/k.y) and then increase again until the present day. These three intervals coincide with, and are probably related to, the succession in global climate change from "Greenhouse" to "Doubthouse" to "Icehouse." Site 1172, like Site 1168, appears to have been strategically located to sensitively record these overall shifts in global climate associated with the development of the Antarctic cryosphere. The higher rates of sedimentation during the early Paleogene and late Neogene resulted from more stable climatic conditions. These were associated with the early Paleogene "Greenhouse" world lacking any significant Antarctic cryosphere and the late Neogene "Icehouse" world marked by a permanent Antarctic ice sheet. Reduced sedimentation rates during the middle Cenozoic at Site 1172 were associated with more highly variable climatic conditions leading to higher rates of deep-sea erosion. The lower-than-normal regional rates of sedimentation during most of the Paleogene at Site 1172 may have resulted from pervasive, but gentle sediment winnowing in shallow waters by the East Australian Current. Relatively higher rates of sedimentation in the late Neogene probably resulted from higher marine productivity caused by stimulation of surface-water circulation upon expansion of the Antarctic cryosphere in the middle Miocene.

The geothermal gradient is lower at this site than in the other Leg 189 sites. Despite TOC contents that are similar to other Paleogene sequences at earlier sites (0.5–1.0 wt%), complete sulfate reduction is not observed and only traces of methane are present. Organic matter is less mature thermally and more labile; however, there is evidence of bitumen in the older siliciclastic sediments, which may indicate the migration of hydrocarbons from below the drilled section. As at other sites, the presence of fresher pore waters was observed on the ETP, which indicates the regional extent of these low chloride fluids.

The sedimentary succession of Site 1172 is similar to that in the other Leg 189 sites in recording three major phases of paleoenvironmental development:

1. Maastrichtian to early late Eocene deposition of shallow-water siliciclastic sediments during rifting between Antarctica and the STR, a time of minimal or no connection between the Pacific Ocean and the southern Indian Ocean.

2. A transitional interval of slow sedimentation, with shallow-water late Eocene-age glauconitic siliciclastic sediments giving way suddenly to earliest Oligocene-age deep-water clayey pelagic carbonates representing the activation of bottom currents as the Tasmanian Gateway opened and deepened during early drifting.
3. Oligocene through Quaternary deposition of pelagic carbonate sediments in increasingly deep waters and more open-ocean conditions as the Southern Ocean developed and expanded with the northward flight of ETP and the Australian continent.

The sediment succession at Site 1172 generally reflects an upward increase in ocean ventilation. Like the other sites drilled during Leg 189, this resulted from a fundamental change in paleogeography associated with increasing dispersal of the southern continents and the opening up of the ocean basins at high latitudes in the Southern Hemisphere. Thus, the sluggish ocean circulation and restricted environments of sedimentation of the Late Cretaceous and early Paleogene were eventually replaced by well-ventilated open-ocean conditions of the later Cenozoic.

The Paleocene to middle Eocene was relatively warm based on the character of dinocyst assemblages. Terrestrial palynomorphs, also indicative of warm conditions, are especially abundant in the lower Paleogene (Paleocene–early Eocene) sediments. Assemblages suggest especially shallow water and restricted conditions at this time with marked runoff. An absence of foraminifers, and even nannofossils, in most parts of the Paleocene to middle Eocene confirms the attribution to marginal marine settings. Maastrichtian sediments were deposited in more open-ocean conditions based on higher abundances of calcareous microfossils and more offshore dinocyst assemblages.

The middle/late Eocene boundary is marked by a change from inner neritic depositional environments with marked freshwater influence and sluggish circulation to more offshore, deeper marine environments with increased ventilation and bottom-water current activity. Concomitant cooling is indicated by the increased numbers of endemic Antarctic dinocyst species, whereas warmer episodes are also recognized. The Eocene–Oligocene transition (~34.0–33.3 Ma) is marked by a series of distinct stepwise environmental changes reflecting increasingly cool conditions and coeval rapid deepening of the basin. Sediments and biota indicate increasing bottom-water ventilation and the appearance of conditions supporting highly productive surface waters, in outer neritic to bathyal depositional settings, with increasingly cold conditions. This trend culminates in the early Oligocene (33–30 Ma) when rigorous ventilation, and generally oxygen-rich waters, precluded sedimentation of organic matter despite overall high surface-water productivity. The condensed calcareous sequence contains abundant siliceous microfossils and was deposited in an oceanic bathyal environment. Oligocene to present-day pelagic carbonates were deposited in well-ventilated open-ocean conditions.

Although Site 1172 reflects the broad patterns of Cenozoic sedimentation for the Tasmanian region, differences are almost certainly related to the site's position astride the East Australian Current. A distinct increase in neritic diatoms during much of the middle Eocene appears to reflect higher productivity in this current than elsewhere on the Tasmanian margin. Increased productivity may have resulted from increased nutrient input into neritic environments swept by the East Australian Current as it moved south adjacent to Australia. A distinct upward increase in kaolinite (and illite) following the middle Miocene (~15 Ma) may reflect the increasing aridity of Australia and the transport of clays into the East Australian Current as it was swept southward along the Australian margin.

A complete composite-core record was successfully obtained for the last ~8 m.y. The successful drilling of Site 1172 capped off a highly productive and satisfying coring campaign in the Southern Ocean. Much was learned at sea and postcruise research is expected to further contribute significantly toward understanding of Southern Ocean and Antarctic environmental development and its role in Cenozoic global climate change.

SUMMARY OF RESULTS

Lithostratigraphy

We recovered a range of biogenic and siliciclastic sediments from the latest Cretaceous to Quaternary (Fig. 16), including the interval of sediments recording the seaway opening south of Australia showing the development of Southern Ocean circulation. The sedimentary sequences allow recognition of three distinct phases of sedimentation (a siliciclastic interval, a transitional unit, and a biogenic carbonate sequence) and three sedimentary provinces (the more restricted west Tasmanian margin [Site 1168], the transitional STR [Sites 1169, 1170, and 1171] and the more ventilated ETP [Site 1172]).

The siliciclastic sequence extends from the late Maastrichtian (drilled on the ETP) to the late Eocene and consists of shallow-water silty claystone and clayey siltstone for the entire Tasmanian region. The siliciclastics are associated with abundant neritic diatoms from the middle Eocene in the Pacific region of the ETP. The sediment is enriched in organic matter in the poorly ventilated western Australo-Antarctic Tasmanian region. Such siliciclastics are widespread on the margins of Australia and Antarctica and have been observed from the Eocene Great Australian Bight (Feary, Hine, Malone, et al., 2000) to the Ross Sea Margin near Cape Adare (Hayes, Frakes, et al., 1975).

The initiation of the transitional unit coincides with the preservation of abundant neritic diatoms in the upper Eocene on the STR, followed by the occurrence of glauconitic siltstones and sands throughout the Tasmanian region. This is indicative of greater bottom-water activity near the Eocene/Oligocene boundary. Siliciclastic sediments decrease rapidly above the glauconitic interval in the lowermost Oligocene of the ETP and the STR but persist in the early Oligocene of the west Tasmanian margin (until ≈ 31 Ma.).

The STR and the ETP pelagic carbonate sequence starts abruptly with the first occurrence of nannofossil chalk and limestone in the lowermost Oligocene. The STR sequence also contains common to abundant siliceous microfossils. On the west Tasmanian margin, the pelagic carbonates increase progressively in the lower Oligocene and consist of almost-pure nannofossil chalk by the middle Miocene. The pelagic carbonate ooze contains increased foraminifers and clay content in the whole Tasmanian region from the late Pliocene to the Pleistocene.

Tectonics and Sedimentation

The upper Paleocene and lower Eocene sediments on the STR decrease in grain size upsection as the clay assemblage evolves from a complex assemblage of kaolinite, illite, and smectite to predominant smectite. This pattern reflects decreased erosion and continental relief at the end of the stage of tectonic activity that led to the formation of transtensional basins from Antarctica to much of the STR.

Beginning in the late middle Eocene, increasing grain size of the shallow-marine siliciclastics on the STR and west Tasmanian margin, together with a clay assemblage dominated by illite and kaolinite, resulted from erosion of steep-continental relief. This interval correlates with a stage of late middle and late Eocene tectonism resulting from increased spreading in the Australo-Antarctic Gulf, and strike-slip activity on the western STR. This stage of tectonism ultimately led to a final separation of Australia from Antarctica. The presence of volcanic glass on the Pacific side of the Tasmanian region and ash layers on the ETP indicate that the late Eocene interval of tectonism was associated with intensified volcanic activity that may have persisted into the early Oligocene. How much of this volcanism was associated with the presumed hot spot volcano of Cascade Seamount on the ETP and how much was related to the general tectonism remains to be determined.

Environment of Sedimentation

Extensive bioturbation of the entire late Maastrichtian- to late Eocene-age sequence on the ETP and of Eocene sediments on the STR indicates significant ventilation of bottom waters. However, the absence of carbonate microfossils and the presence of siliceous microfossils suggest that major dissolution occurred and may have been associated with restricted environmental conditions. Darker sediment colors and decreased bioturbation on the western STR, together with abundant organic matter and intervals of lamination on the western Tasmanian margin, indicate poor ventilation of the Australo-Antarctic Gulf during the middle and late Eocene. Anoxic to suboxic conditions prevailed in the sheltered troughs of the Tasmanian margin. Abundant latest Eocene-age glauconite includes foraminifer infillings indicative of in situ formation. Widespread glauconite in the entire Tasmanian region indicates strong bottom-current activity and winnowing at shelf water depths.

Bottom-water ventilation increased sharply in the earliest Oligocene, producing the light-colored sediments of the ETP and the STR, whereas ventilation increased slowly from the early

Oligocene to the middle Miocene on the western Tasmanian margin as attested by the persistence of laminations and weak bioturbation. The predominance of pelagic carbonates from the earliest Oligocene is unusual at southern high latitudes. The carbonates are likely related to the warm marine influence of subtropical currents transporting heat to the Tasmanian region. This is in sharp contrast with the Ross Sea margin (Site 274), then adjacent to the STR, where biosiliceous microfossils have been predominant since the Oligocene (Hayes, Frakes, et al., 1975).

Climate and Sedimentation

No glacial or ice-rafted deposits were found at any site, even in Oligocene sediments when the Tasmanian region was still close to Antarctica, indicating the absence of significant ice cover in nearby East Antarctica. Smectite or kaolinite dominates in most Eocene sediments of the entire Tasmanian region, indicating that warm climates prevailed on emerged adjacent areas of the Tasmanian land bridge and Antarctic margin. An increasing trend of illite and random mixed-layered clays in the lower Oligocene of Site 1170 on the western STR suggests the development of physical weathering on the adjacent emerged areas, like that in other sectors of East Antarctica (Ehrmann, 1991; Robert and Kennett, 1997). This trend immediately follows the strike-slip activity on the western STR during the transition to the more ventilated biogenic sequence.

The continued presence of common to abundant kaolinite on the western Tasmanian margin and the ETP from the lower Eocene to the Pliocene indicates the persistence of relatively warm climates with significant precipitation in the adjacent coastal areas of Australia. Episodes of increased kaolinite content on the western Tasmanian margin in the lower Oligocene and in the upper to middle Miocene correlate with intervals of intensified precipitation at midlatitudes. The early to middle Miocene interval immediately preceded the expansion of Antarctic ice at 14–15 Ma (Kennett, 1977). Kaolinite on the ETP increased continuously from the middle Eocene to the Pliocene as Australia moved north to warmer latitudes. Beginning in the Pliocene, an increase in the sediment clay fraction is associated with a mineralogical change to increased illite and kaolinite, a composition very similar to that in different latitudes of the Lord Howe Rise in the Tasman Sea. This pattern suggests the development of a dust supply from arid central Australia, most probably by tropospheric winds associated with cold fronts (Pye, 1987).

There are pervasive alternations of lighter and darker intervals from the Eocene to the Pleistocene in the entire Tasmanian region. Preliminary spectral analyses have been conducted on lightness and magnetic susceptibility data from the west Tasmanian margin during a chronologically well-constrained Pliocene–Pleistocene interval. Three important cycles of ~200, 100, and 40 k.y. may indicate some orbital control on regional sedimentation. High sedimentation rates of the STR during the Eocene suggest that some variation of the sedimentation at higher frequencies (104–105 yr) might be expected.

Biostratigraphy

Leg 189 has provided a wealth of new and exciting biostratigraphic and paleoenvironmental information in a part of the Southern Ocean that is critical to understanding Earth's Cenozoic history. We drilled five sites in the Tasmanian region, north and south of the Subtropical Convergence, and in the Indian and Pacific Ocean sides of the STR (Fig. 17). The recovered record spans the Late Cretaceous to Quaternary (Fig. 18) but is commonly punctuated by a late Miocene hiatus and a possible Eocene–Oligocene hiatus (Fig. 19). The integrated microfossil record from all five sites will help unravel the southern history of the East Australian Current, which bathed the Pacific Ocean sites, and also the history of the "Proto-Leeuwin" Current, which bathed the Indian Ocean sites. The activity of both of these currents brought warmer waters to the study area, resulting in markedly different faunal associations when compared with other circum-Antarctic sites (e.g., Leg 113). The late Miocene hiatus is marked by a strong dissolution event in the foraminifers and is restricted to the southernmost sites (Sites 1169, 1170, and 1171), though strong fragmentation of foraminifers was also observed at Sites 1168 and 1172. The transition from "Greenhouse" to "Doubthouse" is strikingly seen at four of the five sites (Fig. 19). The latest Eocene to earliest Oligocene period of slow sedimentation (~1 cm/k.y.), which may be continuous or marked by hiatuses, records the history of this dramatic change in Earth's history. Five major microfossil groups are represented over this interval and provide the opportunity for shore-based collaboration to elucidate the details of this event. At Site 1172, a thick sequence of upper Cretaceous to Eocene fine-grained mudstones of the "Greenhouse" period, often glauconitic and organic rich, contains a continuous dinocyst record. Sporadic calcareous nannofossils and planktonic and benthic foraminifers through this interval will provide age control, as well as paleodepth information.

The planktonic foraminiferal distribution reflects the northward drift of Australia during the Cenozoic. For the Paleogene, because of the southern location of Australia at that time, the subantarctic zonal scheme was used in place of the traditional temperate scheme. This temperate scheme was appropriate for the late Paleogene and Neogene. In addition, the Neogene faunas reflect changing paleoceanography throughout the "Icehouse" period in their diversity, preservation, and phylogeny. The expanded Oligocene and Neogene section of the two northern sites (with sedimentation rates between 1.7 and 4.3 cm/k.y.), and of Site 1168 in particular, means that a standard biostratigraphic section can be established for the shelfal and land exposures to the north (this applies also to the other microfossil groups). The *Globoconella* group is widely distributed through the Neogene section and phylogenetic studies coupled with paleoceanographic results should provide an improved planktonic foraminiferal biostratigraphy for the region. The low-diversity planktonic foraminiferal assemblages of the Late Cretaceous and Paleogene are generally very well preserved, but their abundances are low.

Benthic foraminifers at all sites show a clear change between neritic water depths in the Cretaceous to Eocene interval and deeper waters of the Oligocene and Neogene. At all sites except one (Site 1168), subsidence across the Eocene/Oligocene boundary appears to be a rapid

event, whereas the trend at Site 1168 is more gradual. However, this site is the only one with an expanded Oligocene sequence. Benthic foraminiferal assemblages indicate a more pronounced regional influence in the Eocene, whereas low-resolution sampling across the Oligocene and Neogene suggests that the general trends at all sites are similar for the Neogene, with only Site 1168 showing clear differences throughout the Oligocene.

The Neogene standard nannofossil zonal scheme and the Paleogene nannofossil zonation for the Southern Ocean were successfully applied to Leg 189 sites to provide some of the most useful subantarctic temperate biostratigraphic records to date. In particular, the Oligocene to Pliocene interval is among the most detailed of the Southern Ocean sites of similar latitudes. This sequence will serve as an important reference section for the Southern Hemisphere. Eocene through lower Oligocene nannofossil assemblages at Leg 189 sites show warmer-water characteristics than comparable paleolatitude sites in other sectors of the Southern Ocean (Sites 512, 513, 699, 703, and 747), which reflects the activity of the warm-water Proto-Leeuwin and the East Australian Currents.

Diatoms are abundant in Oligocene to Quaternary sediments at all sites drilled during Leg 189, except Site 1168, and will be used to construct the first calibrated Oligocene–Holocene diatom biostratigraphy south of Australia. In particular, high-resolution biostratigraphy looks especially promising for Sites 1170 and 1171. Integration with other Paleogene and Neogene diatom biostratigraphies being developed from recent ODP legs to the Southern Ocean (e.g., Leg 177) will contribute to a scheme applicable to northern parts of the Southern Ocean. Neritic diatoms are prolific in upper Eocene and lowermost Oligocene sediments at Sites 1170, 1171, and 1172. In conjunction with dinocysts, they will be useful for reconstructing paleoenvironmental conditions across the Eocene/Oligocene boundary including productivity (trophic status), water energy levels, relative salinity, and sea level for both the Indian and Pacific Oceans. During the early Oligocene, the marked floral changes and increased diversity within Sites 1170, 1171, and 1172 imply increasing oceanic influence and productivity. The Neogene diatom floras indicate fluctuations in the influence of warm-temperate and subantarctic water masses over Site 1170, heralding meridional shifts in the position of the Subtropical Convergence as well as the presence of the Proto-Leeuwin Current. At Site 1172, similar fluctuations may signal variations in the influence of the East Australian Current.

Radiolarians are well represented at all sites except Site 1168, although diversity varies through the sequences. The subantarctic radiolarian biostratigraphic sequence from the middle Eocene through Pleistocene is unique and will provide an important contribution to this group's biostratigraphy in the form of a new zonation. This will provide a linkage between the tropical and Antarctic biostratigraphies. There is a near absence of age-diagnostic species from the Antarctic and tropical realms in the Tasmanian region. The radiolarian faunas from Leg 189 also provide an insight into radiolarian evolution.

The dinoflagellate-cyst studies have provided a number of surprises. The first Neogene and Oligocene dinocyst record of the Southern Ocean was discovered at Site 1168, with excellent

calibration. These microfossils are massively abundant and, with sporomorphs, are common in the Upper Cretaceous to lowermost Oligocene successions. Together with palynofacies analysis, there is a great potential for well-calibrated high-resolution biostratigraphy. Dinoflagellate cysts appear to provide the sole biostratigraphic means for age assessment of the critical uppermost Eocene–lowermost Oligocene interval (the so-called "barren green sands"), whereas sporomorphs are present as well. Together with the diatoms, the palynomorphs will allow detailed paleoenvironmental interpretation. Postcruise paleoenvironmental and paleoclimatological studies, including "land-sea correlation" are possible on all conceivable time scales, down to <20-k.y. cyclicities. Also, the first well-calibrated Paleogene dinoflagellate and sporomorph records from the Southern Hemisphere should result from postcruise studies. Cores have yielded the best imaginable material to study the variability of dinocyst morphology, notably within the *Deflandrea phosphoritica* and *Areosphaeridium diktyoplokum–Enneadocysta partridgei* groups.

Future stable isotopic studies on planktonic foraminifers, together with quantitative analysis of diatoms, nannofossils, and dinocysts, should be useful for detailed reconstruction of the sea surface paleotemperatures and paleoproductivity and other paleoenvironmental parameters, such as fluctuations in the position of the Subtropical Convergence. An outstanding biostratigraphic contribution resulting from Leg 189 will be an integrated zonation scheme, including the six microfossil groups for the Oligocene to the Quaternary for this sector of the Southern Ocean.

Paleomagnetism

Paleomagnetism tends to be a difficult profession during carbonate legs. However, during Leg 189 we were fortunate enough to get some magnetostratigraphy at all sites, and at Sites 1170, 1171, and 1172 the paleomagnetic record was sufficiently good to permit construction of useful age-depth plots. Our work is described in terms of its three main aspects: (1) magnetostratigraphy, (2) rock magnetism, and (3) investigation of magnetic overprints and measurement difficulties.

Magnetostratigraphy

The interpretation of the paleomagnetic record at Sites 1168, 1169, and 1170 in terms of magnetostratigraphy was restricted to the Pliocene–Pleistocene and late Miocene. At Sites 1171 and 1172, the paleomagnetic records were adequate to generate an age-depth plot for the Neogene independent from biostratigraphic datums. At Site 1172, magnetostratigraphy was established down to the middle Miocene. Although the quality of the magnetic record deteriorated in older intervals, a relatively complete magnetostratigraphy was achieved, especially across the Eocene/Oligocene boundary. Unfortunately, at both sites the interpretation of the Eocene record from the inclination was problematic, which led to the development of an approach based upon the sign of the z component. This generated distinctive magnetostratigraphic boundaries, where they were almost totally obscured in the inclination

record. The magnetostratigraphy for Leg 189 is summarized in Table 3, which gives the depths of the observed boundary chrons at the various sites. Where there was more than one core, the depths are from the best record.

Rock Magnetism

Throughout Leg 189, rock magnetism studies have revealed a remarkable homogeneity of magnetic material. Most discretes samples had anhysteretic remanent magnetization (ARM) intensities of order 10^{-3} mA/m and isothermal remanent magnetization (IRM) intensities one order greater. We interpret the ARM/IRM ratio as typical for a detrital source. However, at Site 1168 this ratio was higher, suggesting that the magnetic record was carried in fine, single-domain grains probably of biogenic origin. At Sites 1170 and 1171, attempts to correlate magnetic properties (ARM/IRM, IRM 20/IRM, and IRM 500–IRM 200/IRM 500 ratios) with lithologic units were unsuccessful. Down to the Eocene, magnetic properties were very similar and seemed to characterize a similar source, as if magnetic inputs were not influenced by environmental changes. However, there were some changes weakly correlated with lithology, and the origin of the hard carriers observed in some sections remains to be determined from shore-based studies.

Measurement Techniques

The techniques used during this leg varied a little from the standard methods. For the most part, we measured unsplit sections instead of archive-half sections. This was carried out ahead of the multisensor track (MST) measurement. Because the paleomagnetic measurement is faster than the MST track, the paleomagnetic analysis of the unsplit section was conducted in dead time, and thus, core flow was improved. A long-standing problem in the paleomagnetism of ODP-recovered sediments, and in particular in results from weak sediments such as carbonates encountered on this leg, has been the bias toward the “0” declination reading. The analysis of the drift of the 2G cryogenic magnetometer indicates that one possible explanation of this phenomenon is improper application of drift corrections, although this needs to be investigated in more detail onshore. The use of nonmagnetic core-barrel assemblies permitted comparisons between magnetic results from standard and nonmagnetic assemblies, which did not appear to make a major difference to the magnetization of recovered cores, although further analysis onshore is needed again.

In summary, during Leg 189 we encountered the usual difficulties of carbonate legs, but considerable magnetostratigraphy was achieved and aspects of measurement and analysis techniques have been improved. Of particular note are the measurement of unsplit sections to increase intensities and reduce potential of overprint from splitting and the utilization of the intensity of the z component to interpret the magnetostratigraphy.

Downhole Measurements

Downhole logging was conducted at four of the sites drilled during Leg 189 (Sites 1168, 1170, 1171, and 1172). The sequences logged included a range of siliciclastic and biogenic sediments deposited in a variety of sedimentary environments spanning from the Late Cretaceous to the late Neogene. The results from all sites show that there are two distinct Cenozoic logging units: (1) an upper unit characterized by low natural gamma, magnetic susceptibility, resisitivity, and an ~4 photoelectric value associated with the Oligocene to Quaternary pelagic carbonate deposits and (2) a lower unit with higher natural gamma, higher magnetic susceptibility, and lower photoelectric values associated with the Paleocene to late Eocene shallow-water siliciclastic deposits (Fig. 20).

Log parameters in the upper unit are fairly uniform with only small variations apparent in magnetic susceptibility, natural gamma, density, and resistivity indicating that relatively homogeneous, carbonate-rich, pelagic sediments have accumulated since the Oligocene because of opening and deepening of the Tasmanian Gateway. The small fluctuations in the natural gamma and susceptibility logs imply that, despite the predominance of pelagic carbonates, variations in the sediment terrigenous content occurred throughout the Neogene. Minor changes in the terrigenous component could result from variations in the supply and delivery of terrigenous material to the site or, alternatively, may represent changes in the overlying production of biogenic carbonates, which dilute a relatively constant terrigenous supply. Discriminating between these various influences, each of which is related to different physical mechanisms with their own relationship to climate changes, will require detailed postcruise sediment geochemical studies.

In contrast to the relative stability of log parameters in the Neogene pelagic sequences, pronounced variability is evident in downhole logs within the underlying shallow-water Paleocene to Eocene siliciclastic deposits. This lower sequence is characterized by a general increase in the downhole natural gamma logs with depth, suggesting the sediment terrigenous fraction increases with age at every site, although the trend is most pronounced at the STR Site 1171. Likewise, the general increase in U-spectral gamma logs with depth suggests that the shallow-water siliciclastic Paleogene deposits have higher organic carbon content than the overlying open-ocean Neogene deposits. Yet, the Th/U >2 suggests that the depositional environment, although less ventilated than the overlying pelagic carbonate sequence, was dysoxic or oxic. Superimposed on this general trend of increasing natural gamma values with depth are intervals containing higher frequency cyclic variations in the spectral gamma, magnetic susceptibility, and resistivity logs at Sites 1170, 1171, and 1172. The regional persistence of these cyclic variations in the Th spectral gamma and magnetic susceptibility logs suggest a common influence on sedimentation, either through changes in sea level or regional climate, which influenced sediment supply and/or delivery. Shipboard biostratigraphic results suggest that the period of these sediment cycles is near 20 or 40 k.y. using nannofossil and dinocyst datums, respectively.

The transition interval between the relatively homogeneous upper, and highly variable lower log unit varies in thickness by site occurring abruptly at Sites 1171 and 1172 but more gradually at Site 1168. In addition, correlative peaks in the density, resistivity, PEF, and K spectral gamma logs, associated with glauconite-rich sediments (typical of sediment-starved environments) are common in late Eocene sediments just below the transition to the overlying deeper, open-ocean carbonate deposits.

Geochemistry

The drilling of five sites in the region off Tasmania, in particular Sites 1168, 1170, 1171, and 1172, provided unique insights into both regional and temporal variation in organic and interstitial water geochemistry. The results of the organic geochemical characterization of sediments cored during Leg 189 have led to the following salient observations. First, a two-tiered carbonate distribution is characteristic of Sites 1170, 1171, and 1172. In this distribution, Paleogene sediments are generally carbonate poor, whereas Neogene sediments are carbonate rich. Second, the transition from Paleogene carbonate-poor to Neogene carbonate-rich sediments appears to be mostly quite abrupt, except at Site 1168 where it is gradual. Third, an antithetic relationship exists between carbonate and TOC content. In this relationship, Paleogene sediments usually contain >0.5 wt% TOC, whereas Neogene sediments are relatively free of organic matter. Fourth, organic matter type determined primarily by Rock-Eval pyrolysis and paleosalinity characterizations using C/S ratios provide a basis for intersite geochemical facies correlation from site to site. The facies show distinct, and perhaps important, changes at the Paleocene/Eocene boundary, in the middle Eocene, and near the Eocene/Oligocene boundary. Fifth, at Sites 1168, 1170, and 1171, methane contents obtained from headspace gas measurements show an abrupt increase in the organic carbon–containing Paleogene sediments.

Paleogene sediments with relatively high TOC and low $CaCO_3$ contents exist at Sites 1168, 1170, 1171, and 1172 (Fig. 21). These sediments are bioturbated and have higher natural gamma values (Fig. 20), in particular Th/U ratios mostly >2. These characteristics indicate dysoxic to oxic conditions on the seafloor during deposition. Most of the relatively high TOC–low $CaCO_3$ sediments may have had enhanced burial efficiency of organic matter associated with more rapid siliciclastic sedimentation. The generally poorer ventilation of the waters during this time also would have promoted high TOC–low $CaCO_3$ sediments relative to the Neogene.

The high carbonate content of Neogene sediments reflects dominance of calcareous nannofossils; foraminifers are secondary in importance. The upward increase in carbonate content at all sites during Leg 189 is a consequence of a change from shallow-marine to pelagic open-ocean conditions. The low organic carbon content of these carbonate-rich sediments suggests deposition through a well-mixed water column to a well-oxygenated seafloor. The transition from carbonate-poor to carbonate-rich sediments appears to be relatively abrupt at Sites 1170, 1171, and 1172, although higher resolution sampling at Site 1172 demonstrates that the change in carbonate content is gradual through ~10 m of section. This observation suggests

that higher resolution sampling across this boundary at Sites 1170 and 1171 may better define the nature of this carbonate-rich/carbonate-poor boundary. Specifically, the presence of a condensed section can be inferred if the carbonate content increases gradationally across the boundary, whereas the presence of an unconformity can be considered where an abrupt change in carbonate content is observed. At Site 1168, the change from siliciclastic to carbonate sedimentation is gradational, perhaps because of its distance from processes affecting the other sites.

The similarity of geochemical facies between sites is significant because it suggests regional-scale changes in seafloor and water-column conditions. Upper Paleocene–lower Eocene sediments encountered at Sites 1171 and 1172 contain elevated TOC content and variations in C/S and HI values indicative of fluctuations between terrestrial and marine inputs (Fig. 21). These characteristics suggest rapidly changing environmental conditions across the Paleocene/Eocene boundary in the Tasmanian region. A middle Eocene episode of elevated organic carbon burial was widespread in shallow-marine environments. During this time, a clear gradient in organic matter from terrestrially influenced to dominantly marine is observed from Site 1170 to Sites 1171 and 1172. These observations may reflect deposition at Site 1170 within the Australo-Antarctic Gulf, whereas Sites 1171 and 1172 were more strongly influenced by the Paleogene Pacific Ocean.

The highest organic carbon contents observed during Leg 189 are from upper Eocene sediments at Site 1168. Here, TOC content exceeds 5 wt% and is nearly wholly terrestrial in origin. Such characteristics were not encountered at any of the other sites and likely reflect the lower latitudes and proximity of Site 1168 to hinterland source regions, as well as the site location well within the restricted Australo-Antarctic Gulf. However, upper Eocene sediments at Sites 1168, 1170, and 1171 share a C/S record of brackish water conditions before the transition from carbonate-poor to carbonate-rich sedimentation. This signal is difficult to resolve within a setting of relative water deepening. Perhaps, the seaway conditions were deeper, but climatic fluctuations were sufficient to cause episodes of “freshening” of the water column and/or sediments. Alternatively, the brackish water signature in C/S values may actually represent unrecognized periods of decreased pyrite formation. In either case, more analyses will be needed to understand the significance of the geochemical record from this interval.

Headspace gases at all Leg 189 sites are best characterized as biogenic, although thermogenic inputs were observed at the base of most holes. Rock-Eval pyrograms from Paleogene sediments often display a double S_2 peak character, suggesting the presence of bitumen. T_{max} values obtained by Rock-Eval pyrolysis indicate that organic matter is immature generally, although values characteristic of the “oil window” occur at depth in most holes. Methane gas content is closely tied to pore-water sulfate concentrations at Sites 1168, 1170, 1171, and 1172 (Fig. 22), which in turn is closely tied to the lithostratigraphic separation between carbonate-rich and carbonate-poor sediments. The onset of methanogenesis immediately beneath the zone of sulfate reduction exhibits the characteristics of microbially driven diagenetic depth zonation. In this model, carbonate-poor Paleogene sediments contain sufficient organic matter for complete

sulfate reduction, whereas the sulfate reducers in carbonate-rich Neogene sediments inhibit methanogens. At Site 1172, however, the presence of dissolved sulfate is likely inhibiting methanogenesis in the organic carbon–bearing Paleogene sediments. This observation is unusual because the TOC content of these low-gas sediments appears to be sufficient to have already driven sulfate concentrations to zero.

One of the surprising discoveries of the Leg 189 interstitial water geochemistry program was the presence of regionally extensive low-chloride (Cl^-) pore fluids in the older sediments throughout the region, including on the west Tasmania margin (Site 1168), the STR (Sites 1170 and 1171), and the ETP (Site 1172) (Fig. 22). In general, the fresher pore waters are located in the older part of the cored interval but are in different age sediments and are not restricted to specific lithologies. These fresher fluids are manifested in the Cl^- profiles by multiple distinct maxima and minima rather than smoothly decreasing values. Minimum Cl^- values at the four sites range from 486 to 440 mM, a 13%–21% decrease relative to the mean seawater value (559 mM). At three of the sites, pore-water freshening coincides with the onset of methanogenesis; however, low Cl^- fluids were encountered at Site 1172, where only traces quantities of methane are present (Fig. 22).

At present, the origin of the low-Cl^- fluids is enigmatic. Low Cl^- values in marine pore waters have been observed in environments ranging from accretionary prisms to passive continental margins. One possible external source of low-Cl^- fluids in passive continental margins is the advection of meteoric waters from the continent (e.g., Austin, Christie-Blick, Malone, et al., 1998). However, the geographic separation of the sites (Fig. 3) and the general geologic setting make it improbable that there are links to continental recharge areas.

Possible internal sources that may provide low-Cl^- fluids include (1) gas hydrate dissociation, (2) dehydration reactions of hydrous minerals, such as clays and biogenic opal, (3) clay membrane ion filtration (e.g., Kastner et al., 1991; Hesse and Harrison, 1981; Paull, Matsumoto, Wallace, et al., 1996), and perhaps (4) connate fluids. Gas hydrate dissociation is a common cause of such profiles in continental margin settings. However, crude estimates of the base of the gas hydrate stability zone (GHSZ) at Sites 1168, 1170, and 1171, assuming a pure methane and seawater system, indicate the low-Cl^- fluids are below the stability zone. The depth of the hydrate stability zone will be sensitive to the chemistry of the pore fluids and incorporation of other gases into the hydrate structure (Dickens and Quinby-Hunt, 1997; Sloan, 1998). Therefore, a more rigorous calculation of gas hydrate stability may extend the depth of the stability zone. However, the presence of low-Cl^- fluids at Site 1172, with only traces of methane present, appears to eliminate gas hydrates as a possible mechanism, at least at Site 1172.

At present, we cannot eliminate connate fluids as the possible source of fresher fluids. However, it is hard to imagine that the distinct maxima and minima evident in all Cl^- profiles would not have been smoothed by diffusional processes that are clearly at work with other interstitial water constituents (Fig. 22). In fact, the jagged nature of the Cl^- profiles suggests that the emplacement of fresher fluids has occurred relatively recently. Clay mineral reactions are a

well-known source of fresh fluids, and clay content does increase in the older part of the sedimentary succession. Although reaction kinetics are also important, previous research, both experimental and natural observations, indicates that dehydration reactions (e.g., alteration of smectite) occur at elevated temperatures of 80°C or higher (e.g., Perry and Hower, 1972; Velde, 1983). Temperature measurements made during Leg 189 indicate geothermal gradients of ~50°–60°C/km, and all sites were drilled <1 km deep. Thus, the origin of these regionally extensive fresher pore fluids remains unresolved, and postcruise isotopic analysis of the interstitial waters will be required to better understand these diagenetically and/or paleoenvironmentally important fluids.

In addition to the low-Cl^- fluids, pore-water profiles are characterized by reactions involving alteration of silicate minerals, carbonate recrystallization, and organic matter degradation (Fig. 22). Alteration of silicate minerals, within and below the cored section, lead to covarying decreases in Mg^{2+} and K^+ and increases in Li^+ within the pore fluids. The smooth, diffusional Mg^{2+} and K^+ profiles observed at all sites are likely the result of uptake in reactions below the cored interval. Carbonate recrystallization is most pronounced in the Oligocene and Neogene pelagic carbonates, resulting in increases in interstitial Sr^{2+}. The thinnest carbonate sequence (Site 1171) has the lowest Sr^{2+} concentrations with the thinnest interval of elevated Sr^{2+} (cf. Sr^{2+} to carbonate profiles in Fig. 21). As described above, organic matter reactions are most active in the thick, organic-rich Eocene sediments in the lower part of the cored intervals, which may result in differing sulfate gradients (i.e., thicknesses of the sulfate reduction zone) as sulfate is rapidly depleted in the organic-rich Eocene sections.

DISCUSSION AND CONCLUSIONS

Regional Sedimentation

The sedimentary succession in the Tasmanian region generally records three major phases of sedimentary deposition:

1. Paleocene to early upper Eocene rapid deposition of shallow-water siliciclastic sediments during rifting between Antarctica and Southeast Australia, a time of minimal or no connection between the southern Indian and Pacific Oceans.
2. A transitional interval of slow sedimentation, with shallow-water upper Eocene glauconitic siliciclastic sediments giving way suddenly to lowermost Oligocene pelagic carbonates (often clayey initially). The transition was caused by the activation of bottom currents during the late Eocene as the Tasmanian Gateway opened and deepened during early drifting. Cooling reduced precipitation and the flow of siliciclastic sediment, and currents swept the shelves. Sedimentation no longer kept up with subsidence, and pelagic carbonate deposition took over in the early Oligocene.

3. Oligocene through Quaternary deposition of pelagic carbonates in increasingly deep waters and in increasingly open-ocean conditions as the Southern Ocean developed and expanded with the northward flight of the STR and the Australian continent. The sedimentary sequence seems to record an integrated history of interplay between decreasing continental influence, rifting and subsidence of the rise, Antarctic Circumpolar Current development and Antarctic cooling, and other related factors.

In general, sedimentation rates throughout the region changed dramatically in relation to these distinct phases of sedimentation. These were rapid (~10 cm/k.y.) during the siliciclastic sedimentation of the early rifting phase of the late Paleocene to early late Eocene; slow to condensed during the Eocene–Oligocene transition, when more glauconitic sediments were deposited, and generally slow during the biogenic sedimentation from the earliest Oligocene to the present day. There were periods of minimal sedimentation or erosion affecting the late Oligocene and late Miocene sequences.

Considerable variation in thickness is evident for different time periods among the sites. The two major sediment types, the pelagic carbonates of the Neogene and the shallow-water siliciclastic mudstones of the Paleogene and Late Cretaceous, are dealt with separately below. In regard to the pelagic carbonates, the Quaternary is thickest at the two southern sites (Sites 1170 and 1171). The Pliocene is thickest at the western sites on the STR and especially thick at Site 1169, which was protected from scouring by currents from the west by its great depth and the ridge of the TFZ. The Miocene is affected by the onset of the strong Antarctic Circumpolar Current, with the thickest and most complete section in the protected northern Site 1168. The other northern site (Site 1172) has a fairly complete but thinner section. The lower Miocene is especially thin at the southern Sites 1169, 1170, and 1171, probably because of current scouring. The Oligocene, too, was strongly affected by the Antarctic Circumpolar Current and/or the East Australian Current, with the protected northern Site 1168 as the only one with a thick and reasonably complete sequence.

In regard to the siliciclastic mudstones, the upper Eocene is thin everywhere, apparently because fine-grained sediments were swept away by the newly forming Antarctic Circumpolar Current in the shallow-water depths at all sites. In contrast, the lower and middle Eocene are thick everywhere because siliciclastic supply was rapid and there was little current erosion. The same interpretation probably applies to the Paleocene at the southern Site 1171, whereas there is little Paleocene at the northeastern Site 1172. The uppermost Cretaceous mudstones penetrated at Site 1172 may be quite thick judging from seismic evidence only.

Tectonic Evolution

During the Mesozoic, the Tasmanian region was well within east Gondwana, and although the locations of all the sites eventually remained part of Australia, the four deep sites are all on different blocks of continental crust that behaved somewhat differently through time as

Gondwana fragmented. According to the plate tectonic reconstruction of Royer and Rollet (1997), during the mid-Cretaceous (Fig. 5) the locations of Sites 1169 and 1170 were close together on the Antarctic side of the northwest–southeast strike-slip zone along which Australia was moving northwest relative to Antarctica, here named the Tasmania-Antarctic Shear Zone (TASZ). Across the TASZ were the locations of Sites 1168 and 1171, some 600 km apart. Site 1172 was nearly 400 km east of Site 1170 and well away from the rift zone.

An east-west rift along the southern margin of Australia and the northern margin of Antarctica and slow northwest–southeast separation may have begun as early as the Late Jurassic (Willcox and Stagg, 1990). This rift continued eastward in the Otway, Bass, and Gippsland Basins between Australia and Tasmania. Crustal thinning and subsidence occurred along the developing east-west rift, which was filled with thousands of meters of nonmarine Lower Cretaceous sediments. From the mid-Cretaceous (95 Ma) to the middle Eocene (43 Ma), Australia moved northwest relative to Antarctica at a slow rate of ~10 m/m.y. As the east-west rift widened into the Australo-Antarctic Gulf, the sea transgressed from the west depositing shallow-marine and deltaic Late Cretaceous to Eocene sediments. In the Late Cretaceous (75 Ma), the Tasman Sea began to form and rifting in the Bass Strait failed.

In the Tasmanian region, the TASZ terminated the east-west rift. The block east of the TASZ, consisting of southeast Australia, Lord Howe Rise, and Campbell Plateau, moved northwestward along it. Some crustal thinning occurred along the TASZ, with possible deposition of Early Cretaceous-age sediments. By the Late Cretaceous, the TASZ was subsiding steadily, marine transgression took place through the Gulf from the west, and shallow-marine deltaic sediments began to be deposited in the extreme eastern part of the Australo-Antarctic Gulf. This deposition continued into the Eocene.

In the Late Cretaceous (75 Ma), the Lord Howe Rise, Campbell Plateau, and the ETP all began to move away from Australia and Antarctica to the east-northeast (relative to Australia). At 65 Ma, in the latest Cretaceous, the ETP (with Site 1172) stopped moving with the other blocks, but a legacy of rifting before that movement was its thinned crust and the partially oceanic depression between the ETP and what became the STR. Site 1171 showed that strike-slip movement within the central and eastern STR (e.g., on the Balleny Fracture Zone) occurred during a short period in the late Paleocene, when spreading started south of the STR. This agrees with the plate tectonic reconstruction of Cande et al. (2000), which shows the east-west spreading extending from south of the STR and north of the Transantarctic Mountains (TAM) across to New Zealand from the late Paleocene. This is the period when uplift of the TAM has been considered to have begun (Fitzgerald, 1992). However, evidence from the 1999 Cape Roberts drilling, in the western Ross Sea, indicates that Victoria Land Basin first formed by ~3000 m of rapid subsidence east of the TAM at ~34 Ma, close to the Eocene/Oligocene boundary (Cape Roberts Science Team, 2000), suggesting that much of the uplift of TAM may have been synchronous.

This tectonic scenario for Antarctica seems to have been reflected in the structurally interconnected Tasmanian region. If late Paleocene uplift of the TAM did occur, this would have corresponded to the period of strike-slip movement, and associated vertical displacement, on the central and eastern STR. The end of this movement corresponds to the onset of spreading between the TAM and the STR, which separated the strike-slip faults within most of the STR from tectonic movement in Antarctica. However, the early Oligocene collapse of the continental margins everywhere in the Tasmanian region, documented in part by Leg 189 drilling, coincides precisely with the age of formation of the Victoria Land Basin on the conjugate Antarctic margin (~34 Ma). It would seem that there should be a causal relationship, but determining that relationship awaits postcruise research.

The Site 1168 region was part of the Tasmanian block throughout its Cretaceous and Cenozoic history and, within the depocenter caused by crustal thinning along the TASZ, the Sorell Basin. The Sorell Basin was fully separated from the conjugate eastern end of the Wilkes Land Basin in Antarctica once large quantities of oceanic crust began to form in the easternmost Australo-Antarctic Gulf during the middle Eocene (43 Ma). In regard to the oldest seafloor spreading, Pyle et al. (1995) Ar-Ar dated the basalt at the base of DSDP Site 282 on nearby thinned continental crust at 60.7 Ma, but doubts remain about this date because of the extent of alteration of the basalt. Royer and Rollet (1997) suggest the presence of some oceanic crust as old as Chron 24 (55 Ma). Like the basins to the north, the Sorell Basin subsided throughout the Cretaceous and Cenozoic. This basin was filled with thick shallow-marine Upper Cretaceous to Eocene deltaic sediments derived largely from Tasmania. Strike-slip faulting, active into the Paleocene, cut the basin into a number of subbasins and ridges, between a pair of which Site 1168 is located. In the earliest Oligocene, the Sorell Basin subsided rapidly into deep water and the deposition of pelagic carbonate commenced, as also occurred to the northwest in the Otway Basin. In both cases, the subsidence appears to have been about hinge lines near the present coastlines. The cause of the initial rapid subsidence remains unclear, but it was a regional event. It may have resulted from the final clearance of southeast Australia (the southwestern tip of the STR) from Antarctica (Wilkes Land) near the Eocene/Oligocene boundary (Fig. 6). Site 1168 contains a remarkably continuous Eocene to Holocene sequence, but with a clear transition from siliciclastic deposition in the Eocene to pelagic carbonate deposition in the early Oligocene as the margin sank rapidly.

According to Royer and Rollet (1997), Site 1170 was part of the Antarctic block (Wilkes Land) in the early Late Cretaceous, separated from Southeast Australia by the TASZ. After collision with the central STR block in the latest Cretaceous (66 Ma), the western STR block formed, on which Site 1170 is located. This block began to separate from Antarctica by strike-slip motion, with the TASZ transferring to its western side, and by the latest Paleocene, it was firmly welded to Southeast Australia. During the middle Eocene (43 Ma), the onset of fast spreading in the Australo-Antarctic Gulf increased the rate of movement along the TASZ to ~30 m/m.y. At the same time, fast spreading started south of the STR. Much of this block is covered

by the Ninene Basin, which is cut by Cenozoic strike-slip faults into subbasins and ridges. The basin is filled by fairly thick Upper Cretaceous to Eocene siliciclastic sediments that are prograded and of shallow-marine facies, at least in part. This western block was substantially thinned by tectonism and now lies much lower than the adjacent central block of the STR. Site 1170 is located only 10 km from the eastern side of the Ninene Basin, where the basin abuts against the north-south fault (and modern fault scarp) that marks the suture with the central block.

During the earliest Oligocene, Site 1170 and the Ninene Basin subsided rapidly into deep water, as at Site 1168. The initial fast subsidence is a regional event involving Southeast Australia and the Victoria Land Basin in Antarctica, at least. The final clearance of the western block from Antarctica near the Eocene/Oligocene boundary probably had an effect at Site 1170. The unusually thin upper Oligocene sequence may have been caused by increased current erosion caused by shallowing as the spreading axis, with its heat source, passed 100 km to the west (~26 Ma). Site 1170 contains a less complete Upper Eocene to Holocene sequence than Site 1168 because of generally greater current activity caused by its greater proximity to the opening of the Tasmanian Gateway between the STR and Antarctica and the associated Antarctic Circumpolar Current. The transition from Eocene siliciclastic sediments to pelagic carbonate, as the basin sank rapidly during the earliest Oligocene, was much sharper than at Site 1168. This more transitional change at Site 1168 was probably caused by the ongoing supply of siliciclastic sediments from the high hinterland of Tasmania.

During the Early Cretaceous, the southernmost Site 1171 was located on the east Gondwana block consisting of Australia, the Lord Howe Rise, and the Campbell Plateau across the strike-slip TASZ from Antarctica. Some Early Cretaceous-age sediments must have been deposited along the TASZ, but there is no evidence of them near the site. According to Royer and Rollet (1997), the central and eastern blocks of the STR separated from the Tasmanian block in the early Late Cretaceous (95–83 Ma). Site 1171 is located near the boundary between the two blocks, which jostled as they moved. As Australia moved northwest, the two blocks were "braked" by Antarctica until the latest Cretaceous (65.6 Ma), with a total stretching of 150 km between this and the Tasmanian block forming the South Tasman Saddle. Strike-slip basins and ridges developed within the two STR blocks, but there was only limited thinning of these cratonic blocks. Seismic profiles suggest that the basins were filled by prograded Upper Cretaceous and Paleocene sediments (probably shallow marine) derived from the subaerially exposed ridges and along the basins from higher areas to the north. In the Late Cretaceous, at 75 Ma, seafloor spreading started to the east with the Campbell Plateau and the ETP separating from the composite block and moving away east-northeast relative to Site 1171. The continental crust of the blocks was thick, so subsidence was limited.

The initiation of seafloor spreading to the south is open to interpretation, as profiles with magnetic anomalies are limited and the older anomalies are close together and questionable. Royer and Rollet (1997) reliably identify Anomaly 20 (45 Ma), questionably identify Anomaly

24 (55 Ma), and very doubtfully identify Anomaly 31 (67 Ma). Fast spreading clearly began in the middle Eocene (43 Ma). Pyle et al. (1995) Ar-Ar dated the basalt at the base of DSDP Site 280 on nearby oceanic crust at 64.2 Ma, but because of its alteration, doubts remain about this date. Further information on the breakup comes from Site 1171 itself, which lies in a small north-south basin bounded to the east by an arm of the Balleny Fracture Zone, the boundary between the central and eastern STR blocks. From this site, seismic and palynological information shows an unconformity between very broadly and gently folded sediments of Cretaceous to late Paleocene (58 Ma) age and onlapping and flat-lying sediments of early Eocene (54 Ma) age. This shows that much of the movement within continental crust along the Balleny Fracture Zone (which has been active in oceanic crust ever since) was confined to the latest Paleocene (~55 Ma). The end of this strike-slip faulting and associated folding agrees with the Anomaly 21 identification above, confirming that final separation south of the STR (from Wilkes Land) was in the late Paleocene.

During the earliest Oligocene, Site 1171 and the central STR block subsided into deep water, similar to Sites 1168 and 1170. The amount of subsidence was less than at those sites because of the greater crustal thickness. The likely cause of at least part of the early Oligocene subsidence (contemporaneously with that of the margins elsewhere in Southeast Australia and the Victoria Land Basin) is again the final clearance of the attached western STR block from Antarctica. Site 1171 contains a much thinner and less complete upper Eocene and Oligocene sequence than Sites 1168 and 1170 because of its immediate proximity to the opening of the Tasmanian Gateway between the STR and Antarctica and its exposure to the Antarctic Circumpolar Current thereafter. The transition from Eocene siliciclastic sediments to pelagic carbonate, as the basin sank rapidly in the earliest Oligocene, was more rapid than in the less current-swept and expanded sequences at Site 1168.

During the Early Cretaceous, the eastern Site 1172 was in the east Gondwana block consisting of Australia, the Lord Howe Rise, and the Campbell Plateau well away from the TASZ. Seismic data suggest that dipping and faulted Early Cretaceous-age sediments exist at depth. It is probable that a highly reflective sequence above these sediments consists of Late Cretaceous breakup volcanics, perhaps including the undated rhyolite dredged from the eastern scarp of the ETP (Exon et al., 1997a). According to Royer and Rollet (1997), breakup began to form the ETP during the Late Cretaceous (75–65 Ma), both to the plateau's west and east. The plateau moved east-northeast relative to Tasmania and the STR, initially with the continental block of the Lord Howe Rise and Campbell Plateau. However, this block soon separated, leaving the Tasman Sea oceanic crust to the east of the ETP. In the west, some oceanic crust formed between the ETP and the STR, forming L'Atalante Depression, and crustal thinning occurred between the ETP and Tasmania, eventually forming the East Tasman Saddle.

Although the ETP formed in the Late Cretaceous and might well have had a very different subsidence history from the other Tasmanian blocks drilled during Leg 189, this proved not to be the case, with a close similarity between the two Pacific Ocean Sites 1172 and 1171. At both

sites, Paleocene and Eocene sediments are similar shallow-marine (neritic) siliciclastics, and at both sites there was rapid subsidence and a switch to deposition of pelagic carbonate beginning in the earliest Oligocene. The plateau had been planated by erosion and deposition during the latest Cretaceous and Paleogene, with siliciclastic sediment coming from the marginal granitic highs and perhaps from Tasmania, if the East Tasman Saddle subsided late. An additional feature of the ETP was the formation of a large hot spot volcano in its center during the late Eocene. According to Quilty (1997), calcareous microfossils show that the upper part of this 1500-m-high guyot, the Cascade Seamount, was in shallow-marine depths during the late Eocene. This clearly conflicts with the evidence of upper bathyal deposition of latest Eocene-age sediments at Site 1172 below the base of the seamount. An explanation awaits postcruise investigation.

A tabulation of vital information from ODP Leg 189 and DSDP Leg 29 sites (Kennett and Houtz, 1975) summarizes much of the above (Table 4). It shows that three breakup ages (75, 55, and 34 Ma) affected the various sites in various ways. The first breakup was at 75 Ma for the central and eastern Sites 1171, 281, 1172, and 283 and at 55 Ma for the western and southern Sites 282, 1168, and 280. The last breakup was at 34 Ma on the STR for Sites 1170, 281, and 1171. The subsidence since the Eocene is large on oceanic crust or thinned continental crust (Sites 282, 1168, 1170, 280, and 283) at 3100–3800 m. It is less on the thick continental crust of the central STR and the ETP (Sites 281, 1171, and 1172) at 1600–2500 m. The transition from siliciclastic to biogenic sedimentation is Eocene/Oligocene at most Leg 189 sites in basinal settings in shallow Eocene water depths, but it is Oligocene/Miocene in several Leg 29 sites on local highs in deeper Eocene water depths. This variation is probably caused in part by the position of the CCD relative to the sites during the Eocene to Miocene.

Evolution of the Tasmanian Gateway

In the Early Cretaceous, east Gondwana was intact and ocean currents flowed west and north of Australia and east of the continental block of the Lord Howe Rise, the Campbell Plateau, and New Zealand (LCNZ). The situation began to change early in the Late Cretaceous, when an east-west rift caused marine transgression into the Australo-Antarctic Gulf. Despite a continuation of the rift eastward through present-day Bass Strait into the Lord Howe Rise, the Tasmanian-Antarctic land bridge east of the Gulf survived, and the eastern part of the rift filled with nonmarine sediments. By the Late Cretaceous the northwest-southeast TASZ was well developed, and Gulf waters began to transgress southward along it. In the Late Cretaceous at 75 Ma, continental breakup occurred and seafloor spreading began between Australia and the LCNZ. This rift propagated northward forming the Tasman Sea. Final breakup off northeastern Australia was during the Paleocene at ~60 Ma, and thereafter major ocean currents could flow along the eastern coast of Australia, Tasmania, the ETP, the STR, and the Antarctic margin to the south. However, the Tasmanian Land Bridge between Southeast Australia and Antarctica remained essentially intact, separating the Australo-Antarctic Gulf from the Pacific Ocean.

By the latest Paleocene, the areas of continental crust in the land bridge that had been thinned during the Cretaceous—the future Bass Strait, the South Tasman Saddle between Tasmania and the STR, and parts of the TASZ between Antarctica and STR—had subsided and were near sea level. From then on, limited interchange of shallow-marine waters may have occurred between the Australo-Antarctic Gulf and the Pacific Ocean. The plate tectonic reconstructions of Royer and Rollet (1997) and Cande et al. (in press) suggest, and a variety of other tectonic and sedimentary evidence (including that from Leg 189) support, the idea of a shallow-marine connection during the middle Eocene (Fig. 7). However, the very different character of the shallow-marine Eocene sediments recovered at Sites 1168 and 1170 in the restricted waters of the Gulf, and at Sites 1171 and 1172 in the open waters of the Pacific Ocean, indicates that this interchange was not significant.

However, the same lines of evidence suggest that Antarctica and the STR separated during the Eocene–Oligocene transition (Fig. 6). The ODP sites clearly show a rapid change in the earliest Oligocene to similar open-ocean conditions on both sides of the former Tasmanian Land Bridge, and a shallow-water Antarctic Circumpolar Current was established at that time. By the late Oligocene, the Tasmanian Seaway was hundreds of kilometers wide and at abyssal water depths south of the STR, and a shallow to deep Antarctic Circumpolar Current from the west was eroding older sediments. Nearly all of the former land bridge south of Tasmania had by then submerged, and the expanding current was scouring the ocean floor in places. The Tasmanian Gateway was fully open at all depths by the time Drake Passage, south of South America, is inferred to have opened to deep water during the early Miocene (Barker and Burrell, 1977) and could accommodate an ever-increasing circumpolar flow. This increasing strength continued through the remainder of the Cenozoic as the Australian mainland and Tasmania continued to move northward and Drake Passage opened further. The expanding influence of circumpolar circulation led to bottom-water erosion and winnowing over certain areas and was particularly strong during the late Neogene. The expansion of the Antarctic cryosphere during the middle and late Cenozoic, and its effect of strengthening thermohaline circulation at deep and intermediate water depths, contributed to the deep-ocean erosion and formation of hiatuses in the sequences. Examples of this include the middle Miocene scouring east of Site 1170 that removed the Oligocene and the scouring during the Miocene–Pliocene transition in the southern part of the STR.

Paleocene–Eocene Paleoenvironments: Before the Gateway Opened

Deposition during the Paleocene through early late Eocene (43–36 Ma) was dominated by continental influences. The sequences drilled are probably quite similar to even older underlying Paleogene sequences, which, based on seismic and other evidence, consist of siliciclastic sediments deposited in deltaic environments that kept up with subsidence and compaction as rifting progressed. The southern sequences (Sites 1170 and 1171) provide unusually good records of Antarctic paleoenvironmental conditions at the Antarctic continental margin at high

latitudes (~67°S), whereas Sites 1168 and 1172 provide comparative records at lower latitudes on the western and eastern margins of Tasmania. At Sites 1170 and 1171, the Paleocene–Eocene dark, fine-grained, organic-rich siliciclastic sediments were deposited on a highly restricted, moderately tranquil, broad shelf near the opening rift between Antarctica and Australia in the extreme southeastern corner of the Australo-Antarctic Gulf (Site 1170) and in the extreme southwestern margin of the Pacific (Site 1171). Benthic foraminiferal assemblages indicate deposition in neritic water depths, probably shallower than 100 m. An absence of sedimentary characteristics indicating turbulence suggests that deposition was below wave base (which may have been shallow in the equable climatic conditions prevailing) and without important current or tidal influences. Persistent reworked early Eocene to Cretaceous radiolarians and organic dinocysts at Site 1170 suggest continuous weathering and erosion of marine sediments of this age in the hinterland.

Highly restricted nearshore conditions in the middle to early late Eocene at all sites are indicated by a wide range of criteria including pervasive pollen and spore assemblages, abundant continuous low-diversity assemblages of organic dinocysts indicative of eutrophic and brackish surface waters, and limited representation of open-ocean planktonic microfossils. Diverse pollen and spore assemblages are particularly abundant in the Paleocene sequence at Site 1171, indicating particularly strong continental influence with abundant, diverse plant communities. In situ assemblages of planktonic foraminifers and radiolarians are largely absent, diatoms are rare, and calcareous nannofossils are uncommon. Good preservation of calcareous nannofossils suggests that they are uncommon, not because of dissolution, but because of the restricted coastal setting in conjunction with high sedimentation rates. However, the presence of foraminiferal linings suggests dissolution of foraminifers at some levels.

Ventilation on the shelves over much of the region was poor to limited throughout the middle to early late Eocene judging from high TOC, limited bioturbation, and benthic foraminiferal assemblages dominated by agglutinated forms and nodosariids. The sediments at Sites 1168 and 1170 suggest that the eastern, remote end of the narrow, restricted Australo-Antarctic Gulf was poorly ventilated. Low oxygen levels in waters of the eastern Gulf would have developed because of the restricted circulation (2000 km from the open Indian Ocean) and the proximity of inferred abundant terrestrial organic sources from the surrounding land masses, including Antarctica, warm climatic conditions, and possible high marine biotic productivity in eutrophic conditions. Ventilation was especially poor at Site 1168, off western Tasmania, as indicated by laminated sediments. Deeper water sediments at nearby Site 282 were also poorly oxygenated. Anoxic to dysoxic depositional environments would be expected within an expanded oxygen minimum zone that extended up onto the continental shelf at Site 1168. Eocene sediments at Site 1170, in the extreme southeastern corner of the Gulf, were also deposited in poorly oxygenated conditions on a tranquil shelf. Here, the absence of laminations and a slight increase in bioturbation in some intervals suggest greater shelf ventilation than at Site 1168, but circulation was almost certainly sluggish.

The poor ventilation in such shallow-water depths at Site 1170 suggests that the Tasmanian Gateway generally was closed to even shallow waters (~100 m) during the middle and early late Eocene, at least in the developing rift basin between Antarctica and the STR. This is supported by the contrasting Eocene record at Site 1171, near the developing seaway on the Pacific side of the Tasmanian Land Bridge, where the shelf sediments are well bioturbated, suggesting with other evidence more strongly ventilated conditions than in the Gulf and no oxygen minimum zone. If the Tasmanian Gateway had been open widely at shallow depths, there would have been little basin to basin fractionation and, hence, little contrast in sedimentary environments. Middle Eocene sedimentation at Site 1172 bears considerable resemblance to that at Site 1171, but it was in a more oceanic, better ventilated environment within the open Pacific Ocean. The proximity of Site 1172 to the large and newly formed subaerial Cascade Seamount may have increased the speed of bottom currents nearby, thus enhancing ventilation.

The middle through upper Eocene sediment sequence at Sites 1170 and 1171 reveals distinct cycles in physical properties, sediments, and microfossil assemblages. Alternations between dark, poorly bioturbated, nannofossil-poor sediments lacking glauconite and lighter, more nannofossil-abundant, bioturbated sediments containing glauconite probably result from changes in water-mass ventilation. Quantitative changes in dinocyst assemblages are cyclic. The darker sedimentary intervals are associated with higher abundances of dinocysts (including massive monotaxic blooms) characteristic of eutrophic conditions and suggesting high nutrient supply to surface waters. In contrast, dinocysts characteristic of more oligotrophic surface waters dominate the lighter intervals in association with more abundant calcareous nannofossils. Clear cyclicity with probable Milankovitch periodicity is also evident in Th abundance in the logging data.

These middle to late Eocene shelfal cycles almost certainly will be shown to correlate with changes in sediment and biotic characteristics. The cause of the cycles is yet to be determined, but they probably resulted from minor climatic oscillations at high southern latitudes, perhaps associated with small sea-level changes, which caused changes in siliciclastic sediment supply, upwelling, and nutrient supply, and associated changes in bottom-water ventilation. The relative importance of marine vs. terrestrial sources of organic carbon varied at the different margin locations during the Eocene. At Site 1168, terrestrial carbon sources dominate, but marine organic carbon dominates at Sites 1170 and 1171, where marine productivity was high in a restricted nearshore setting. In contrast, Paleocene sediments, sampled only at Site 1171 on the southern STR, clearly exhibit a much stronger terrestrial influence with abundant terrestrial plant materials (e.g., pollen and spores). Throughout the Paleocene to middle Eocene, sedimentation kept up with subsidence and compaction.

Evidence for glaciation is completely lacking during the Paleocene and Eocene. Both marine and terrestrial microfossils indicate cool, temperate conditions throughout the middle and late Eocene. Calcareous nannofossil assemblages are of relatively high diversity and appear to be slightly warmer in this sector of the Antarctic than at comparable latitudes elsewhere (although almost completely lacking warmth-loving discoasters). Their diversity suggests an absence of

seasonal sea ice over the shelf and marine conditions during much of the time. Middle Eocene clay assemblages at Site 1170 are completely dominated by smectite, suggesting warm temperatures, seasonal rainfall, and a predominance of chemical over physical weathering.

Relatively warm, cosmopolitan dinocyst assemblages of the middle Eocene were in part replaced during the late Eocene by cooler, endemic Antarctic forms. This inferred cooling is consistent with stable isotopic records that indicate progressive cooling of the Southern Ocean during the middle and late Eocene (Shackleton and Kennett, 1975; Stott et al., 1990; Kennett and Stott, 1990). Cooler continental conditions during the late Eocene are indicated by conspicuous increases in illite relative to smectite clays at Sites 1170 and 1171, suggesting a reduction in continental chemical weathering, perhaps in combination with increased tectonism near the expanding rift. Nevertheless, the character and abundance of the organic dinocyst and diatom assemblages throughout the entire middle to upper Eocene suggest that at no time was cooling sufficient to form important seasonal sea ice in this Antarctic region. Pollen and spore records suggest that the middle and late Eocene plant communities on the hinterlands were diverse and cool temperate. Floras were dominated by Nothofagus, podocarps, and other forms with an understory of ferns, similar to a floral assemblage of similar age previously documented in the Weddell Sea sector of Antarctica (Mohr, 1990). Although upper Eocene pollen assemblages appear cooler, they still indicate relative warmth along the Antarctic margin compared with the distinctly cooler Oligocene that followed. Oligocene floras, if they existed, left no record because palynomorphs were not preserved in the pervasive carbonate sediments, probably because of oxidation. Therefore, a nonglaciated, cool, temperate climate prevailed on this sector of the Antarctic margin during the middle to late Eocene. This contrasts with the Prydz Bay margin, where clear evidence exists for late Eocene glaciation (Barron et al., 1991a) and early Oligocene development of a major ice sheet (Zachos et al., 1992, 1993, 1996).

In summary, the contrast between the poorly oxygenated, shallow-marine waters of the shelf of the Australo-Antarctic Gulf and the better oxygenated waters in the Pacific Ocean suggests a general lack of interchange between southern Indian and Pacific Ocean waters. The evidence discussed above suggests that the Tasmanian Gateway remained more or less closed, even to shallow-surface waters, until the late Eocene at ~36 Ma. Sites 1168 and 1170 in the Gulf are much more poorly ventilated than Sites 1171 and 1172 in the Pacific Ocean.

The Eocene–Oligocene Transition: The Gateway Opens

Major paleoenvironmental changes occurred during the Eocene–Oligocene transition, the most profound change in the entire Cenozoic (Kennett, 1977; Zachos et al., 1993), at all four deep sites (Sites 1168, 1170,1171, and 1172). The sites contain a variably continuous record of this interval, which shows that almost all aspects of the depositional environment changed. The late Eocene is represented by a condensed sequence of continentally influenced glauconite-rich silty claystones to glauconitic muddy green siltstones and the early Oligocene by biogenic carbonates. A transitional change upward in the late Eocene from more muddy to more sandy

sediments, associated with increasing glauconite and quartz and the deposition of glauconitic quartz-rich sandy silts ("green sands"), reflects an upward increase in bottom-current activity and winnowing. The near absence of calcareous microfossils in the "green sands" at Sites 1170, 1171, and 1172 made dating difficult. However, dinocysts and diatoms suggest a relatively complete upper Eocene sequence up to and including the "green sands." This is supported by the clear upward gradation in lithology into the "green sands," the general succession of microfossil datums, and the unexceptional changes in the assemblages of organic dinocysts, pollen, and spores.

Within the "green sands," despite the winnowing and hiatuses, the angularity of the quartz at some levels indicates periods with little reworking. During the late Eocene, diatoms and benthic foraminifers indicate deepening of the "green sand" environment from neritic to upper bathyal. With steadily increasing water depths in the early Oligocene, deposition changed to open-water pelagic carbonates. This reflects a change during the early late Eocene to early Oligocene, from siliciclastic to biogenic sedimentation, from a poorly to a well-oxygenated benthic environment, from tranquil to moderately dynamic environments, and from relatively warm to cool climatic conditions. The sequence of change over the Eocene–Oligocene transition is remarkable in its consistency over the width and breadth of the Tasmanian-Antarctic margin, as determined from our four deep cored sequences. Differences in detail are clearly related to individual setting at the time of deposition, such as latitude and proximity to the ocean and landmasses.

The glauconitic sediments are strongly bioturbated and were deposited in well-oxygenated bottom waters. The lack of carbonate microfossils in the "green sands" suggests a dissolution episode related to the expansion of the Antarctic cryosphere. This episode is recorded widely in deep-sea carbonate sequences and is associated with the well-known positive oxygen isotopic shift in the early Oligocene (33 Ma) (e.g., Shackleton and Kennett, 1975; Miller, 1991; Zachos et., 1994). Based on our biochronology, the changes in the sediments suggest the opening of the Tasmanian Gateway to some cool shallow-water flow in the late Eocene and intensifying current flow toward the Eocene/Oligocene boundary. This was followed in the earliest Oligocene by expansion of the Antarctic cryosphere and deep-water interchange between the southern Indian and Pacific Oceans. This interchange heralds the initiation of the circumpolar current in this segment of the Southern Ocean. Although planktonic microfossils indicate climatic cooling during this interval, there is no evidence of glacial activity. Indeed, the calcareous nannofossil assemblages suggest somewhat warmer conditions than in sequences at equivalent latitudes elsewhere in the Southern Ocean (Wei and Wise, 1990; Wei and Thierstein, 1991; Wei et al., 1992). The Oligocene clay assemblages at Site 1170 also suggest a transitional climate based on the co-occurrence of both smectite, indicating chemical weathering, and illite, indicating physical weathering.

Water depths throughout the region began to increase rapidly from the lowermost Oligocene upper bathyal depths. They reached upper abyssal depths during the early Neogene with a total water-depth increase averaging 2000 m. Clearly, such a depth increase must reflect rapid

subsidence of the STR and the Tasmanian margin during the Oligocene along with expansion of the Tasmanian Gateway. The major and rapid reduction in siliciclastic sediment supply to the margin would also have contributed to the initial depth increase.

The late Eocene "green sands" in the sequences closest to Antarctica (Sites 1170 and 1171) are overlain, with little gradation, by ooze and chalk of early Oligocene age. Near western Tasmania (Site 1168), a similar sequence shows more gradation upward in the Oligocene. From the earliest Oligocene onward, sedimentation in these sequences was completely dominated by relatively slow deposition of nannofossil ooze and chalks, faster than in the "green sands," but much slower than during the early and middle Eocene. Although the age of the base of the carbonates requires better constraint, existing stratigraphic data suggest deposition commenced soon after the earliest Oligocene oxygen isotopic shift at 33 Ma. This isotopic shift represents major cooling and the initial major cryospheric development of East Antarctica (Shackleton and Kennett, 1975; Miller, 1991; Wei, 1991; Zachos et al., 1994) and major expansion of the psychrosphere with its deep-ocean circulation (Kennett and Shackleton, 1976). Therefore, the synchronous commencement of biogenic carbonate deposition at all sites appears to reflect major climatic and oceanographic changes that affected broad regions of the STR and Tasmanian margins. This created a more dynamic, well-ventilated ocean with increased upwelling and higher surface-water biogenic productivity that increased rates of sedimentation of calcareous nannofossils and diatoms and decreased preservation of organic carbon. Open-ocean planktonic diatoms replaced neritic diatoms, which suggests coastal upwelling had begun on the STR and Tasmanian margin during the earliest Oligocene. Furthermore, associated cooling of the Antarctic continent apparently decreased weathering rates and transport of siliciclastic sediments to the margin. The environment of deposition was, thus, transformed from the late Eocene to the earliest Oligocene, from dominance of siliciclastics to dominance of calcareous nannofossils.

Sequences from other areas of the Antarctic margin show a similar drastic reduction in siliciclastics and increase in biogenic sedimentation during the Eocene–Oligocene transition. The lowermost Oligocene is often marked by an increase in biogenic sediments or of biogenic components in otherwise relatively slowly deposited siliciclastic sediments including diamictites (Diester-Haass and Zahn, 1996; Kennett and Barker, 1990; Salamy and Zachos, 1999). However, outside the Tasmanian region, the biogenic component is usually biogenic silica (diatoms) rather than calcium carbonate (calcareous nannofossils and foraminifers). On the shallow (probably neritic) northwest margin of the Weddell Sea, carbonate-free diatom ooze was deposited during the earliest Oligocene, suggesting significant cool-water upwelling (Barker, Kennett, et al., 1988). On the margins at Prydz Bay and southern Ross Sea, diatoms became an important component in diamictites (Barron et al., 1991a; Barron et al., 1991b; Exon, Kennett, Malone, in press).

Why was there such a sharp change from siliciclastic to carbonate sedimentation at the Eocene/Oligocene boundary? A very broad, shallow Australian-Antarctic shelf had been supplied with siliciclastics for tens of millions of years, and even though rifting, subsidence, and

compaction had started early in the Cretaceous, sedimentation had kept up and shallow-marine sediments were rapidly deposited through until the end of the middle Eocene. In the Tasmanian region, there was also subsidence related to the Late Cretaceous opening of the Tasman Sea. Rifting between Australia and Antarctica gave way to almost complete separation of the continents and fast spreading in the middle Eocene (43 Ma), and this could be expected to increase the rate of subsidence. At Sites 1170, 1171, and 1172, glauconitic and siliciclastic upper Eocene sedimentation almost kept up with subsidence until the Eocene/Oligocene boundary (33 Ma), some 10 m.y. after the onset of fast spreading, even though the sedimentation rate was now low.

Then came the change to much faster subsidence at the Eocene/Oligocene boundary, an effect mirroring the rapid subsidence that formed the Victoria Land Basin in nearby Antarctica at the same time (Cape Roberts Scientific Team, 2000). This subsidence clearly had a regional cause and reduced the area available for erosion in the Tasmanian region. The contemporaneous climatic cooling would have led to greatly reduced rainfall and, thus, weathering and erosion, further reducing siliciclastic supply. Thereafter, the sea deepened rapidly, and slow deposition of pelagic carbonate dominated completely. This appears to have been the most significant interval of sediment starvation along the Antarctic margin.

Paleogene Margin Carbonates: Interplay between Tectonics and Climate

The sequences at Sites 1170 and 1171 have revealed a marked difference in the Eocene–Oligocene sediment transition as compared with other parts of the Antarctic margin. As far as we can tell, no other margin sectors experienced pelagic carbonate deposition immediately following the Eocene/Oligocene boundary. Other areas experienced deposition of biosiliceous sediments or more slowly accumulating siliciclastic sediments with an increased siliceous biogenic component. The environment at the Tasmanian-Antarctic margin apparently favored biogenic carbonate preservation and relatively low biosiliceous productivity. Here, even Eocene siliciclastic sediments generally contain a better record of better preserved calcareous nannofossils and foraminifers than elsewhere. These observations suggest different climatic regimes in different sectors of the Antarctic margin during the Eocene and Oligocene. Circum-Antarctic climatic and oceanographic similarity, a hallmark of the modern Antarctic, did not exist during the Paleogene. Biogeographic evidence from calcareous nannofossils and lack of any evidence for glaciation in the Tasmanian sector indicate that conditions were slightly warmer than in other margin sectors, even during the Oligocene. The earliest Oligocene was a time of major cryosphere expansion in the southern Indian Ocean sector and in the southern Ross Sea. Thus, circum-Antarctic circulation was still insufficiently developed in the Oligocene to unify the character of paleoenvironmental change around the Antarctic margin.

Why are carbonates generally better preserved on the STR during the Paleogene than elsewhere on the Antarctic margin? This region may have been under the strong influence of warm low-latitude surface waters carried southward along the eastern margin of Australia by the

East Australian Current and southward around western Australia into the Australo-Antarctic Gulf. Southward flow of warm waters along the east Australian margin would have been enhanced by constriction in the Indonesian Seaway in the Oligocene (Hall, 1996). These warm tropical waters would have been relatively saline and, thus, would have helped promote production of deep waters. Hence, this sector of the margin may have operated in an antiestuarine mode (Berger et al., 1996) marked by a downward flux of deep waters and an inward flow of surface waters, as in the modern North Atlantic. In this case, upwelling of nutrient-rich waters is diminished and carbonate accumulation is favored. Other sectors of the Antarctic margin, marked by strong carbonate dissolution at shallow water depths and high biosiliceous accumulation, may have operated in estuarine mode, marked by an upwelling of nutrient-rich deep waters and an outflow of surface waters. There, carbonate dissolution is favored by the upwelling of old, deep, low-alkalinity, high pCO_2 waters such as in the modern north Pacific Ocean.

A major strengthening of oceanic thermohaline circulation occurred at the climatic threshold of the Eocene–Oligocene transition. This resulted largely from the major cooling and cryospheric development of Antarctica (Kennett and Shackleton, 1976). This cooling, in turn, led to increased aridity of the continent and a major reduction of freshwater flow to the surrounding continental margin, which is reflected by marked reduction in the transport of siliciclastic sediments to the Antarctic margin. Surface waters near the margin would therefore have increased in salinity. A major positive feedback almost certainly would have resulted, with further strengthening of bottom-water production and expansion of the oceanic psychrosphere (deep-ocean circulation). Thus, the delivery of high salinity surface waters to the STR sector of the Antarctic margin, caused by its unusual plate tectonic setting, may well have especially enhanced bottom-water production and, in turn, increased carbonate-biogenic accumulation on the margin.

Southern Ocean Development and Paleoceanography

Drilling during Leg 189 was conducted to test the hypothesis formulated during DSDP Leg 29 (Kennett, et al., 1974; Kennett, Houtz, et al., 1975; Kennett, 1977) that initial development and evolution of Antarctica cryosphere during the middle and late Cenozoic resulted from thermal isolation of the Antarctic by the development of the Antarctic Circumpolar Current and the Southern Ocean. The Cenozoic expansion of the Southern Ocean resulted from plate tectonic movements that caused northward movement of Australia and its southern continental extension—Tasmania and the STR—and the opening of Drake Passage (Weissel and Hayes, 1972; Barker and Burrell, 1977; Lawver et al., 1992; Cande et al., 2000). The opening of the Tasmanian Gateway created initial thermal isolation and resulted in the major cooling of Antarctica that also produced, through feedback mechanisms, the first ice sheets on at least some sectors of the continent. The four major sites drilled during Leg 189 penetrated to middle Eocene or even Upper Cretaceous sediments, thus providing a climatic and paleoceanographic record for the last 40 to 70 m.y., depending on the site. The sediment sequences reveal a remarkably

coherent regional picture reflecting major paleoceanographic changes, especially during the mid- to late Paleogene and continuing into the Neogene, resulting from critical plate tectonic changes related to final separation of the STR from East Antarctica.

Paleogene

Changes in the sediment records drilled during Leg 189 are consistent with plate tectonic reconstructions (Royer and Rollet, 1997; Cande et al., 2000). These reconstructions suggest that before the late Eocene, the Tasmanian land bridge effectively blocked even shallow water connections between the Australo-Antarctic Gulf and the southwest Pacific Ocean (Fig. 23). Initial opening of the Tasmanian Gateway to shallow waters occurred some time in the late Eocene after ~37 Ma, and deeper waters by 33 Ma (earliest Oligocene) (Fig. 24). The two crucial effects of plate tectonics were therefore the initial development of a gateway to shallow waters, followed by subsidence of the STR and establishment of deep-interocean communication. The sediment sequences recovered during Leg 189 suggest that major subsidence of the margins cored was very rapid, beginning near the Eocene/Oligocene boundary and becoming well advanced by the earliest Oligocene. The gateway was then fully open (Fig. 24), and the Tasmanian Seaway, involving both shallow to abyssal water flow, continued to expand during the remainder of the Cenozoic (Fig. 25) as it does today.

Major reorganization of Southern Ocean circulation occurred during the Eocene–Oligocene transition, as proposed by Kennett, Houtz, et al. (1975), Kennett (1977), Murphy and Kennett (1986), as circum-Antarctic circulation commenced through the developing Tasmanian Seaway. Until the early late Eocene (Fig. 23), no Antarctic Circumpolar Current existed to interfere with the influence of the southward-flowing warm-subtropical arm of the South Pacific gyre (East Australian Current). These warm waters were transported close to Antarctica, warming this region and contributing toward the well-known relative warmth of the continent before the late Eocene, a trend supported by Leg 189 data. The opening of the Tasmanian Gateway and the development of circum-Antarctic circulation closely coincides with major cooling and cryospheric development of Antarctica during the Eocene–Oligocene transition (Shackleton and Kennett, 1975; Miller, 1991; Zachos et al., 1994). This allowed relatively cooler waters from the Australo-Antarctic Gulf into the South Pacific as the Antarctic Circumpolar Current, which led to initial decoupling of the warm-subtropical gyre from the Southern Ocean (Fig. 24) and cooling of South Pacific waters at high latitudes (Kennett, 1977; Kennett, 1978; Murphy and Kennett, 1986). The decoupling strengthened as the Tasmanian Seaway continued to open during the Oligocene (Fig. 25) and throughout the remainder of the Cenozoic, with the expansion of the Southern Ocean. The ever-increasing strength and width of the Antarctic Circumpolar Current led to increased Cenozoic thermal isolation of Antarctica that, in turn, led to further positive feedbacks reinforcing Antarctic cooling and cryosphere expansion. Although the late Oligocene through Neogene record of this climatic evolution was not immediately apparent during

shipboard investigations, we expect that this will be revealed as a result of postcruise isotopic and quantitative microfossil studies.

Major changes in the sediments from Leg 189 are consistent with the hypothesis that major Antarctic cooling occurred during the Eocene–Oligocene transition at the time of the Antarctic Circumpolar Current development through the Tasmanian Gateway. The most conspicuous sedimentological change for the entire last 65 m.y. was the Eocene–Oligocene transition from rapidly deposited siliciclastic sediments to pelagic carbonates. In our sequences, the transition is associated with an increase in bottom currents, while the margins were still relatively shallow, in neritic to upper bathyal depths, leading to a conspicuous reduction in sedimentation rates and deposition of glauconitic silts and sands. Widespread hiatuses in the lower to mid-Oligocene indicate increased and pervasive current activity down to abyssal depths. Increased current strength in the narrow Gateway resulted in increased thermohaline circulation synchronous with psychrospheric development. This, in turn, was linked to enhanced bottom-water production around the now seasonally freezing Antarctic margin (Kennett and Shackleton, 1976).

As discussed above, the relatively sudden decrease in deposition of siliciclastic sediments along the margins of the Tasmanian land bridge is inferred to have resulted largely from sediment starvation caused by a dramatic decrease in precipitation, humidity, chemical weathering, and, hence, run-off and sediment supply from Antarctica associated with the major cooling. This change corresponds to the large positive shift in oxygen isotopic values detected globally in the deep ocean, which reflects both cooling of the deep ocean upon development of the psychrosphere (deep-ocean cool waters) and significant ice accumulation on Antarctica, initiating the cryosphere. The change closely coincides with rapid subsidence of the STR and the Tasmanian margin, which led to open-ocean conditions and encouraged upwelling and increased biogenic sedimentation. Increased upwelling elsewhere, over broad areas of the Antarctic margin, lead to the onset of biosiliceous sedimentation, unlike the pelagic carbonate sedimentation of the Tasmanian margin.

Major glacial development of the Antarctic is inferred to have begun in the earliest Oligocene in a number of areas from the evidence of diamictites (Barron et al., 1991b; Larsen et al., 1991; Cape Roberts Science Team, 2000) and ice-rafted sediments (Hayes, Frakes, et al., 1975; Barker, Kennett, et al., 1988; Zachos et al., 1992). Shipboard investigations during Leg 189 revealed no evidence for Oligocene glacial activity on the Antarctic margin in the offshore Tasmanian region. This is consistent with the observations made during DSDP Leg 29 (Kennett, Houtz, et al., 1975). Furthermore, evidence is lacking for early Oligocene glacial activity at DSDP Site 274 in an equivalent sequence on the conjugate Antarctic margin near Cape Adare, where, even in the late Oligocene, glacial activity is extremely rare (Piper and Brisco, 1975). Our combined results strongly suggest that this sector of the Antarctic margin was relatively warm compared with others, especially in the Kerguelen sector in the southern Indian Ocean. We present the hypothesis that relative warmth of the Tasmanian region resulted from long-term transport of heat toward the Southern Ocean by the warm East Australian Current (Figs. 23, 24). However,

the influence of this warm current apparently did not extend into the southern Ross Sea in the early Oligocene, when marine diamictites were deposited at 77°S at Cape Roberts (Cape Roberts Scientific Team, 2000). Thus, a strong meridional climatic gradient existed in the Ross Sea sector of Antarctica. Indeed, a corollary of Leg 189 interpretations is that Antarctica was clearly marked by strong regional differences in climate during the Oligocene.

Earlier ideas of continent-wide ice sheets of present-day proportions in the Oligocene are unlikely based on descriptions of several margin sediment sequences drilled during the DSDP and ODP programs (e.g., Kennett and Barker, 1990; Hayes, Frakes, et al., 1975), including results from Leg 189. This probably includes the earliest Oligocene interval of inferred major ice growth (Zachos et al., 1992), evidence for which is also apparently lacking in the Leg 189 sequences. This conclusion appears reasonable considering that the Antarctic Circumpolar Current was still developing in the Oligocene, so its unifying circumpolar influence probably had not developed until the Neogene. Until then, regional climatic differences probably existed around the margin. Indeed, if it is correct that deep circum-Antarctic circulation formed in the earliest Miocene (Barker and Burrell, 1977), fundamental paleoceanographic changes associated with this development may have been the basis for differentiation by earth scientists of the Paleogene and Neogene in the dawn of the scientific era.

Neogene

Neogene sedimentation at Leg 189 sites on the STR and the Tasmanian margin was completely dominated by nannofossil oozes with a significant foraminiferal component. Sedimentation of these pelagic carbonates was largely continuous, except during the late Miocene and earliest Pliocene, at a number of sites. The Miocene–Pliocene transition is missing in a hiatus at Sites 1169 and 1171, and the lower-upper Miocene is missing at Site 1168. Otherwise, the lower and upper Miocene and the Pliocene to Quaternary appear to be largely complete in the sequences. The uppermost Miocene hiatus appears to have resulted from increased thermohaline circulation associated with Antarctic cryospere expansion at that time (Hodell et al., 1986). Altogether, the Neogene sequences cored during Leg 189 provide a fine suite of sequences in present-day temperate (cool subtropical) and subantarctic water masses of the Southern Ocean. These represent a treasure chest for high-resolution Neogene paleoclimatic and biostratigraphic investigations of the Southern Ocean. The Neogene carbonates exhibit changes that record changing environmental conditions in response to the northward movement of the STR, Tasmania, and the ETP from Antarctica and shifting positions of the Subtropical Convergence and the Subantarctic Front.

The pelagic carbonates accumulated at relatively low rates (~2–4 cm/k.y.) typical of the open ocean. Relatively low-diversity benthic foraminiferal assemblages indicate deposition in abyssal depths under generally well-ventilated conditions characteristic of the Antarctic Circumpolar Current region. Other than a small, pervasive clay fraction, siliciclastic sediments are absent throughout the Neogene, except in the early Neogene of Site 1168, which is the site closest to a

present land mass. Nannofossil oozes are conspicuously pure white on the STR in the lower Neogene, which corresponds to when the STR was well clear of the siliciclastic influences of Antarctica and yet had not come under the late Neogene influence of increasing aridification and associated dustiness of Australia. Diatoms are consistently present throughout the Neogene carbonates but exhibit a distinct increase in abundance and diversity after the middle Miocene. This almost certainly reflects an increase in upwelling within the Southern Ocean at that time in response to the well-known expansion of the Antarctic cryosphere. A marked increase in carbonate ooze deposition during the early Pliocene at Sites 1169 and 1170, on the southeastern STR, is not observed at other sites, suggesting local concentrations of calcareous nannofossils rather than any regional trend like that in the southwest Pacific (Kennett and von der Borch, 1986). During the latest Neogene, planktonic foraminifers become much more important relative to calcareous nannofossils. This may reflect increased winnowing by deep currents and/or a decrease in relative importance of calcareous nannofossils compared to planktonic foraminifers during the late Neogene.

Postcruise investigations of Leg 189 Neogene sequences will lead to a significant increase in understanding of paleoclimatic and paleoceanographic history of the Southern Ocean. Upper Neogene sections have been satisfactorily spliced from multiple cores in four of the sites (Sites 1168 and 1170–1172) to provide essentially continuous paleoclimatic records. Pervasive sedimentary cycles are apparent throughout the entire Neogene, based on observations of the sediment record and changes in the physical properties of the sediments. Shipboard investigations of clay assemblages suggest relatively warmer conditions during the early Neogene until ~15 Ma. After that, clay assemblages suggest general regional cooling. During the late Neogene, clays became increasingly important in the pelagic carbonates, in part because of increasing dust transport from Australia. A distinct influx of kaolinite in several sites, including the southern STR, during the late Pliocene and Quaternary probably reflects increasing southeastward wind transport of relict clays from an increasingly arid Australia. The uppermost Neogene sediments at Site 1172, which is downwind from Tasmania, exhibit distinct cycles in clay abundance in the biogenic oozes, almost certainly in response to glacial-interglacial oscillations in Australian continental aridity.

REFERENCES

Austin, J.A., Jr., Christie-Blick, N., Malone, M.J., et al., 1998. *Proc. ODP, Init. Repts.,* 174A: College Station, TX (Ocean Drilling Program).

Barker, P.F., and Burrell, J., 1977. The opening of the Drake Passage. *Mar. Geol.,* 25: 15–34.

Barker, P.F., Kennett, J.P., et al., 1988. *Proc. ODP, Init. Repts.,* 113: College Station, TX (Ocean Drilling Program).

Barrett, P.J., 1994. Progress towards a Cenozoic Antarctic glacial history. *Terra Antarct.,* 1:247–248.

Barron, J.A., Baldauf, J.G., Barrera, E., Caulet, J.-P., Huber, B.T., Keating, B.H., Lazarus, D., Sakai, H., Thierstein, H.R., and Wei, W., 1991a. Biochronologic and magnetochronologic synthesis of Leg 119 sediments from the Kerguelen Plateau and Prydz Bay, Antarctica. *In* Barron, J., Larsen, B., et al., *Proc. ODP, Sci. Results,* 119: College Station, TX (Ocean Drilling Program), 813–847.

Barron, J.A., Larsen, B., and Baldauf, J.G., 1991b. Evidence for late Eocene to early Oligocene Antarctic glaciation and observations on late Neogene glacial history of Antarctica: results from Leg 119. *In* Barron, J., Larsen, B., et al., *Proc. ODP, Sci. Results,* 119: College Station, TX (Ocean Drilling Program), 869–891.

Barrows, T.T., Jugins, S., DeDeckker, P., Thiede, J., and Martinez, J.I., 2000. Sea-surface temperatures of the southwest Pacific Ocean during the Last Glacial Maximum. *Paleoceanogrpahy,* 15:95–109.

Berger, W.H., Bickert, T., Yasuda, M.K., and Wefer, G., 1996. Reconstruction of atmospheric CO_2 from the deep-sea record of Ontong Java Plateau: the Milankovitch chron. *Geol. Rundsch.,* 85:466–495.

Cande, S.C., and Kent, D.V., 1995. Revised calibration of the geomagnetic polarity timescale for the Late Cretaceous and Cenozoic. *J. Geophys. Res.,* 100:6093–6095.

Cande, S.C., Stock, J.M., Muller, R.D., Ishihara, T., 2000. Cenozoic motion between east and west Antarctica. *Nature,* 404:145–150.

Cape Roberts Science Team, 2000. Studies from the Cape Roberts Project, Ross Sea, Antarctica: initial Report on CRP-3. *Terra Antarct.,* 7.

Dickens, G.R., and Quinby-Hunt, M.S., 1997. Methane hydrate stability in pore water: a simple theoretical approach for geophysical applications. *J. Geophys. Res.,* 102:773–783.

Diester-Haass, L., and Zahn, R., 1996. Eocene-Oligocene transition in the Southern Ocean: history of water mass circulation and biological productivity. *Geology,* 24:163–166.

DiVenere, V.J., Kent, D.V., and Dalziel, I.W.D., 1994. Mid-Cretaceous paleomagnetic results from Marie Byrd Land, West Antarctica: a test of post-100 Ma relative motion between East and West Antarctica. *J. Geophys. Res.,* 99:15115–15139.

Ehrmann, W.U., 1991. Implications of sediment composition on the southern Kerguelen Plateau for paleoclimate and depositional environment. *In* Barron, J., Larsen, B., et al., *Proc. ODP, Sci. Results,* 119: College Station, TX (Ocean Drilling Program), 185–210.

Exon, N.F., Berry, R.F., Crawford A.J., and Hill, P.J., 1997a. Geological evolution of the East Tasman Plateau, a continental fragment southeast of Tasmania. *Aust. J. Earth Sci.,* 44:597–608.

Exon, N.F., Lee, C.S., Felton, E.A., Heggie, D., McKirdy, D., Penney, C., Shafik, S., Stephenson, A., and Wilson, C., 1992. BMR Cruise 67: Otway Basin and west Tasmanian sampling. *Rep.—Bur. Miner. Resour.* (Aust.), No. 306.

Exon, N.F., Moore, A.M.G., and Hill, P.J., 1997b. Geological framework of the South Tasman Rise, south of Tasmania, and its sedimentary basins. *Aust. J. Earth Sci.,* 44:561–577.

Exon, N.F., Royer, J-Y., and Hill, P.J., 1996. Tasmante cruise: swath-mapping and underway geophysics south and west of Tasmania. *Mar. Geophys. Res.,* 18:275–287.

Feary, D.A., Hine, A.C., Malone, M.J., et al., 2000. *Proc. ODP, Init. Repts.,* 182 [CD-ROM]. Available from: Ocean Drilling Program, Texas A&M University, College Station, TX 77845-9547, U.S.A.

Fitzgerald, P.G., 1992. The Transantarctic Mountains of southern Victoria Land: the application of apatite fission track analysis to rift shoulder uplift. *Tectonics,* 11:634–662.

Garner, D.M., 1959. The Subtropical Convergence in New Zealand waters. *N. Z. J. Geol. Geophys.,* 2:315–337.

Hall, R., 1996. Reconstructing Cenozoic SE Asia. *In* Hall, R., and Blundell, D.J. (Eds.), *Tectonic Evolution of Southeast Asia.* Geol. Soc. Spec. Publ. London, 106:153–184.

Haq, B.U., Hardenbol, J., and Vail, P.R., 1987. Chronology of fluctuating sea levels since the Triassic. *Science,* 235:1156–1167.

Hayes, D.E., Frakes, L.A., et al., 1975. *Init. Repts. DSDP,* 28: Washington (U.S. Govt. Printing Office).

Hesse, R., and Harrison, W.E., 1981. Gas hydrates (clathrates) causing pore-water freshening and oxygen isotope fractionation in deep-water sedimentary sections of terrigenous continental margins. *Earth Planet. Sci. Lett.,* 55:453–462.

Heusser, L.E., and Van de Geer, G., 1994. Direct correlation of terrestrial and marine paleoclimate records from four glacial-interglacial cycles; DSDP Site 594, Southwest Pacific. *In* Murray-Wallace, C.V.(Ed.), Quaternary marine and terrestrial records in Australasia; do they agree? *Quat. Sci. Rev.,* 13:273–282.

Hill, P.J., Exon, N.F., Royer, J.-Y., Whitmore, G., Belton, D., and Wellington, A., 1997a. Atlas of the offshore Tasmanian region: swath-mapping and geophysical maps from AGSO's 1994 Tasmante survey. *Aust. Geol. Surv. Organ.*

Hill, P.J., Meixner, A.J., Moore, A.M.G., and Exon, N.F., 1997b. Structure and development of the West Tasmanian offshore sedimentary basins: results of recent marine and aeromagnetic surveys. *Aust. J. Earth Sci.,* 44:579–596.

Hinz, K., and Shipboard Party, 1985. Geophysical, geological, and geochemical studies off west Tasmania and on the South Tasman Rise. *Bundes. Geowiss. Rohs. Cruise Rep.,* SO36B.

Hodell, D.A., Elmstrom, K.M., and Kennett, J.P., 1986. Latest Miocene benthic $\delta^{18}0$ changes, global ice volume, sea level, and the "Messinian salinity crisis." *Nature,* 320:411–414.

Hodell, D.A., and Venz, K., 1992. Toward a high-resolution stable isotopic record of the Southern Ocean during the Pliocene-Pleistocene (4.8 to 0.8 Ma). *In* Kennett, J.P., Warnke, D.A. (Eds.), *The Antarctic Paleoenvironment: A Perspective on Global Change* (Pt. 1). Am. Geophys. Union, Antarct. Res. Ser., 56:265–310.

Howard, W.R., and Prell, W.L., 1992. Late Quaternary surface circulation of the southern Indian Ocean and its relationship to orbital variations. *Paleoceanography,* 7:79–117.

Howard, W.R., and Prell, W.L., 1994. Late Quaternary carbonate production and preservation in the Southern Ocean: implications for oceanic and atmospheric carbon cycling. *Paleoceanography,* 9:453–482.

Imbrie, J., Boyle, E.A., Clemens, S.C., Duffy, A., Howard, W.R., Kukla, G., Kutzbach, J., Martinson, D.G., McIntyre, A., Mix, A.C., Molfino, B., Morley, J.J., Peterson, L.C., Pisias, N.G., Prell, W.L., Raymo, M.E., Shackleton, N.J., and Toggweiler, J.R., 1992. On the structure and origin of major glaciation cycles, 1. Linear responses to Milankovitch forcing. *Paleoceanography,* 7:701–738.

Imbrie, J., Boyle, E.A., Clemens, S.C., Duffy, A., Howard, W.R., Kukla, G., Kutzbach, J., Martinson, D.G., McIntyre, A., Mix, A.C., Molfino, B., Morley, J.J., Peterson, L.C., Pisias, N.G., Prell, W.L., Raymo, M.E., Shackleton, N.J., and Toggweiler, J.R., 1993. On the structure and origin of major glaciation cycles, 2. The 100,000-year cycle. *Paleoceanography,* 8:698–736.

Kastner, M., Elderfield, H., and Martin, J.B., 1991. Fluids in convergent margins: what do we know about their composition, origin, role in diagenesis and importance for oceanic chemical fluxes? *Philos. Trans. R. Soc. London A,* 335:243–259.

Kennett, J.P., 1977. Cenozoic evolution of Antarctic glaciation, the circum-Antarctic Ocean, and their impact on global paleoceanography. *J. Geophys. Res.,* 82:3843–3860.

Kennett, J.P., 1978. The development of planktonic biogeography in the Southern Ocean during the Cenozoic. *Mar. Micropaleontol.,* 3:301–345.

Kennett, J.P., and Barker, P.F., 1990. Latest Cretaceous to Cenozoic climate and oceanographic developments in the Weddell Sea, Antarctica: an ocean-drilling perspective. *In* Barker, P.F., Kennett, J.P., et al., *Proc. ODP, Sci. Results,* 113: College Station, TX (Ocean Drilling Program), 937–960.

Kennett, J.P., Houtz, R.E., Andrews, P.B., Edwards, A.R., Gostin, V.A., Hajos, M., Hampton, M.A., Jenkins, D.G., Margolis, S.V., Ovenshine, A.T., and Perch-Nielsen, K., 1974. Development of the Circum-Antarctic Current. *Science,* 186:144–147.

Kennett, J.P., Houtz, R.E., Andrews, P.B., Edwards, A.E., Gostin, V.A., Hajos, M., Hampton, M., Jenkins, D.G., Margolis, S.V., Ovenshine, A.T., and Perch-Nielsen, K., 1975. Cenozoic paleoceanography in the southwest Pacific Ocean, Antarctic glaciation, and the development of the Circum-Antarctic Current. *In* Kennett, J.P., Houtz, R.E., et al., *Init. Repts. DSDP,* 29: Washington (U.S. Govt. Printing Office), 1155–1169.

Kennett, J.P., Houtz, R.E., et al., 1975. *Init. Repts. DSDP,* 29: Washington (U.S. Govt. Printing Office).

Kennett, J.P., and Shackleton, N.J., 1976. Oxygen isotopic evidence for the development of the psychrosphere 38 Myr ago. *Nature,* 260:513–515.

Kennett, J.P., and Stott, L.D., 1990. Proteus and Proto-oceanus: ancestral Paleogene oceans as revealed from Antarctic stable isotopic results: ODP Leg 113. *In* Barker, P.F., Kennett, J.P., et al., *Proc. ODP, Sci. Results,* 113: College Station, TX (Ocean Drilling Program), 865–880.

Kennett, J.P., and von der Borch, C.C., 1986. Southwest Pacific Cenozoic paleoceanography. *In* Kennett, J.P., von der Borch, C.C., et al., *Init. Repts. DSDP,* 90 (Pt. 2): Washington (U.S. Govt. Printing Office), 1493–1517.

Lavin, C.J., 1997. The Maastrichtian breakup of the Otway Basin margin—a model developed by integrating seismic interpretation, sequence stratigraphy and thermochronological studies. *Explor. Geophys.* (Sydney), 28:252–259.

Lawver, L.A., Gahagan, L.M., and Coffin, M.F., 1992. The development of paleoseaways around Antarctica. *In* Kennett, J.P., and Warnke, D.A. (Eds.), *The Antarctic Paleoenvironment: a Perspective on Global Change.* Antarct. Res. Ser., 56:7–30.

McKerron, A.J., Dunn, V.L., Fish, R.M., Mills, C.R., and van der Linden-Dhont, S.K., 1998. Bass Strait's Bream B reservoir development: success through a multi-functional team approach. *APEA J.,* 38:13–35.

Miller, K.G., Fairbanks, R.G., and Mountain, G.S., 1987. Tertiary oxygen isotope synthesis, sea-level history, and continental margin erosion. *Paleoceanography,* 2:1–19.

Miller, K.G., Wright, J.D., and Fairbanks, R.G., 1991. Unlocking the Ice House: Oligocene-Miocene oxygen isotopes, eustasy, and margin erosion. *J. Geophys. Res.,* 96:6829–6848.

Mohr, B.A.R., 1990. Eocene and Oligocene sporomorphs and dinoflagellate cysts from Leg 113 drill sites, Weddell Sea, Antarctica. *In* Barker, P.F., Kennett, J.P., et al., *Proc. ODP, Sci. Results,* 113: College Station, TX (Ocean Drilling Program), 595–612.

Moore, A.M.G., Willcox, J.B., Exon, N.F., and O'Brien, G.W., 1992. Continental shelf basins on the west Tasmania margin. *APEA J.,* 32:231–250.

Müller, R.D., Royer, J.Y., and Lawver, L.A., 1993. Revised plate motions relative to the hotspots from combined Atlantic and Indian-Ocean hotspot tracks. *Geology,* 21:275–278.

Murphy, M.G., and Kennett, J.P., 1986. Development of latitudinal thermal gradients during the Oligocene: oxygen-isotope evidence from the southwest Pacific. *In* Kennett, J.P., von der Borch, C.C., et al., *Init. Repts. DSDP,* 90: Washington (U.S. Govt. Printing Office), 1347–1360.

Mutter, J.C., Hegarty, K.A., Cande, S.C., and Weissel, J.K., 1985. Breakup between Australia and Antarctica: a brief review in the light of new data. *Tectonophysics,* 114:255–279.

Oppo, D.W., Fairbanks, R.G., Gordon, A.L., and Shackleton, N.J., 1990. Late Pleistocene Southern Ocean $\delta^{13}C$ variability. *Paleoceanography,* 5:43–54.

Orsi, A.H., Whitworth, T., III, and Nowlin, W.D., Jr., 1995. On the meridional extent and fronts of the Antarctic Circumpolar Current. *Deep-Sea Res.,* 42:641–673.

O'Sullivan, P.B., Foster, D.A., Kohn, B.P., Gleadow, A.J.W., and Raza, A., 1995. Constraints on the dynamics of rifting and denudation on the eastern margin of Australia: fission track evidence for two discrete causes of rock cooling. *In* Mauk, J.L., and St. George, J.D. (Eds.), *Proceedings of the 1995 Pacific Rim Congress: Exploring the rim.* Australas. Inst. Min. Metall. Publ. Ser., 9:441–446.

Paull, C.K., Matsumoto, R., Wallace, P.J., et al., 1996. *Proc. ODP, Init. Repts.,* 164: College Station, TX (Ocean Drilling Program).

Perry, E.A., and Hower, J., 1972. Late-stage dehydration in deeply buried pelitic sediments. *AAPG Bull.,* 56:2013–2021.

Piper, D.J.W., and Brisco, C.B., 1975. Deep-water continental-margin sedimentation, DSDP Leg 28, Antarctica. *Init. Repts., DSDP,* 28: Washington (U.S. Govt. Printing Office), 727–755.

Pyle, D.G., Christie, D.M., Mahoney, J.J., and Duncan, R.A., 1995. Geochemistry and geochronology of ancient southeast Indian and southwest Pacific seafloor. *J. Geophys. Res.,* 100:22261–22282.

Pye, K., 1987. *Aeolian Dust and Dust Deposits:* London (Academic Press).

Quilty, P.G., 1997. Eocene and younger biostratigraphy and lithofacies of the Cascade Seamount, East Tasman Plateau, Southwest Pacific Ocean. *Aust. J. Earth Sci.,* 44:655–665.

Rintoul, S.R., and Bullister, J.L., 1999. A late winter hydrographic section from Tasmania to Antarctica. *Deep-Sea Res. Part I,* 46:1417–1454.

Robert, C., and Kennett, J.P., 1997. Antarctic continental weathering changes during Eocene-Oligocene cryosphere expansion: clay mineral and oxygen isotope evidence. *Geology,* 25:587–590.

Royer, J.-Y., and Rollet, N., 1997. Plate-tectonic setting of the Tasmanian region. *In* Exon, N.F., and Crawford, A.J. (Eds.), *West Tasmanian Margin and Offshore Plateaus: Geology, Tectonic and Climatic History, and Resource Potential.* Aust. J. Earth Sci., 44:543–560.

Ruddiman, W.F., Raymo, M.E., Martinson, D.G., Clement, B.M., and Backman, J., 1989. Pleistocene evolution: Northern Hemisphere ice sheets and North Atlantic Ocean. *Paleoceanography,* 4:353–412.

Salamy, K.A., and Zachos, J.C., 1999. Latest Eocene-early Oligocene climate change and Southern Ocean fertility: inferences from sediment accumulation and stable isotope data. *Palaeogeogr., Palaeoclimatol., Palaeoecol.,* 145:61–77.

Shackleton, N.J., and Kennett, J.P., 1975. Paleotemperature history of the Cenozoic and the initiation of Antarctic glaciation: oxygen and carbon isotope analyses in DSDP Sites 277, 279, and 281. *In* Kennett, J.P., Houtz, R.E., et al., *Init. Repts. DSDP,* 29: Washington (U.S. Govt. Printing Office), 743–755.

Shipboard Scientific Party, in press. *Proc. ODP, Init. Repts.,* 188: College Station, TX (Ocean Drilling Program).

Smith, G.C., 1985. Bass Basin geology and petroleum exploration. *In* Glenie, R.C. (Ed.), *Second South-Eastern Australia Oil Exploration Symposium: technical papers presented at the PESA symposium.* Pet. Expl. Soc. Aust., 257–284.

Sloan, E.D. Jr., 1998. Clathrate hydrates of natural gases. 2nd Ed. New York: Marcel Dekkenr, Inc. 705.

Stott, L.D., Kennett, J.P., Shackleton, N.J., and Corfield, R.M., 1990. The evolution of Antarctic surface waters during the Paleogene: inferences from the stable isotopic composition of planktonic foraminifers, ODP Leg 113. *In* Barker, P.F., Kennett, J.P., et al., *Proc. ODP, Sci. Results,* 113: College Station, TX (Ocean Drilling Program), 849–863.

Trenberth, K.E., and Solomon, A., 1994. The global heat balance: heat transports in the atmosphere and ocean. *Clim. Dyn.,* 10:107–134.

Velde, B., 1983. Diagenetic reactions in clays. *In* Parker, A., and Sellwood, B.W. (Eds.), *Sediment Diagenesis:* Boston (D. Reidel), 215–268.

Wei, W., 1991. Evidence for an earliest Oligocene abrupt cooling in the surface waters of the Southern Ocean. *Geology,* 19:780–783.

Wei, W., and Thierstein, H.R., 1991. Upper Cretaceous and Cenozoic calcareous nannofossils of the Kerguelen Plateau (southern Indian Ocean) and Prydz Bay (East Antarctica). *In* Barron, J., Larsen, B., et al., *Proc. ODP, Sci. Results,* 119: College Station, TX (Ocean Drilling Program), 467–494.

Wei, W., Villa, G., and Wise, S.W., Jr., 1992. Paleoceanographic implications of Eocene-Oligocene calcareous nannofossils from Sites 711 and 748 in the Indian Ocean. *In* Wise, S.W., Jr., Schlich, R., et al., *Proc. ODP, Sci. Results,* 120: College Station, TX (Ocean Drilling Program), 979–999.

Wei, W., and Wise, S.W., Jr., 1990. Biogeographic gradients of middle Eocene-Oligocene calcareous nannoplankton in the South Atlantic Ocean. *Palaeogeogr., Palaeoclimatol., Palaeoecol.,* 79:29–61.

Weissel, J.K., and Hayes, D.E., 1972. Magnetic anomalies in the southeast Indian Ocean. *In* Hayes, D.E. (Ed.), *Antarctic Oceanology* (Vol. 2): *The Australian-New Zealand Sector.* Antarct. Res. Ser., 19:165–196.

Willcox, J.B., and Stagg, H.M.J., 1990. Australia's southern margin: a product of oblique extension. *Tectonophysics,* 173:269–281.

Wright, J.D., Miller, K.G., and Fairbanks, R.G., 1991. Evolution of modern deepwater circulation; evidence from the late Miocene Southern Ocean. *Paleoceanography,* 6:275–290.

Zachos, J.C., Breza, J.R., and Wise, S.W., 1992. Early Oligocene ice-sheet expansion on Antarctica: stable isotope and sedimentological evidence from Kerguelen Plateau, southern Indian Ocean. *Geology,* 20:569–573.

Zachos, J.C., Lohmann, K.C., Walker, J.C.G., and Wise, S.W., Jr., 1993. Abrupt climate change and transient climates during the Paleogene: a marine perspective. *J. Geol.,* 101:191–213.

Zachos, J.C., Quinn, T.M., and Salamy, K.A., 1996. High-resolution (10^4 years) deep-sea foraminiferal stable isotope records of the Eocene-Oligocene Climate transition. *Paleoceanography,* 11:251–266.

Zachos, J.C., Stott, L.D., and Lohmann, K.C., 1994. Evolution of early Cenozoic marine temperatures. *Paleoceanography,* 9:353–387.

TABLE CAPTIONS

Table 1. Deep Sea Drilling Project sites off Tasmania.

Table 2. Leg 189 operations summary.

Table 3. Summary of magnetostratigraphy.

Table 4. Tectonic history of DSDP and ODP sites in the region.

FIGURE CAPTIONS

Figure 1. Antarctica and surrounding continents at the Cretaceous/Tertiary boundary, during early Oligocene and during earliest Miocene times showing the change from meridional to Antarctic Circumpolar Current circulation that brought about the thermal isolation of Antarctica (modified from Kennett, 1978).

Figure 2. Global sea level, tectonism, and ice volume (after Barrett, 1994). Left curve is from Atlantic benthic foraminifers (Miller et al., 1987); right curve is from seismic sequence analysis (Haq et al., 1987).

Figure 3. Bathymetry of the offshore Tasmanian region, making use of Tasmante swath bathymetry. Solid circles = Leg 189 sites. Crosses = DSDP sites. Squares = *Marion Dufresne* 1997 piston core sites. Seismic profiles shown in Figure 8 are solid lines. Contours are in meters.

Figure 4. Trajectory of the South Tasman Rise with respect to Antarctica (J.-Y. Royer, unpubl. data). Because Antarctica has remained stable relative to the South Pole since the Cretaceous (e.g. Müller et al., 1993; DiVenere et al., 1994), it also shows the paleolatitudes of the South Tasman Rise. The close correspondence between the hot spot trace (dashed line) and the trace with Antarctica fixed (solid line) adds confidence to the interpretation (ages after Cande and Kent, 1995, magnetic reversal time scale; magnetic chrons are in parentheses).

Figure 5. Plate tectonic setting of the Tasmanian region within Gondwana during the earliest Late Cretaceous (95 Ma) modified after Royer and Robert (1997), showing a zone of strike-slip faulting (Tasmanian-Antarctic Shear Zone) and areas of rift sedimentation. W-STR = west South Tasman Rise; E-STR = east South Tasman Rise; ETP = East Tasman Plateau.

Figure 6. Paleogeographic map of Tasmanian region during the middle Eocene (40 Ma) based partly on Royer and Rollet (1997, fig. 10C) and on Leg 189 results. Solid circles = DSDP Leg 29 sites. Open circles with dots = Leg 189 sites. Late Cretaceous oceanic crust was covered with deep Pacific Ocean, and Eocene oceanic crust with bathyal ocean. Most of the Tasmania-South Tasman Rise region was covered in shallow seas. Shallow-water connections between the restricted Australo-Antarctic Gulf to the west and Pacific Ocean may have been established both north and south of the South Tasman Rise.

Figure 7. Paleogeographic map of the Tasmanian region at the Eocene/Oligocene boundary (33.5 Ma) based partly on Royer and Rollet (1997, fig. 8) and Leg 189 results. Solid circles = DSDP Leg 29 sites. Open circles with dots = Leg 189 sites. Most oceanic crust was covered with deep water, and most of the Tasmania/South Tasman Rise region was covered in bathyal seas. A deep-water connection between the restricted Australo-Antarctic Gulf to the west and the Pacific Ocean had just been established south of the STR, allowing the onset of circum-Antarctic circulation.

Figure 8. Cross-sections from seismic profiles across the region showing DSDP and proposed high-priority ODP sites. P1 = West Tasmania; P2, P3 = South Tasman Rise; and P4 = East Tasman Plateau. Site locations are shown in Figure 3.

Figure 9. Map of structures and minimum sediment thickness of the area west and south of Tasmania after Hill et al. (1997a), based on multichannel seismic profiles. ODP and DSDP sites are shown. TWT = two-way traveltime.

Figure 10. Sketch map of Cretaceous and Paleogene movements, relative to a fixed Tasmania, of the western South Tasman Rise block, eastern South Tasman Rise block, and East Tasman Plateau (modified from Exon et al., 1997b).

Figure 11. The oceanographic fronts in the Southern Ocean south of Tasmania after Rintoul and Bullister (1999). STF = Subtropical Front. SAF = Subantarctic Front. PF = Polar Front.

Figure 12. Postdrilling interpretation for local seismic profile SO 36-47, across Site 1168, showing broad ages and lithostratigraphic units. The site is on a gentle slope to the west. Note the thick Oligocene sequence. The long-wavelength hummocks in the late Eocene may represent delta distributaries. There is almost no seismic character in the younger sequences, but three age/lithostratigraphic boundaries are marked by reflectors: Me, Oe, and El. Siliciclastic material has been shed from a ridge upslope into the Eocene and Oligocene sequences. TD = total depth.

Figure 13. Postdrilling interpretation for local seismic profile AGSO 125-14, across Site 1170, showing broad ages and lithostratigraphic units. This shows the site's position just west of the high central block and the evidence of Miocene scouring that removed the Oligocene and late Eocene sequences. Note the thick Pliocene-Pleistocene and the reduced Oligocene sections at this site. TD = total depth.

Figure 14. Postdrilling interpretation for local seismic profile AGSO 202-5, across Site 1171, showing broad ages and lithostratigraphic units. The site is in a north-south strike-slip basin on the central block of the South Tasman Rise, just west of the trace of the Balleny Fracture Zone block (and the eastern block of the Rise). It is the only site that penetrated the Paleocene, and the relationships at the Paleocene/Eocene unconformity indicate that the fracture zone's last movement was in the late Paleocene. This probably represents the time of initial spreading to the south. Note the thick Eocene, the very thin Oligocene, and the thin Pliocene–Pleistocene sections at this site. TD = total depth.

Figure 15. Postdrilling interpretation for local seismic profile AGSO 125-4, across Site 1172, showing broad ages and lithostratigraphic units. Drilling directly dated the three upper unconformities (A–C), and helped control the possible ages of the lower unconformities (D and E). Note the thick middle Eocene and Miocene to Holocene, and the virtually absent Oligocene and late Eocene sections at this site. TD = total depth.

Figure. 16. Summary of lithologies, Leg 189 sites 1168 through 1172. TD = total depth.

Figure 17. Comparison of major age stratigraphic units by depth for Leg 189 Sites 1168 through 1172. TD = total depth. L* = straddles the Eocene/Oligocene boundary.

Figure 18. Summary stratigraphic and sediment facies for Leg 189 sites 1168 through 1172, arranged west to east. Major lithologies against time show major hiatuses.

Figure 19. Sedimentation rate summary curves for Leg 189 sites 1168 through 1172.

Figure 20. Downhole natural gamma and medium resistivity results from Holes 1168A, 1170D, 1171D, and 1172D. Higher gamma values are often indicative of an increased terrigenous component and/or organic material in the sediment, whereas higher resitivities are often associated with increased lithification and/or decreased porosity. The distinct lithologic change close to the Eocene/Oligocene boundary, from siliciclastic glauconitic claystone to nannofossil chalk and ooze, can be clearly seen in Holes 1168A (~260 mbsf), 1171D (~270 mbsf) and 1172D (~360 mbsf).

Figure 21. Summary of organic geochemistry results. The upper panel shows carbonate content (in weight percent $CaCO_3$), whereas the lower panel presents total organic matter content and hydrogen indices. Also shown are regional correlations and approximate location of lithostratigraphic units and age.

Figure 22. Summary of interstitial water geochemistry results for Sites 1168, 1170, 1171, and 1172. The upper panel shows Cl^- and methane profiles. Intervals with Cl^- values less than mean seawater (i.e., fresher waters) are shaded. The lower panel shows concentration-depth profiles for selected interstitial water constituents. The approximate location of the Eocene–Oligocene (E/O) transition is also shown.

Figure 23. Schematic diagram showing inferred surface-water circulation of the Australian-Antarctic region during the middle Eocene (43.7 Ma) with the Tasmanian Gateway closed. Plate tectonic reconstruction is modified from Cande et al. (2000). Note the influence of the East Australian Current on the Antarctic margin in the absence of circum-Antarctic circulation. Weak gyral circulation is inferred in the highly restricted Australo-Antarctic Gulf. ODP Leg 189 and DSDP Leg 29 site locations are indicated.

Figure 24. Schematic diagram showing inferred surface water-circulation of the Australian-Antarctic region during the earliest Oligocene (33 Ma). Plate tectonic reconstruction is modified from Cande et al. (2000). At this time, the Tasmanian Gateway was initially open to deep-water circum-Antarctic circulation between the South Tasman Rise and Antarctica. Note that early development of circum-Antarctic circulation began to decrease the influence of the East Australian Current on the Antarctic continental margin.

Figure 25. Schematic diagram showing inferred surface water circulation of the Australian-Antarctic region during the late Oligocene (26 Ma). Plate tectonic reconstruction is modified from Cande et al. (2000). At this time, the Antarctic cryosphere had increased significantly. The expansion of the Antarctic Circumpolar Current (ACC) continued as the South Tasman Rise and Tasmania moved northward from Antarctica. Note increasing decoupling of the East Australian current from the Antarctic margin associated with the increasing strength of the ACC.

Table 1. Deep Sea Drilling Project sites off Tasmania.

Site	Latitude (S) Longitude (N)	Water depth (m)	Penetration (m)	Total recovery	Maximum age sediment	Basement type
280	48° 57.44' 147° 14.08'	4176	524	19%	early to middle Miocene	Intrusive basalt
281	47° 59.84' 147° 45.85'	1591	169	62%	late Eocene	Late carboniferous schist
282	42° 14.76' 143° 29.18'	4202	310	20%	late Eocene	Pillow basalt
283	43° 54.60' 154° 16.96'	4729	592	10%	Paleocene	Altered basalt

Table 1

Table 2. Leg 189 operations summary.

Hole	Latitude	Longitude	Water depth (mbsl)	Number of cores	Interval cored (m)	Core recovered (m)	Recovery (%)	Interval drilled (m)	Total penetration (mbsf)	Time on site (days)
1168A	42° 36.5809′S	144° 24.7620′E	2463.3	95	883.5	837.10	94.7	0.0	883.5	7.6
1168B	42° 36.5692′S	144° 24.7594′E	2463.6	12	108.4	106.52	98.3	0.0	108.4	0.6
1168C	42° 36.5533′S	144° 24.7614′E	2464.0	31	290.5	248.15	85.4	0.0	290.5	1.4
			Site 1168 totals:	138	1282.4	1191.77	92.9	0.0	1282.4	9.5
1169A	47° 03.9159′S	145° 14.2089′E	3567.9	26	246.3	225.02	91.4	0.0	246.3	2.8
			Site 1169 totals:	26	246.3	225.02	91.4	0.0	246.3	2.8
1170A	47° 09.0435′S	146° 02.9881′E	2704.7	52	464.3	379.83	81.8	0.0	464.3	1.7
1170B	47° 09.0344′S	146° 02.9846′E	2704.6	19	175.8	179.67	102.2	0.0	175.8	2.1
1170C	47° 09.0226′S	146° 02.9871′E	2703.3	19	180.1	179.64	99.7	0.0	180.1	1.2
1170D	47° 09.0107′S	146° 02.9829′E	2704.7	38	354.8	287.69	81.1	425.0	779.8	6.0
			Site 1170 totals:	128	1175.0	1026.83	87.4	425.0	1600.0	11.0
1171A	48° 29.9960′S	149° 06.6901′E	2148.2	14	124.4	117.52	94.5	0.0	124.4	0.9
1171B	48° 29.9854′S	149° 06.6863′E	2148.0	12	108.8	106.73	98.1	0.0	108.8	0.5
1171C	48° 29.9971′S	149° 06.7051′E	2147.8	31	274.8	245.58	89.4	0.0	274.8	1.2
1171D	48° 29.9975′S	149° 06.7222′E	2147.8	75	711.2	525.40	73.9	247.6	958.8	7.4
			Site 1171 totals:	132	1219.2	995.23	81.6	247.6	1466.8	10.0
1172A	43° 57.5854′S	149° 55.6961′E	2621.9	56	522.6	483.87	92.6	0.0	522.6	3.0
1172B	43° 57.5750′S	149° 55.7010′E	2622.3	22	202.4	206.70	102.1	0.0	202.4	1.0
1172C	43° 57.5684′S	149° 57.5684′E	2621.7	18	171.0	172.54	100.9	0.0	171.0	1.1
1172D	43° 57.5545′S	149° 55.7169′E	2621.7	31	297.9	237.09	79.6	468.6	766.5	5.4
			Site 1172 totals:	127	1193.9	1100.20	92.2	468.6	1662.5	10.5
			Leg 189 totals:	551	5116.8	4539.05	88.7	1141.2	6258.0	43.8

Table 2

Table 3. Summary of magnetostratigraphy.

	Chron	Age (Ma)	1168 (mbsf)	1169 (mbsf)	1170 (mbsf)	1171 (mbsf)	1172 (mbsf)		Chron
O	C1n	0.780	3.75	3.5	28.2	12.6	12.5	O	C1n
T	C1r.1n	0.990		6	35	14.9		T	C1r.1n
O	C1r.1n	1.070	9		39.9	16.5		O	C1r.1n
T	C1r.2r-1n	1.201						T	C1r.2r-1n
O	C1r.2r-1n	1.211						O	C1r.2r-1n
T	C2n	1.770	28.1	19.2	60.4	24	17.1	T	C2n
O	C2n	1.950	42.9		68	26	19.55	O	C2n
T	C2r.1n	2.140						T	C2r.1n
O	C2r.1n	2.150						O	C2r.1n
T	C2An.1n	2.581		40.6	83.7	31.75	30.9	T	C2An.1n
O	C2An.1n	3.040				34.5	36.9	O	C2An.1n
T	C2An.2n	3.110				35.6	38.6	T	C2An.2n
O	C2An.2n	3.220			96.2		40.2	O	C2An.2n
T	C2An.3n	3.330					41.7	T	C2An.3n
O	C2An.3n	3.580					46.25	O	C2An.3n
T	C3n.1n	4.180					57.8	T	C3n.1n
O	C3n.1n	4.290			126		60	O	C3n.1n
T	C3n.2n	4.462			128.5		63.4	T	C3n.2n
O	C3n.2n	4.480			130.5		66.6	O	C3n.2n
T	C3n.3n	4.800			133.5			T	C3n.3n
O	C3n.3n	4.890			135.2			O	C3n.3n
T	C3n.4n	4.980			135.8		78.9	T	C3n.4n
O	C3n.4n	5.230			138		94.1	O	C3n.4n
T	C3An.1n	5.894			144.2		100.7	T	C3An.1n
O	C3An.1n	6.137			150.3		105.4	O	C3An.1n
T	C3An.2n	6.269			152.9		107.4	T	C3An.2n
O	C3An.2n	6.567			157.25			O	C3An.2n
T	C3Bn	6.935					121.5	T	C3Bn
O	C3Bn	7.091					124.2	O	C3Bn
T	C3Br.1n	7.135					125.4	T	C3Br.1n
O	C3Br.1n	7.170					126.8	O	C3Br.1n
T	C3Br.2n	7.341						T	C3Br.2n
O	C3Br.2n	7.375						O	C3Br.2n
T	C4n.1n	7.432						T	C4n.1n
O	C4n.1n	7.562						O	C4n.1n
T	C4n.2n	7.650						T	C4n.2n
O	C4n.2n	8.072					146.9	O	C4n.2n
T	C4r.1n	8.225					149.2	T	C4r.1n
O	C4r.1n	8.257					150.3	O	C4r.1n
T	C4An	8.699					154.2	T	C4An
O	C4An	9.025					167	O	C4An
T	C4Ar.1n	9.230					169.2	T	C4Ar.1n
O	C4Ar.1n	9.308					169.8	O	C4Ar.1n
T	C4Ar.2n	9.580					174	T	C4Ar.2n
O	C4Ar.2n	9.642					175	O	C4Ar.2n
T	C5n.1n	9.740				80	176.7	T	C5n.1n
O	C5n.1n	9.880				82.5		O	C5n.1n
T	C5n.2n	9.920				83.5		T	C5n.2n
O	C5n.2n	10.949				107.75	215	O	C5n.2n
T	C5r.1n	11.052				109.5		T	C5r.1n
O	C5r.1n	11.099				113		O	C5r.1n
T	C5r.2n	11.476				123		T	C5r.2n
O	C5r.2n	11.531						O	C5r.2n
T	C5An.1n	11.935				129.75	245	T	C5An.1n
O	C5An.1n	12.078				130.6		O	C5An.1n
T	C5An.2n	12.184				133.4		T	C5An.2n
O	C5An.2n	12.401				134.5		O	C5An.2n

T	C5Ar.1n	12.678						T C5Ar.1n
O	C5Ar.1n	12.708						O C5Ar.1n
T	C5Ar.2n	12.775						T C5Ar.2n
O	C5Ar.2n	12.819						O C5Ar.2n
T	C5AAn	12.991			264			T C5AAn
O	C5AAn	13.139			268.5			O C5AAn
T	C5ABn	13.302			273			T C5ABn
O	C5ABn	13.510			277			O C5ABn
T	C5ACn	13.703			278	156		T C5ACn
O	C5ACn	14.076			283.5	159.35		O C5ACn
T	C5ADn	14.178			286	161.3		T C5ADn
O	C5ADn	14.612			292	167.2		O C5ADn
T	C5Bn.1n	14.800			294			T C5Bn.1n
O	C5Bn.1n	14.888			296			O C5Bn.1n
T	C5Bn.2n	15.034			297.5			T C5Bn.2n
O	C5Bn.2n	15.155						O C5Bn.2n
T	C5Cn.1n	16.014	252.6		308			T C5Cn.1n
O	C5Cn.1n	16.293			310.5			O C5Cn.1n
T	C5Cn.2n	16.327			311			T C5Cn.2n
O	C5Cn.2n	16.488			314			O C5Cn.2n
T	C5Cn.3n	16.556						T C5Cn.3n
O	C5Cn.3n	16.726	257					O C5Cn.3n
T	C5Dn	17.277	264.3					T C5Dn
O	C5Dn	17.615	272.3		323			O C5Dn
T	C5En	18.281	281.9				320	T C5En
O	C5En	18.781	287.6		338		323.5	O C5En
T	C6n	19.048	321.5		341	207.2	326	T C6n
O	C6n	20.131	347.3			223.5	337	O C6n
T	C6An.1n	20.518						T C6An.1n
O	C6An.1n	20.725						O C6An.1n
T	C6An.2n	20.996						T C6An.2n
O	C6An.2n	21.320						O C6An.2n
T	C6AAn	21.768						T C6AAn
O	C6AAn	21.859						O C6AAn
T	C6AAr.1n	22.151						T C6AAr.1n
O	C6AAr.1n	22.248						O C6AAr.1n
T	C6AAr.2n	22.459						T C6AAr.2n
O	C6AAr.2n	22.493						O C6AAr.2n
T	C6Bn.1n	22.588						T C6Bn.1n
O	C6Bn.1n	22.750						O C6Bn.1n
T	C6Bn.2n	22.804						T C6Bn.2n
O	C6Bn.2n	23.069						O C6Bn.2n
T	C6Cn.1n	23.353						T C6Cn.1n
O	C6Cn.1n	23.535						O C6Cn.1n
T	C6Cn.2n	23.677						T C6Cn.2n
O	C6Cn.2n	23.800						O C6Cn.2n
T	C6Cn.3n	23.999						T C6Cn.3n
O	C6Cn.3n	24.118						O C6Cn.3n
T	C7n.1n	24.730			393.4		346	T C7n.1n
O	C7n.1n	24.781			394			O C7n.1n
T	C7n.2n	24.835			395			T C7n.2n
O	C7n.2n	25.183			399			O C7n.2n
T	C7An	25.496			402			T C7An
O	C7An	25.648			403			O C7An
T	C8n.1n	25.823			404.5			T C8n.1n
O	C8n.1n	25.951						O C8n.1n
T	C8n.2n	25.992						T C8n.2n
O	C8n.2n	26.554						O C8n.2n
T	C9n	27.027						T C9n
O	C9n	27.972						O C9n
T	C10n.1n	28.283						T C10n.1n
O	C10n.1n	28.512						O C10n.1n

Table 3 (continued)

T	C10n.2n	28.578				T	C10n.2n
O	C10n.2n	28.745				O	C10n.2n
T	C11n.1n	29.401			356	T	C11n.1n
O	C11n.1n	29.662			356.8	O	C11n.1n
T	C11n.2n	29.765			357.3	T	C11n.2n
O	C11n.2n	30.098			358.6	O	C11n.2n
T	C12n	30.479				T	C12n
O	C12n	30.939				O	C12n
T	C13n	33.058				T	C13n
O	C13n	33.545				O	C13n
T	C15n	34.655				T	C15n
O	C15n	34.940				O	C15n
T	C16n.1n	35.343				T	C16n.1n
O	C16n.1n	35.526				O	C16n.1n
T	C16n.2n	35.685			361	T	C16n.2n
O	C16n.2n	36.341			362.5	O	C16n.2n
T	C17n.1n	36.618			362.8	T	C17n.1n
O	C17n.1n	37.473			366	O	C17n.1n
T	C17n.2n	37.604				T	C17n.2n
O	C17n.2n	37.848				O	C17n.2n
T	C17n.3n	37.920			367.2	T	C17n.3n
O	C17n.3n	38.113			374	O	C17n.3n
T	C18n.1n	38.426			383	T	C18n.1n
O	C18n.1n	39.552				O	C18n.1n
T	C18n.2n	39.631				T	C18n.2n
O	C18n.2n	40.130			415	O	C18n.2n
T	C19n	41.257			430	T	C19n
O	C19n	41.521			432	O	C19n
T	C20n	42.536			440	T	C20n
O	C20n	43.789				O	C20n
T	C21n	46.264		523		T	C21n
O	C21n	47.906		571		O	C21n
T	C22n	49.037				T	C22n
O	C22n	49.714				O	C22n
T	C23n.1n	50.778				T	C23n.1n
O	C23n.1n	50.946			555	O	C23n.1n
T	C23n.2n	51.047			569	T	C23n.2n
O	C23n.2n	51.743				O	C23n.2n
T	C24n.1n	52.364				T	C24n.1n
O	C24n.1n	52.663				O	C24n.1n
T	C24n.2n	52.757				T	C24n.2n
O	C24n.2n	52.801				O	C24n.2n
T	C24n.3n	52.903				T	C24n.3n
O	C24n.3n	53.347		773	594	O	C24n.3n
T	C25n	55.904		889		T	C25n
O	C25n	56.391				O	C25n
T	C26n	57.554				T	C26n
O	C26n	57.911				O	C26n
T	C27n	60.920				T	C27n
O	C27n	61.276				O	C27n
T	C28n	62.499				T	C28n
O	C28n	63.634				O	C28n
T	C29n	63.976				T	C29n
O	C29n	64.745				O	C29n

Notes: O = onset. T = termination.

Table 3 (continued)

Table 4. Tectonic history of DSDP and ODP sites in the region.

Site	Block/basin	Oldest sediment near site	Probable breakup age (Ma)	Siliciclastic/ carbonate transition	Subsidence since Eocene (no correction for sediment loading)
282	Sorell Basin	Early Cretaceous	55 (west)	Oligocene/ Miocene	3800 *
1168	Sorell Basin	Early Cretaceous	55 (west)	Eocene/ Oligocene	3100 †
1170	West STR	Late Cretaceous	55 (south) 34 (west)	Eocene/ Oligocene	3100 †
281	Central STR	Late Cretaceous	75 (east) 55 (south) 34 (west)	Oligocene/ Miocene	1600 †
1171	Central STR	L Cretaceous	75 (east) 55 (south) 34 (west)	Eocene/ Oligocene	2300 †
280	Southern oceanic crust	Eocene	55 (north)	Within Eocene: to diatom ooze	3200 ‡
1172	East Tasman Plateau	Cretaceous	75 (east and west)	Eocene/ Oligocene	2500 †
283	Tasman Sea oceanic crust	Paleocene	75 (west)	none	3700 ‡

Notes: STR = South Tasman Rise. * = assuming latest Eocene water depth of ~500 m. † = assuming latest Eocene water depth of ~100 m. ‡ = assuming latest Eocene water depth of ~1000 m.

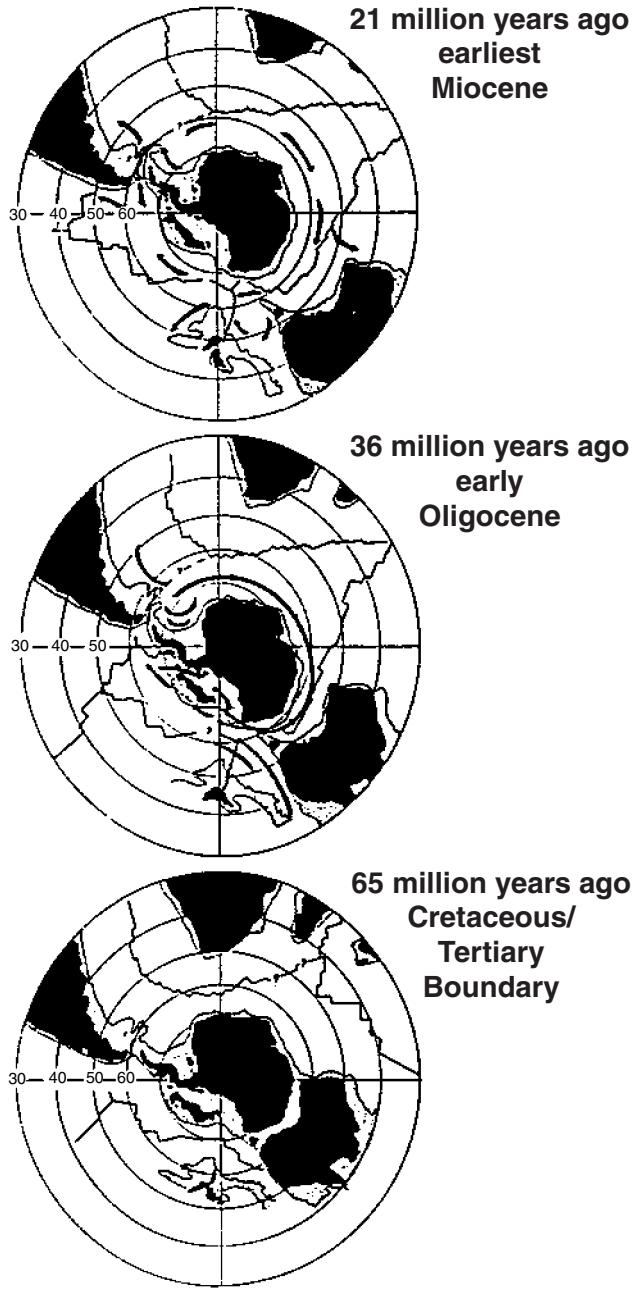
21 million years ago
earliest
Miocene
30
40
50
60
36 million years ago
early
Oligocene
30
40
50
65 million years ago
Cretaceous/
Tertiary
Boundary
30
40
50
60

Figure 1

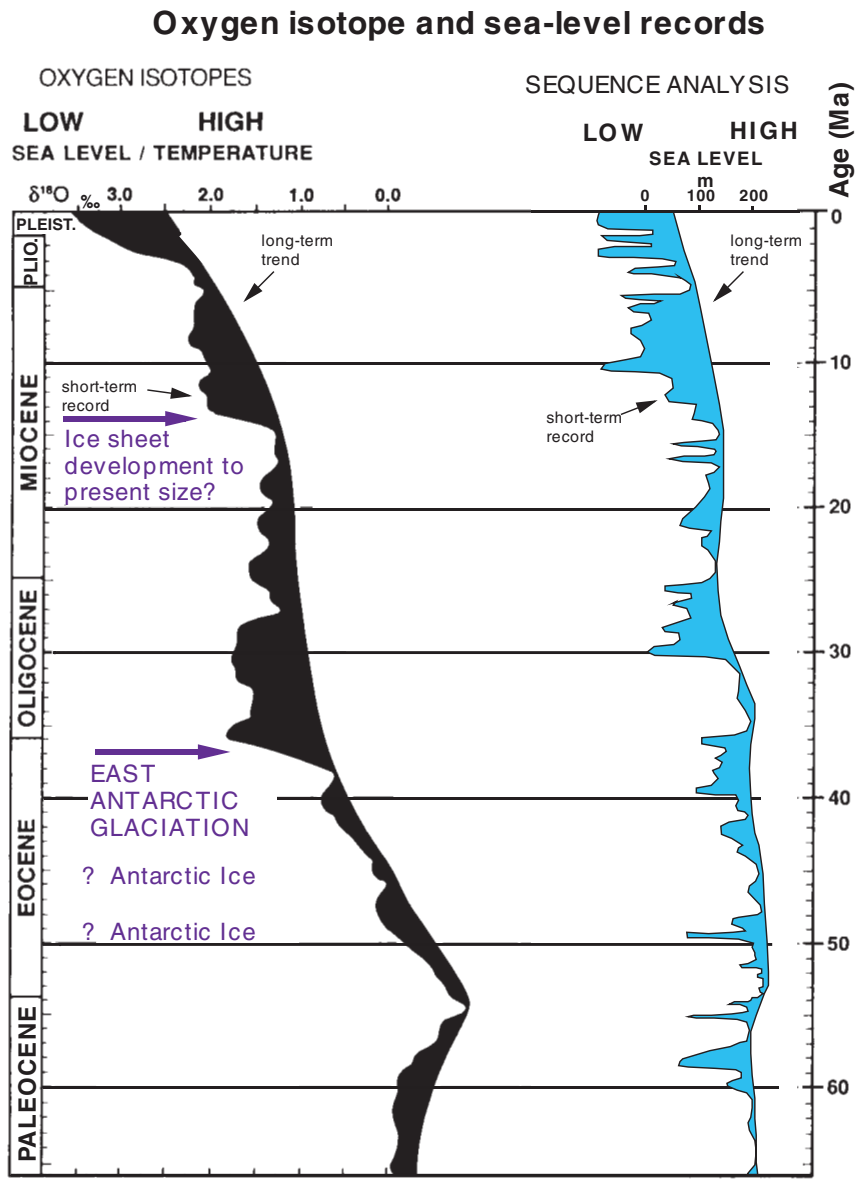

1‰ $\delta^{18}O$ = 110 m below sea level or 4°C water - temperature change
(modified from Barrett, 1994)

Figure 2

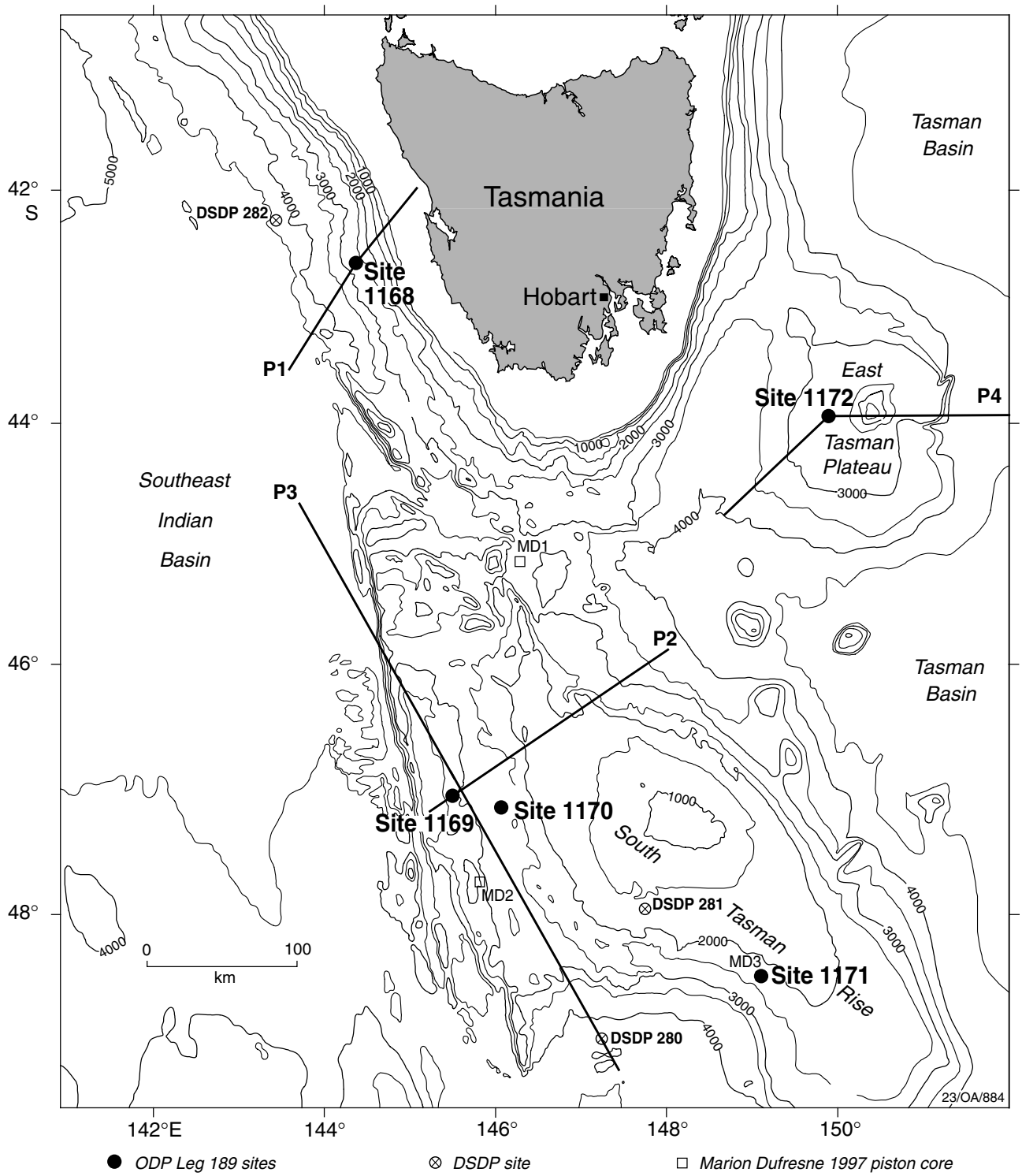
Tasmania
Hobart
Tasman Basin
East Tasman Plateau
Southeast Indian Basin
South Tasman Rise
DSDP 282
DSDP 281
DSDP 280
Site 1168
Site 1169
Site 1170
Site 1171
Site 1172
P1
P2
P3
P4
MD1
MD2
MD3
5000
4000
3000
2000
1000
0
100
km
42° S
44°
46°
48°
142°E
144°
146°
148°
150°
23/OA/884
ODP Leg 189 sites
DSDP site
Marion Dufresne 1997 piston core

Figure 3

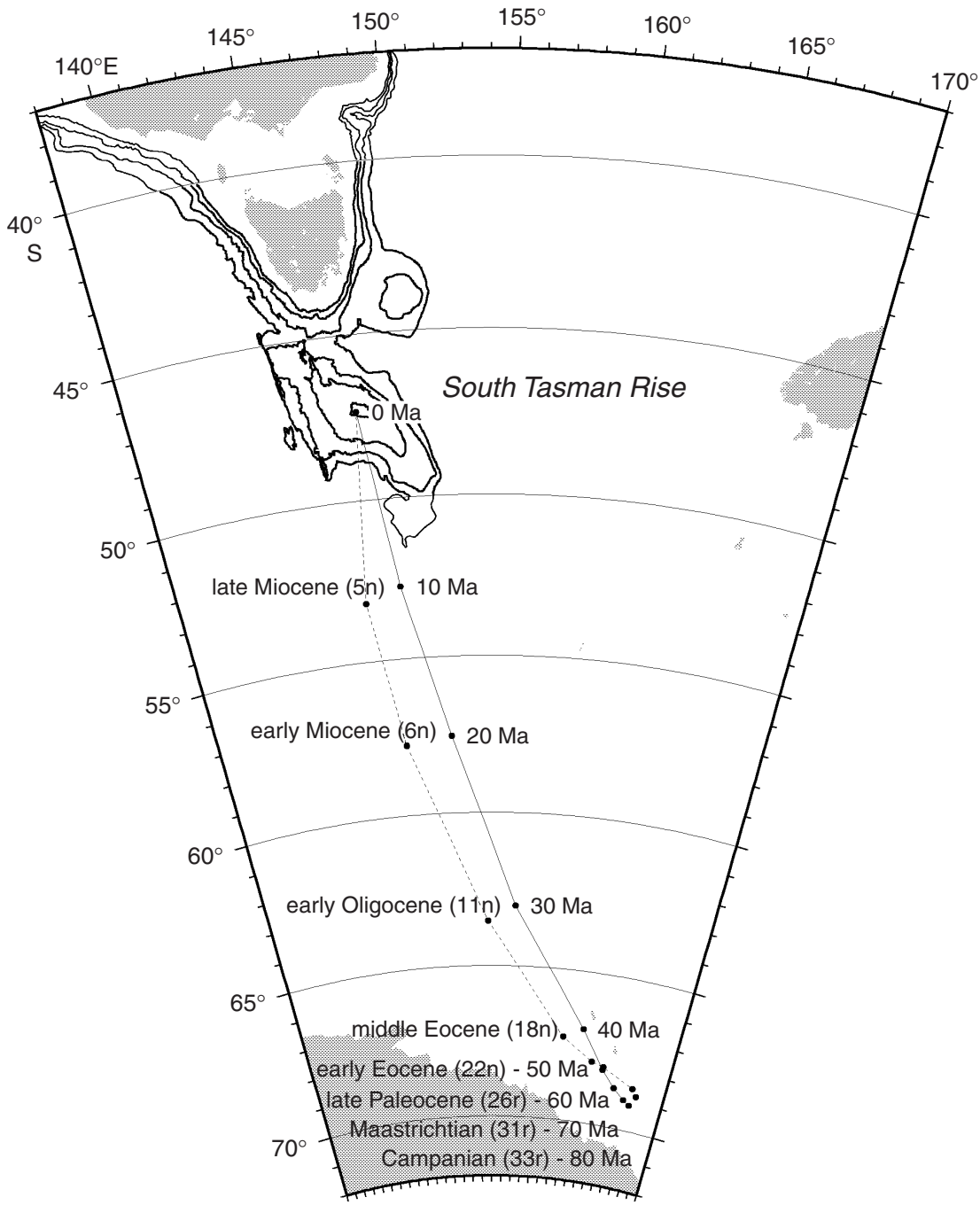
140°E
145°
150°
155°
160°
165°
170°
40°
S
45°
50°
55°
60°
65°
70°
South Tasman Rise
0 Ma
late Miocene (5n)
10 Ma
early Miocene (6n)
20 Ma
early Oligocene (11n)
30 Ma
middle Eocene (18n)
40 Ma
early Eocene (22n) - 50 Ma
late Paleocene (26r) - 60 Ma
Maastrichtian (31r) - 70 Ma
Campanian (33r) - 80 Ma

Figure 4

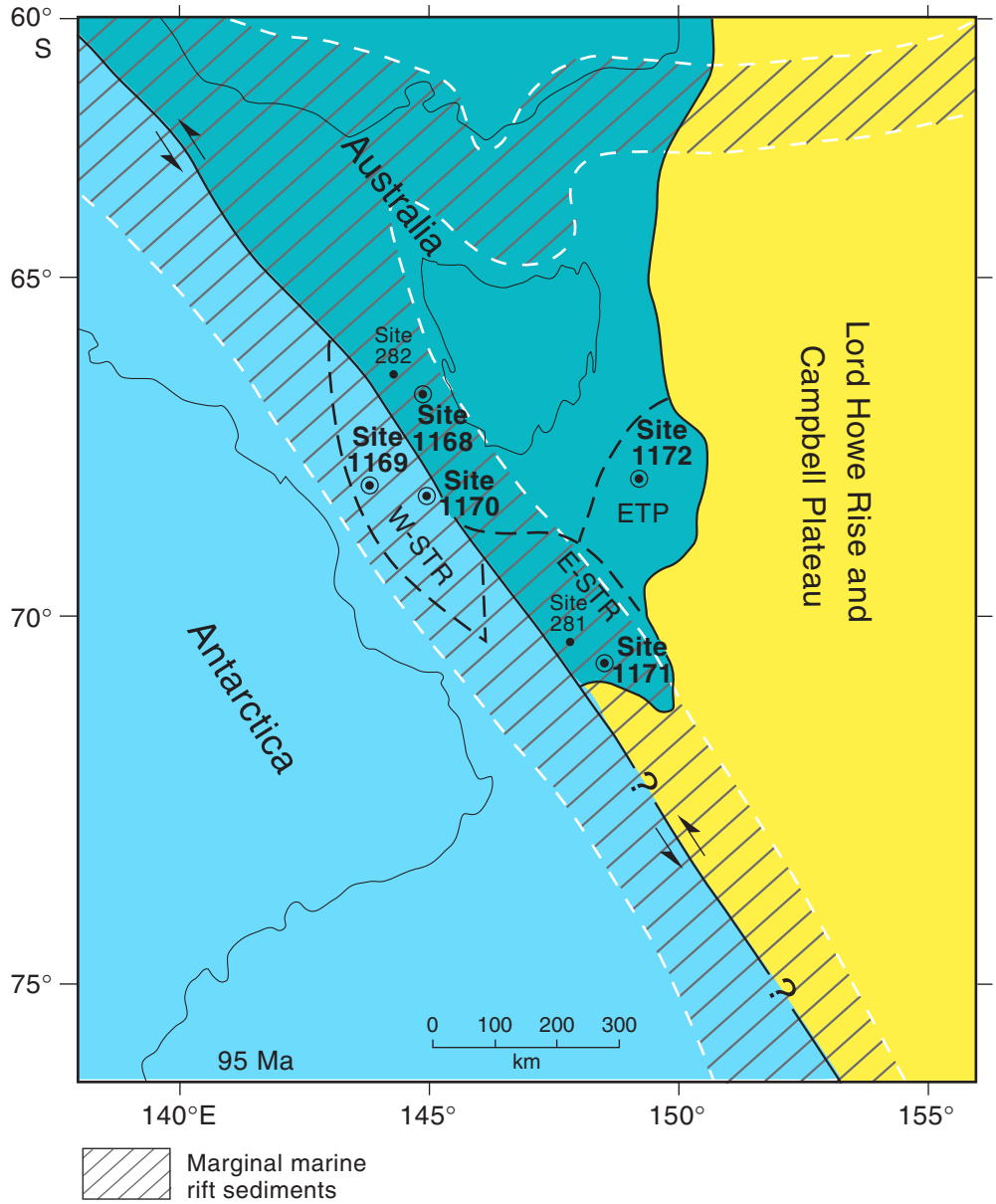
60° S
65°
70°
75°
140°E
145°
150°
155°
Australia
Antarctica
Lord Howe Rise and Campbell Plateau
Site 282
Site 1168
Site 1169
Site 1170
Site 1172
ETP
W-STR
E-STR
Site 281
Site 1171
95 Ma
0 100 200 300
km
Marginal marine rift sediments

Figure 5

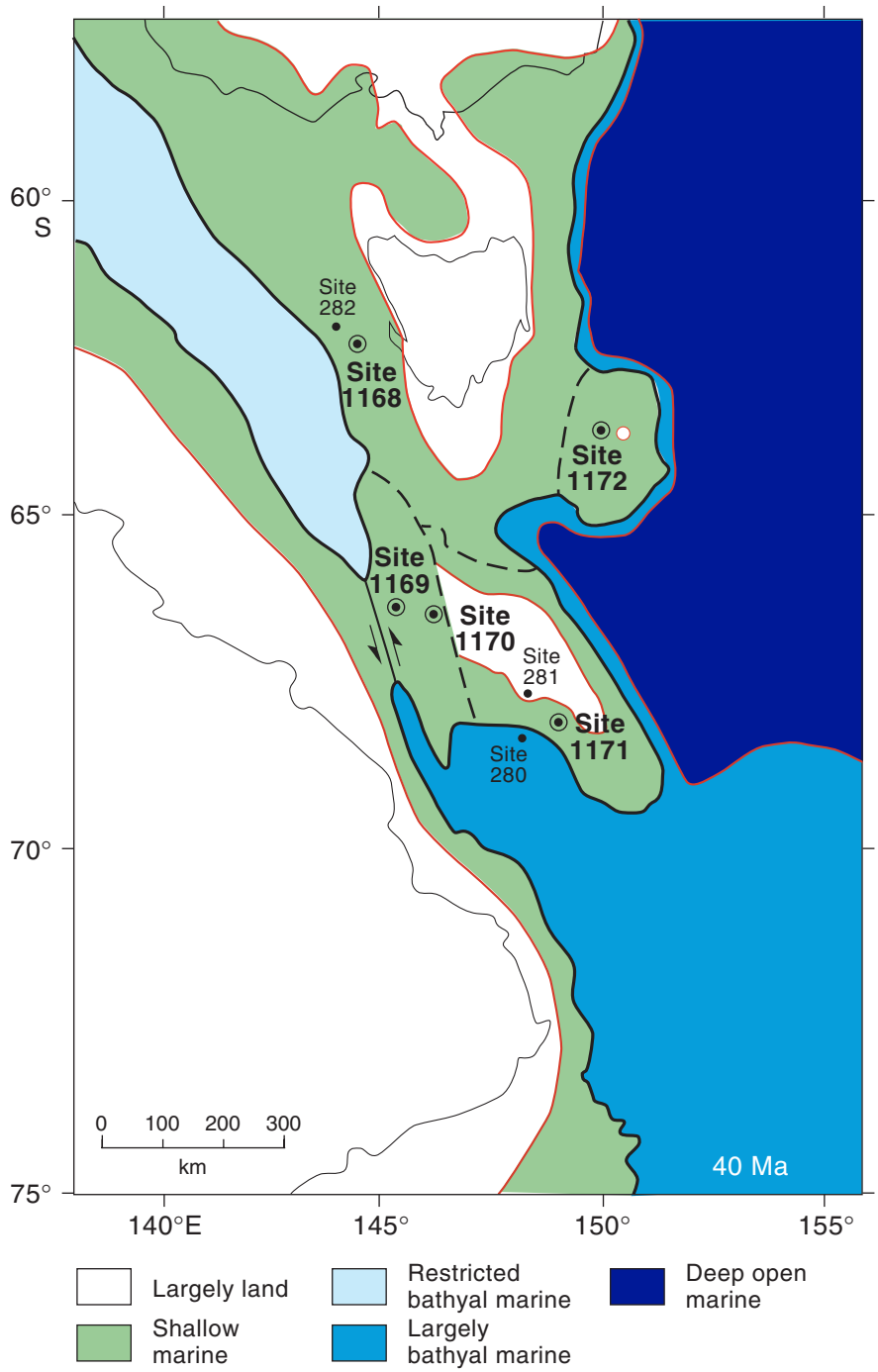
60° S
65°
70°
75°
140°E
145°
150°
155°
Site 282
Site 1168
Site 1172
Site 1169
Site 1170
Site 281
Site 1171
Site 280
0 100 200 300
km
40 Ma
Largely land
Shallow marine
Restricted bathyal marine
Largely bathyal marine
Deep open marine

Figure 6

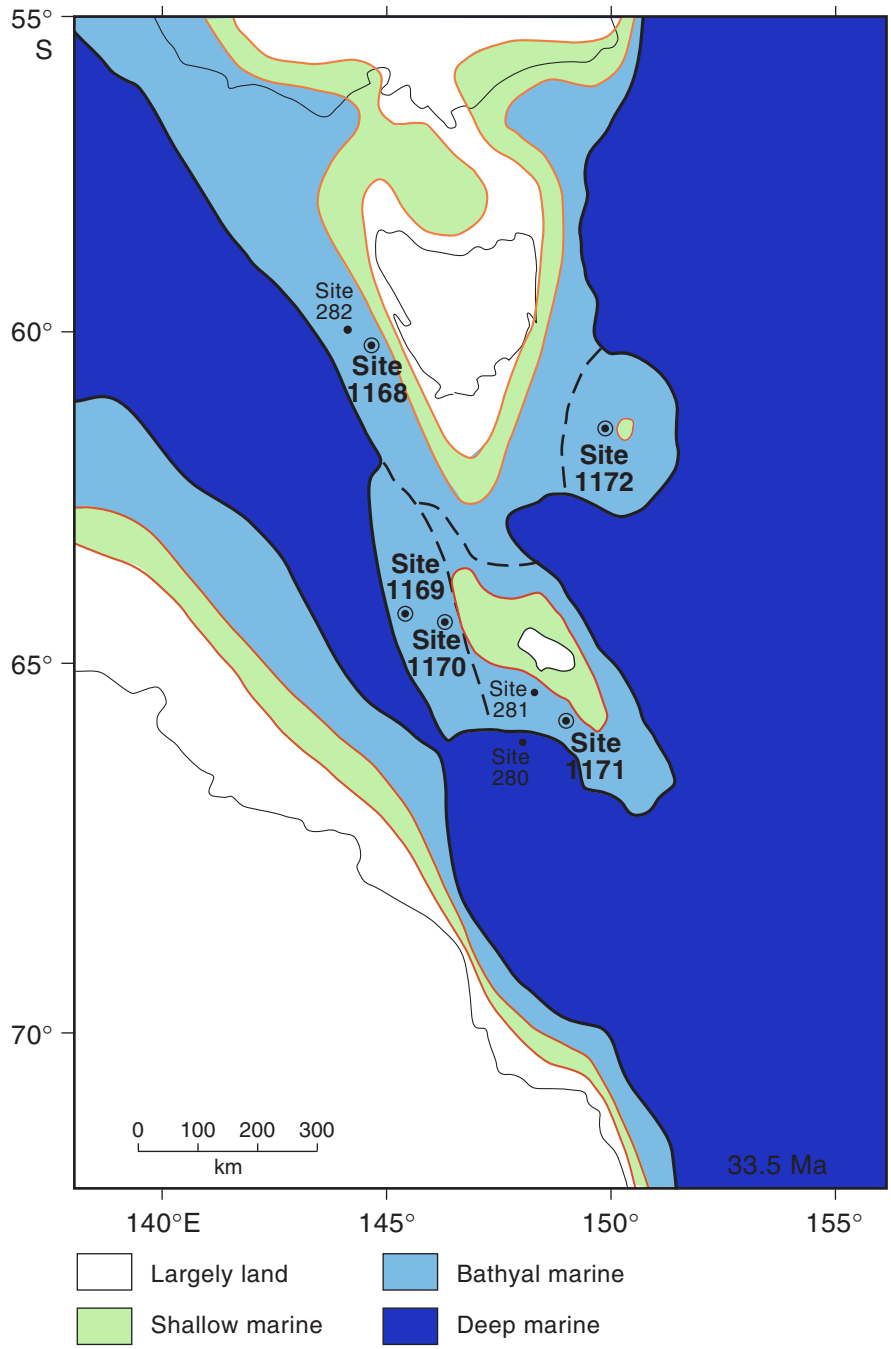
55° S
60°
65°
70°
Site 282
Site 1168
Site 1172
Site 1169
Site 1170
Site 281
Site 280
Site 1171
0 100 200 300
km
33.5 Ma
140°E
145°
150°
155°
Largely land
Bathyal marine
Shallow marine
Deep marine

Figure 7

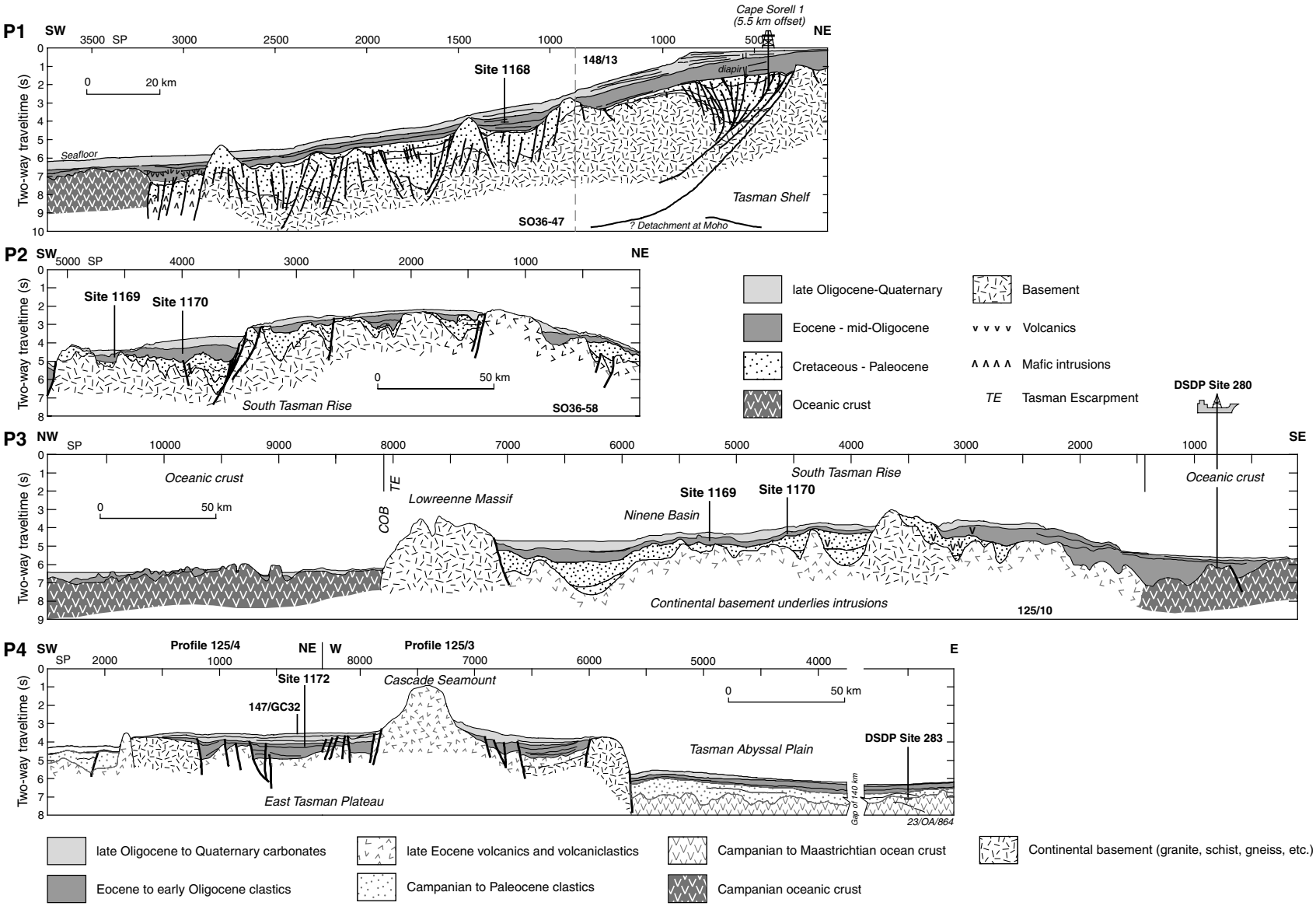
P1
SW
NE
Cape Sorell 1
(5.5 km offset)
Site 1168
148/13
diapir
Seafloor
Tasman Shelf
SO36-47
? Detachment at Moho
Two-way traveltime (s)
P2
SW
NE
Site 1169
Site 1170
South Tasman Rise
SO36-58
P3
NW
SE
Oceanic crust
COB
TE
Lowreenne Massif
Ninene Basin
South Tasman Rise
Site 1169
Site 1170
Oceanic crust
DSDP Site 280
Continental basement underlies intrusions
125/10
P4
SW
NE
W
E
Profile 125/4
Profile 125/3
Site 1172
147/GC32
Cascade Seamount
Tasman Abyssal Plain
DSDP Site 283
East Tasman Plateau
Gap of 140 km
23/OA/864
late Oligocene-Quaternary
Eocene - mid-Oligocene
Cretaceous - Paleocene
Oceanic crust
Basement
Volcanics
Mafic intrusions
TE Tasman Escarpment
late Oligocene to Quaternary carbonates
Eocene to early Oligocene clastics
late Eocene volcanics and volcaniclastics
Campanian to Paleocene clastics
Campanian to Maastrichtian ocean crust
Campanian oceanic crust
Continental basement (granite, schist, gneiss, etc.)

Figure 8

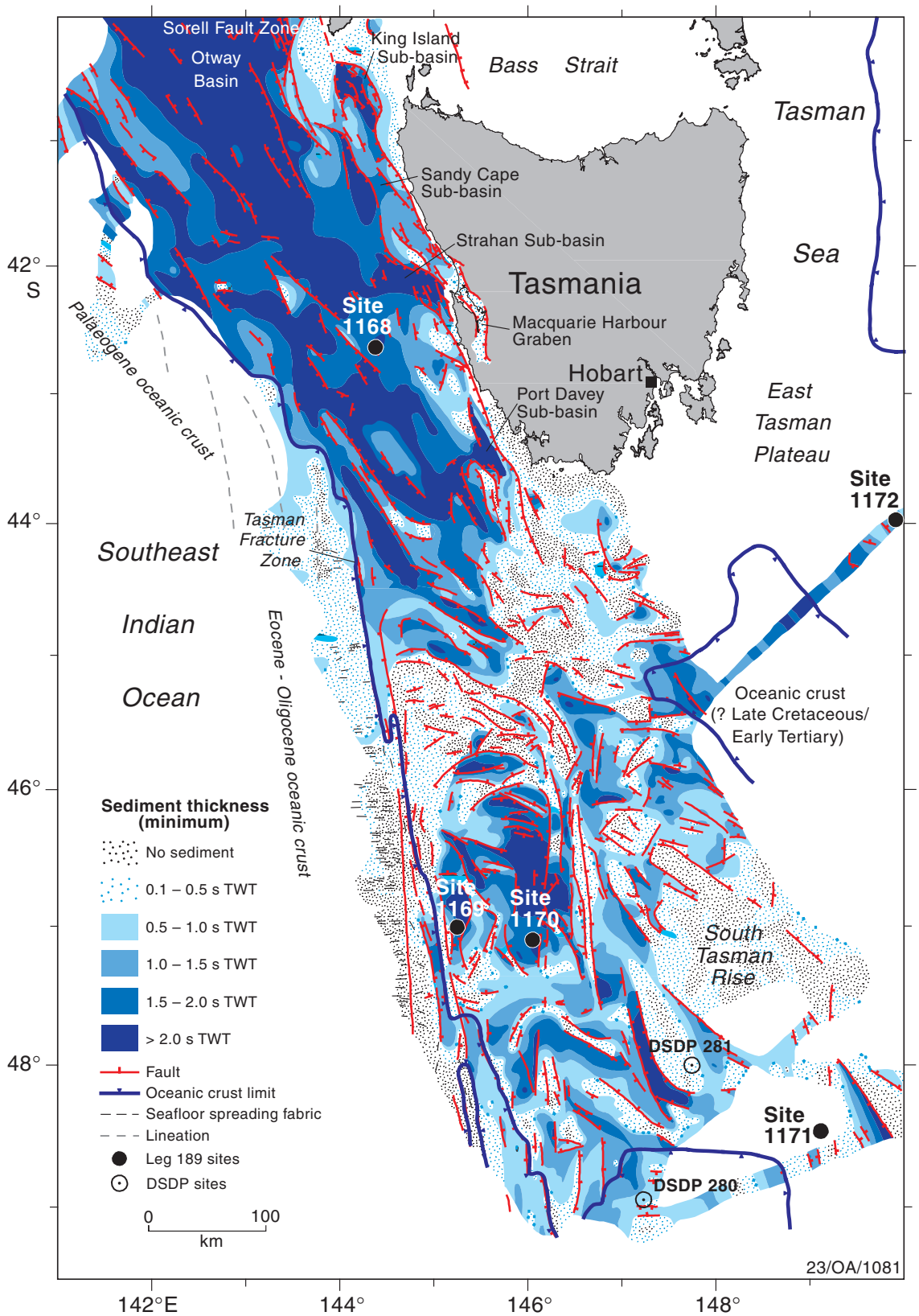
Sorell Fault Zone
Otway Basin
King Island Sub-basin
Bass Strait
Tasman Sea
Sandy Cape Sub-basin
Strahan Sub-basin
Tasmania
Macquarie Harbour Graben
Hobart
Port Davey Sub-basin
East Tasman Plateau
Site 1168
Site 1172
Site 1169
Site 1170
Site 1171
Palaeogene oceanic crust
Tasman Fracture Zone
Southeast Indian Ocean
Eocene - Oligocene oceanic crust
Oceanic crust (? Late Cretaceous/ Early Tertiary)
South Tasman Rise
DSDP 281
DSDP 280
Sediment thickness (minimum)
No sediment
0.1 – 0.5 s TWT
0.5 – 1.0 s TWT
1.0 – 1.5 s TWT
1.5 – 2.0 s TWT
> 2.0 s TWT
Fault
Oceanic crust limit
Seafloor spreading fabric
Lineation
Leg 189 sites
DSDP sites
0
100
km
23/OA/1081
42° S
44°
46°
48°
142°E
144°
146°
148°

Figure 9

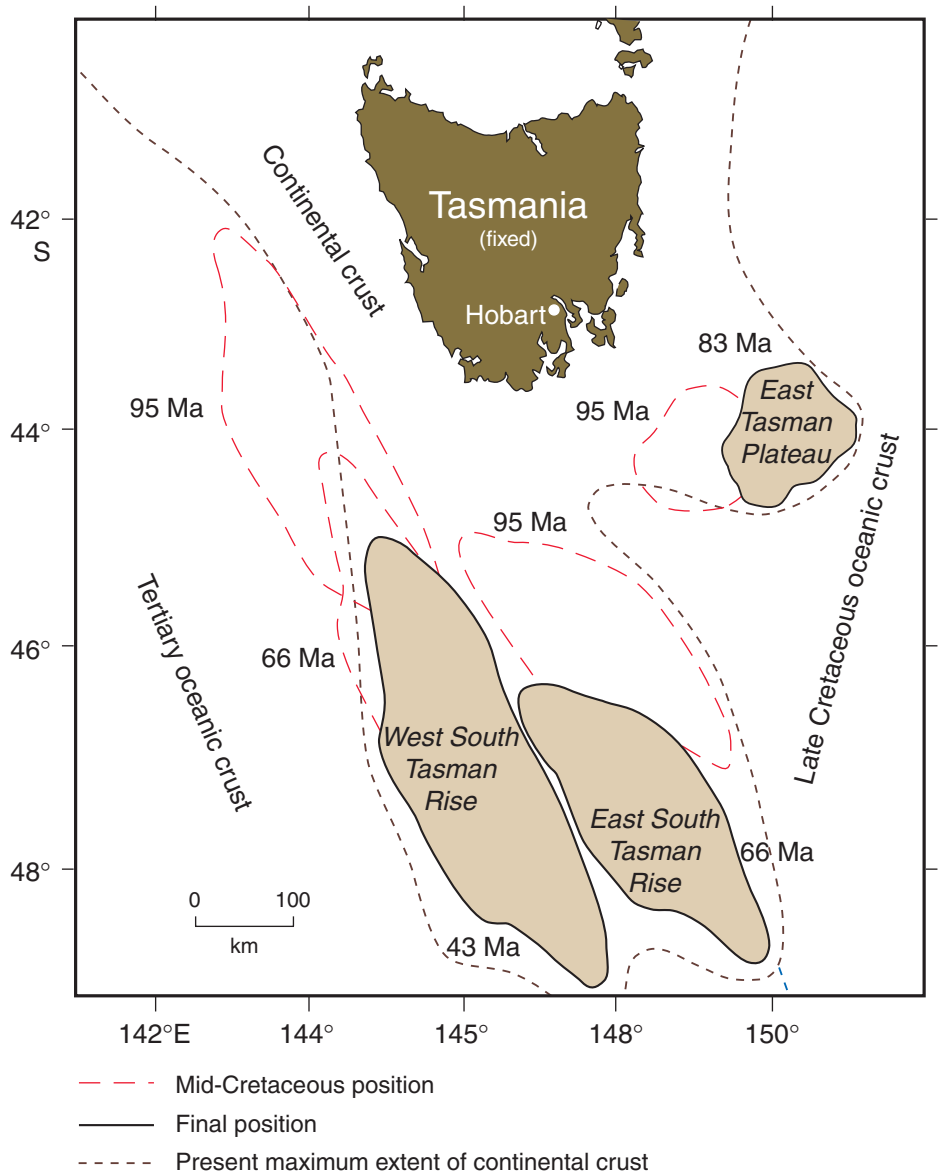
Tasmania
(fixed)
Hobart
Continental crust
42° S
44°
46°
48°
142°E
144°
145°
148°
150°
83 Ma
95 Ma
95 Ma
95 Ma
East Tasman Plateau
Late Cretaceous oceanic crust
Tertiary oceanic crust
66 Ma
West South Tasman Rise
East South Tasman Rise
66 Ma
43 Ma
0
100
km
Mid-Cretaceous position
Final position
Present maximum extent of continental crust

Figure 10

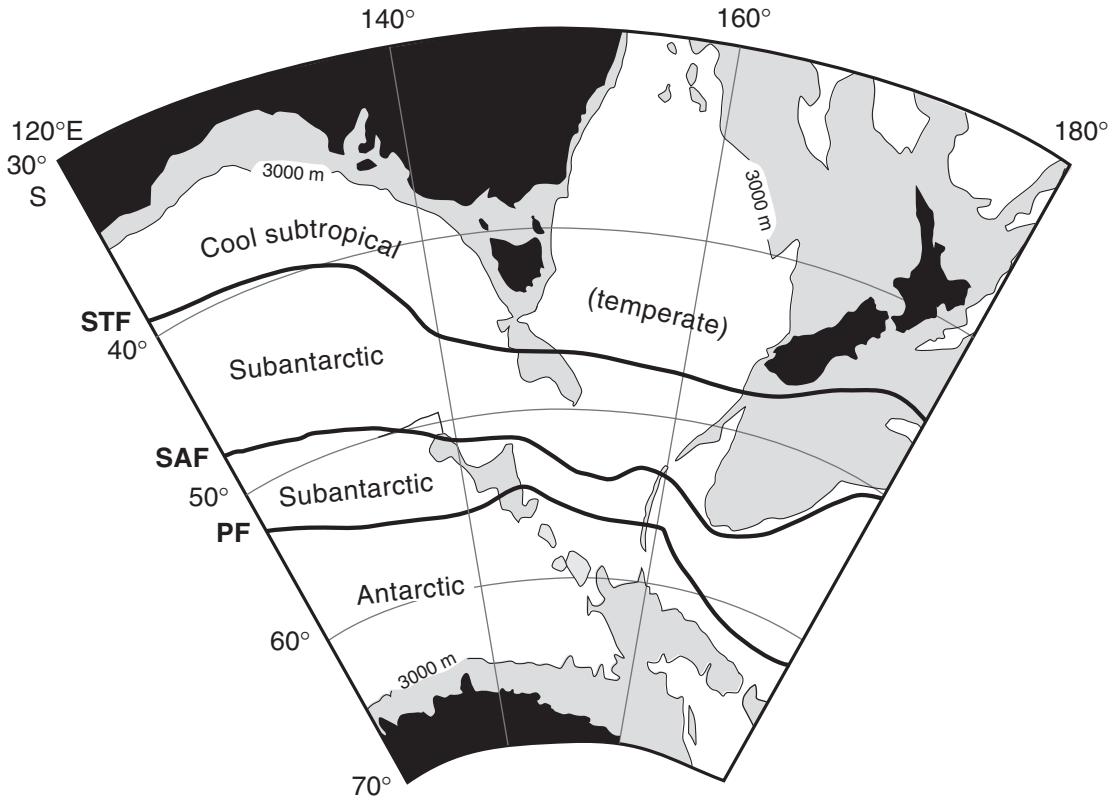
140°
160°
120°E
180°
30°
S
3000 m
3000 m
Cool subtropical
(temperate)
STF
40°
Subantarctic
SAF
50°
Subantarctic
PF
Antarctic
60°
3000 m
70°

Figure 11

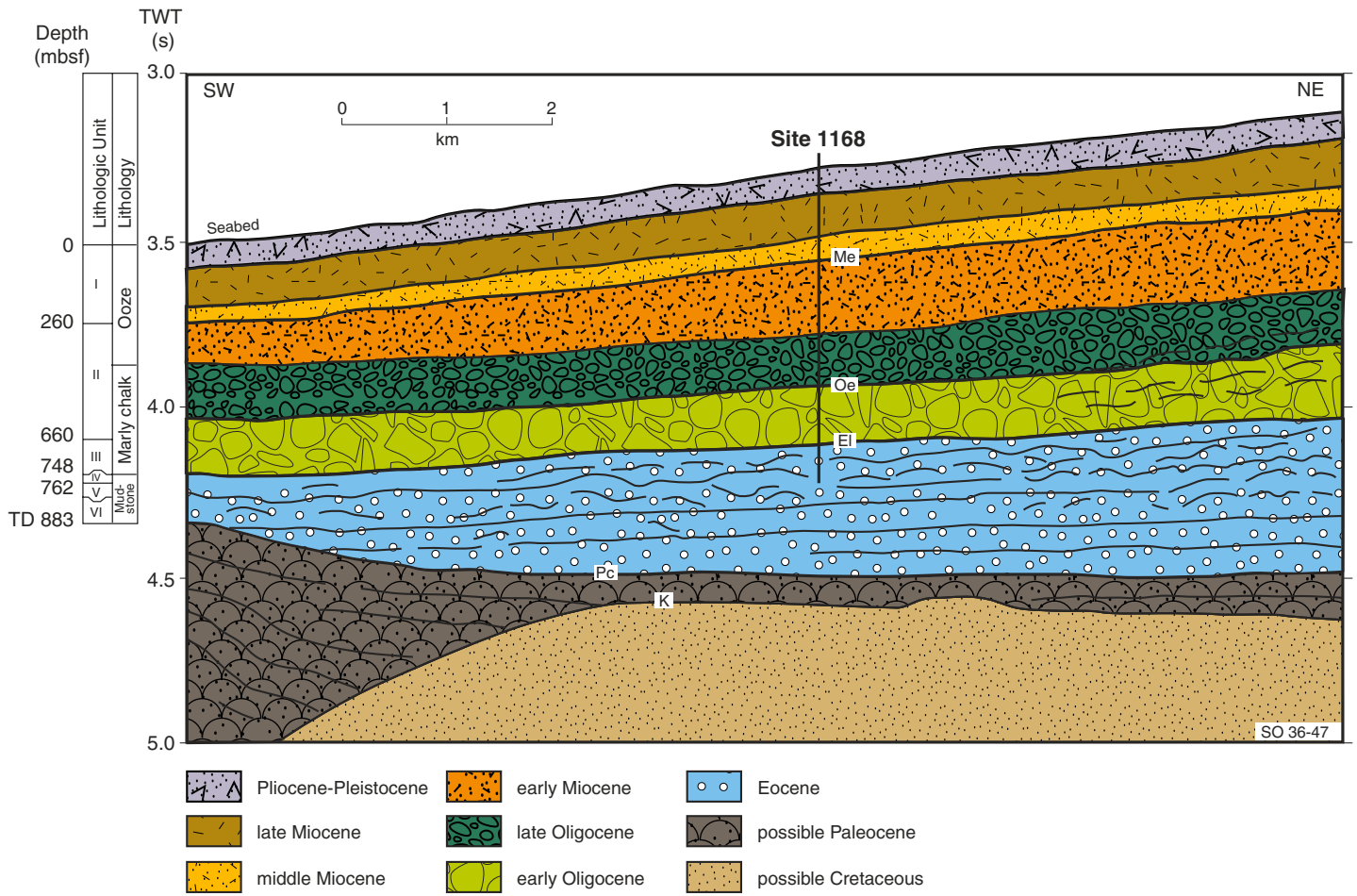
Depth
(mbsf)
TWT
(s)
Lithologic Unit
Lithology
I
II
III
IV
V
VI
Ooze
Marly chalk
Mud-
stone
0
260
660
748
762
TD 883
3.0
3.5
4.0
4.5
5.0
SW
NE
0
1
2
km
Site 1168
Seabed
Me
Oe
El
Pc
K
SO 36-47
Pliocene-Pleistocene
late Miocene
middle Miocene
early Miocene
late Oligocene
early Oligocene
Eocene
possible Paleocene
possible Cretaceous

Figure 12

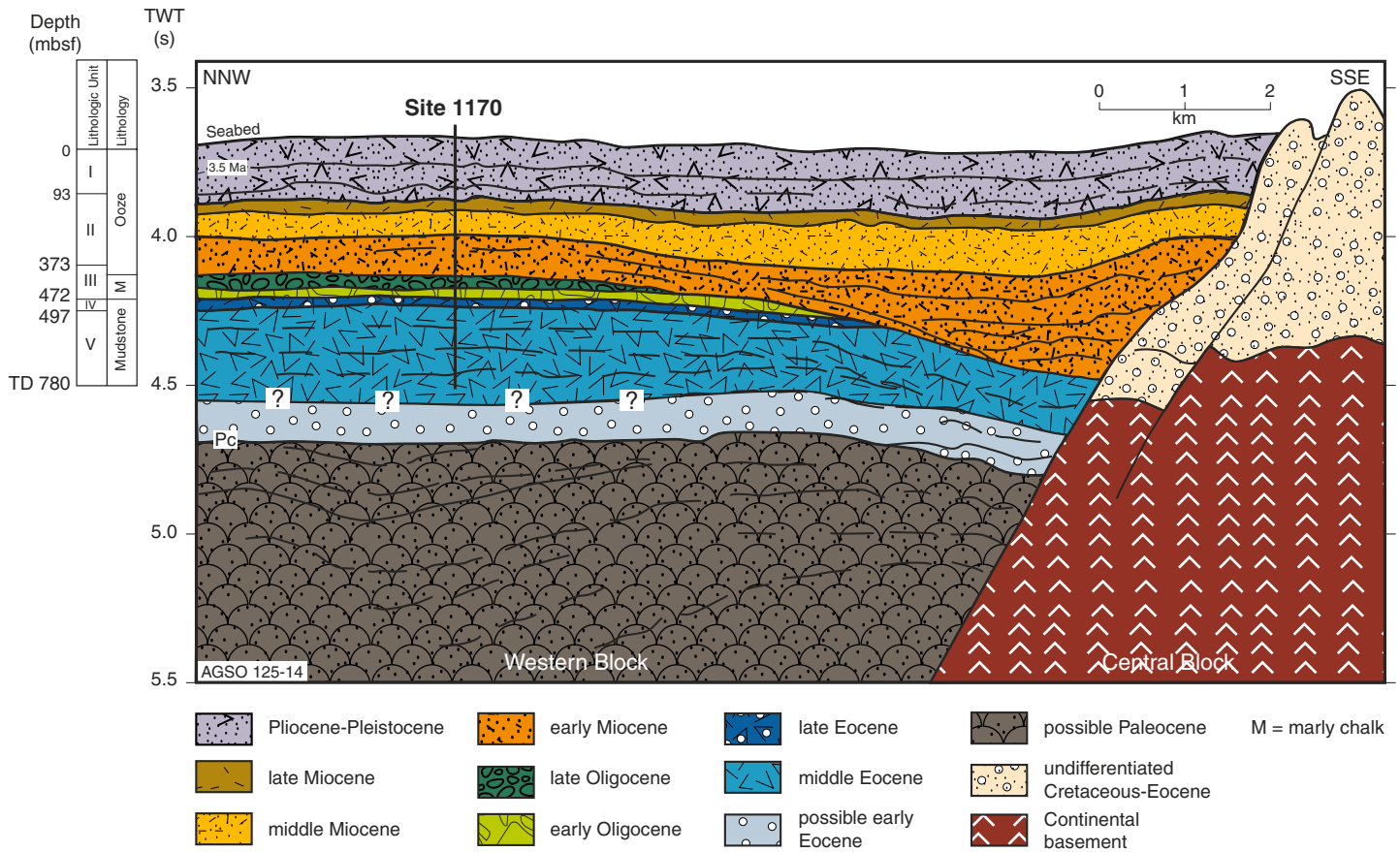
Depth
(mbsf)
TWT
(s)
Lithologic Unit
Lithology
0
I
93
II
Ooze
373
III
M
472
IV
497
V
Mudstone
TD 780
3.5
4.0
4.5
5.0
5.5
NNW
SSE
Site 1170
Seabed
3.5 Ma
0
1
2
km
?
?
?
?
Pc
AGSO 125-14
Western Block
Central Block
Pliocene-Pleistocene
late Miocene
middle Miocene
early Miocene
late Oligocene
early Oligocene
late Eocene
middle Eocene
possible early Eocene
possible Paleocene
undifferentiated Cretaceous-Eocene
Continental basement
M = marly chalk

Figure 13

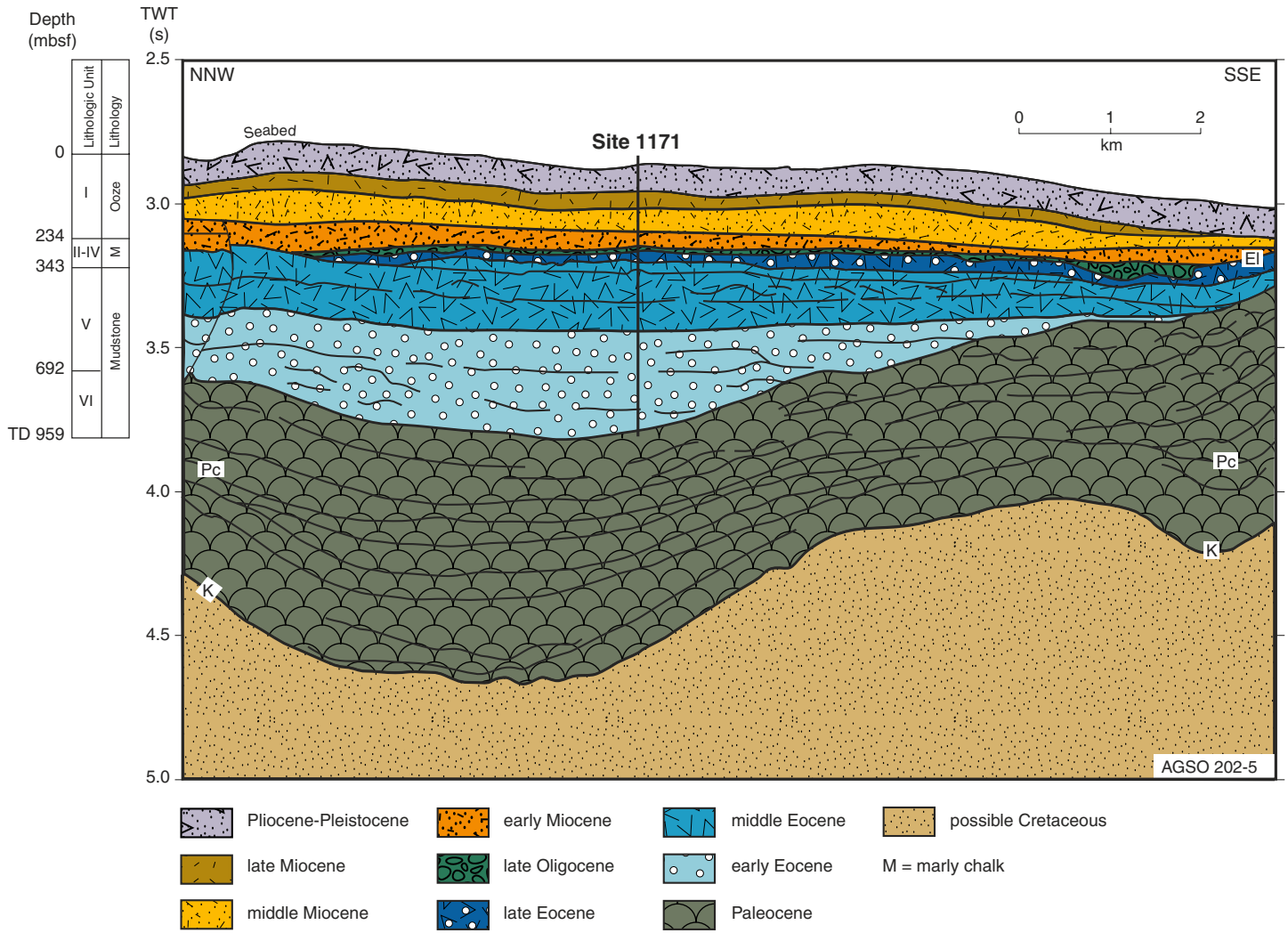
Depth
(mbsf)
TWT
(s)
Lithologic Unit
Lithology
0
I
Ooze
234
II-IV
M
343
V
Mudstone
692
VI
TD 959
2.5
3.0
3.5
4.0
4.5
5.0
NNW
SSE
Seabed
Site 1171
0
1
2
km
El
Pc
Pc
K
K
AGSO 202-5
Pliocene-Pleistocene
early Miocene
middle Eocene
possible Cretaceous
late Miocene
late Oligocene
early Eocene
M = marly chalk
middle Miocene
late Eocene
Paleocene

Figure 14

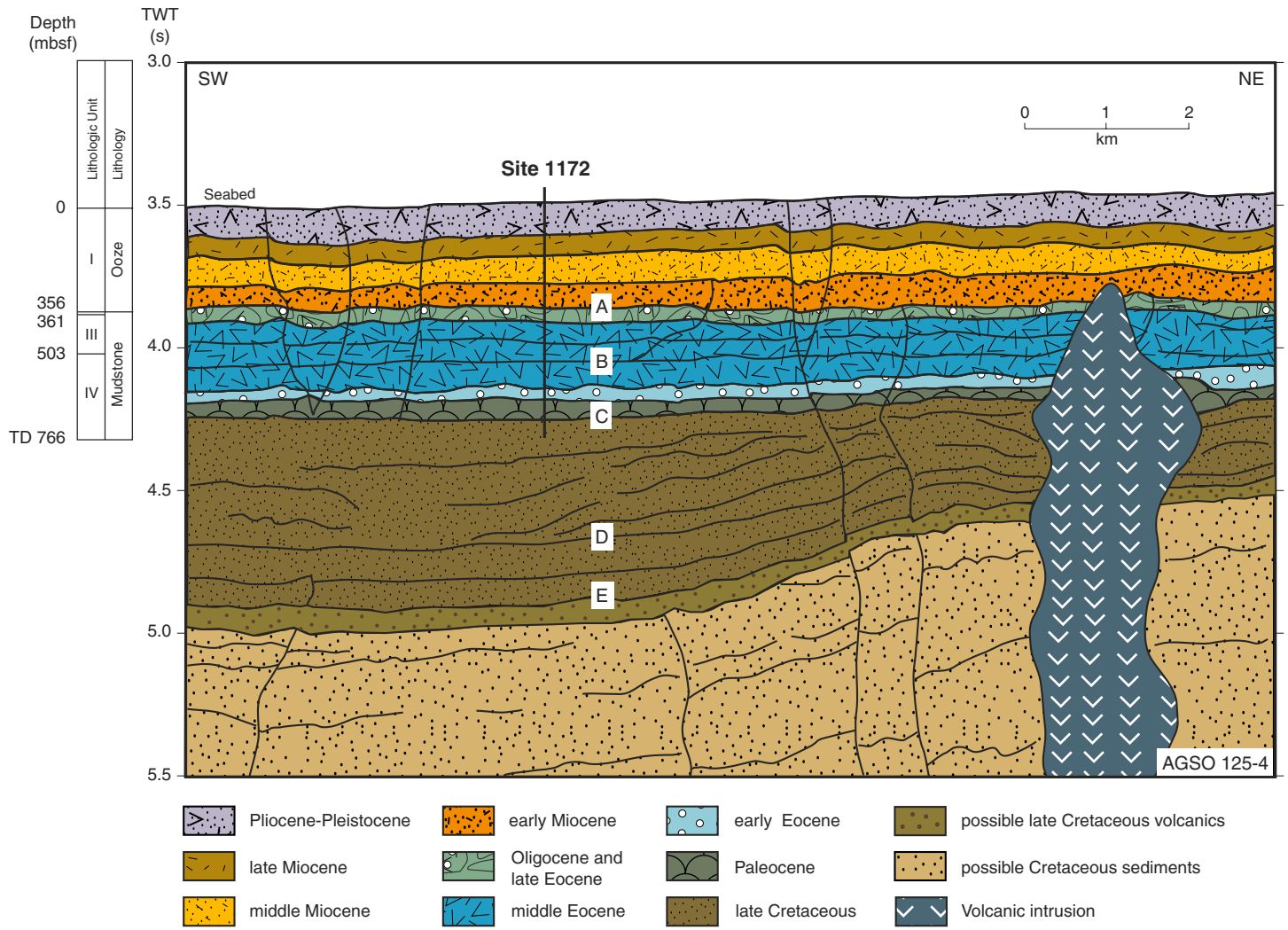
Depth
(mbsf)
TWT
(s)
Lithologic Unit
Lithology
0
I
Ooze
356
361
III
503
IV
Mudstone
TD 766
3.0
3.5
4.0
4.5
5.0
5.5
SW
NE
0
1
2
km
Site 1172
Seabed
A
B
C
D
E
AGSO 125-4
Pliocene-Pleistocene
late Miocene
middle Miocene
early Miocene
Oligocene and
late Eocene
middle Eocene
early Eocene
Paleocene
late Cretaceous
possible late Cretaceous volcanics
possible Cretaceous sediments
Volcanic intrusion

Figure 15

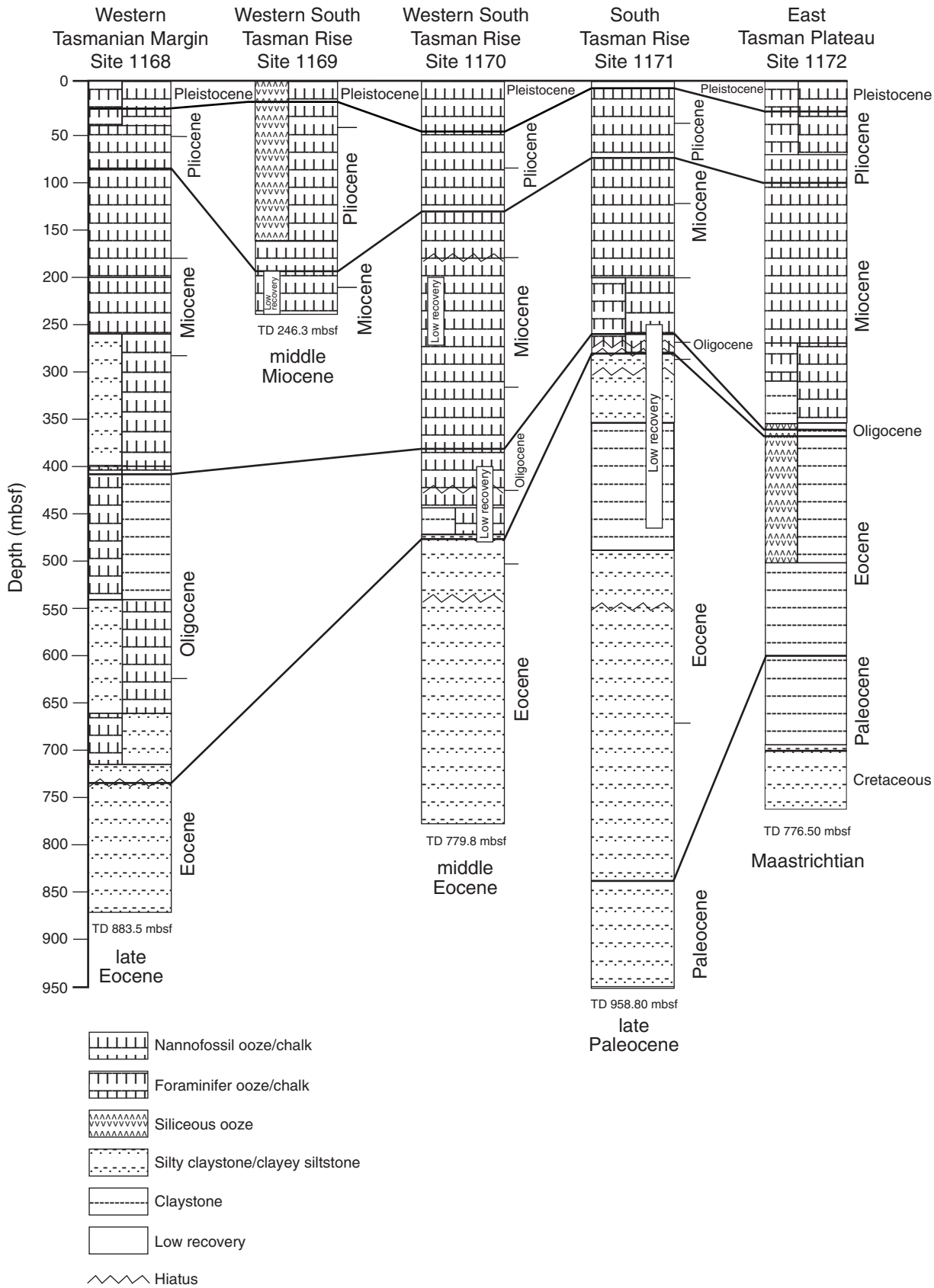
Western Tasmanian Margin Site 1168
Western South Tasman Rise Site 1169
Western South Tasman Rise Site 1170
South Tasman Rise Site 1171
East Tasman Plateau Site 1172
Depth (mbsf)
0
50
100
150
200
250
300
350
400
450
500
550
600
650
700
750
800
850
900
950
Pleistocene
Pliocene
Miocene
Oligocene
Eocene
Paleocene
Cretaceous
Low recovery
TD 883.5 mbsf
late Eocene
TD 246.3 mbsf
middle Miocene
TD 779.8 mbsf
middle Eocene
TD 958.80 mbsf
late Paleocene
TD 776.50 mbsf
Maastrichtian
Nannofossil ooze/chalk
Foraminifer ooze/chalk
Siliceous ooze
Silty claystone/clayey siltstone
Claystone
Low recovery
Hiatus

Figure 16

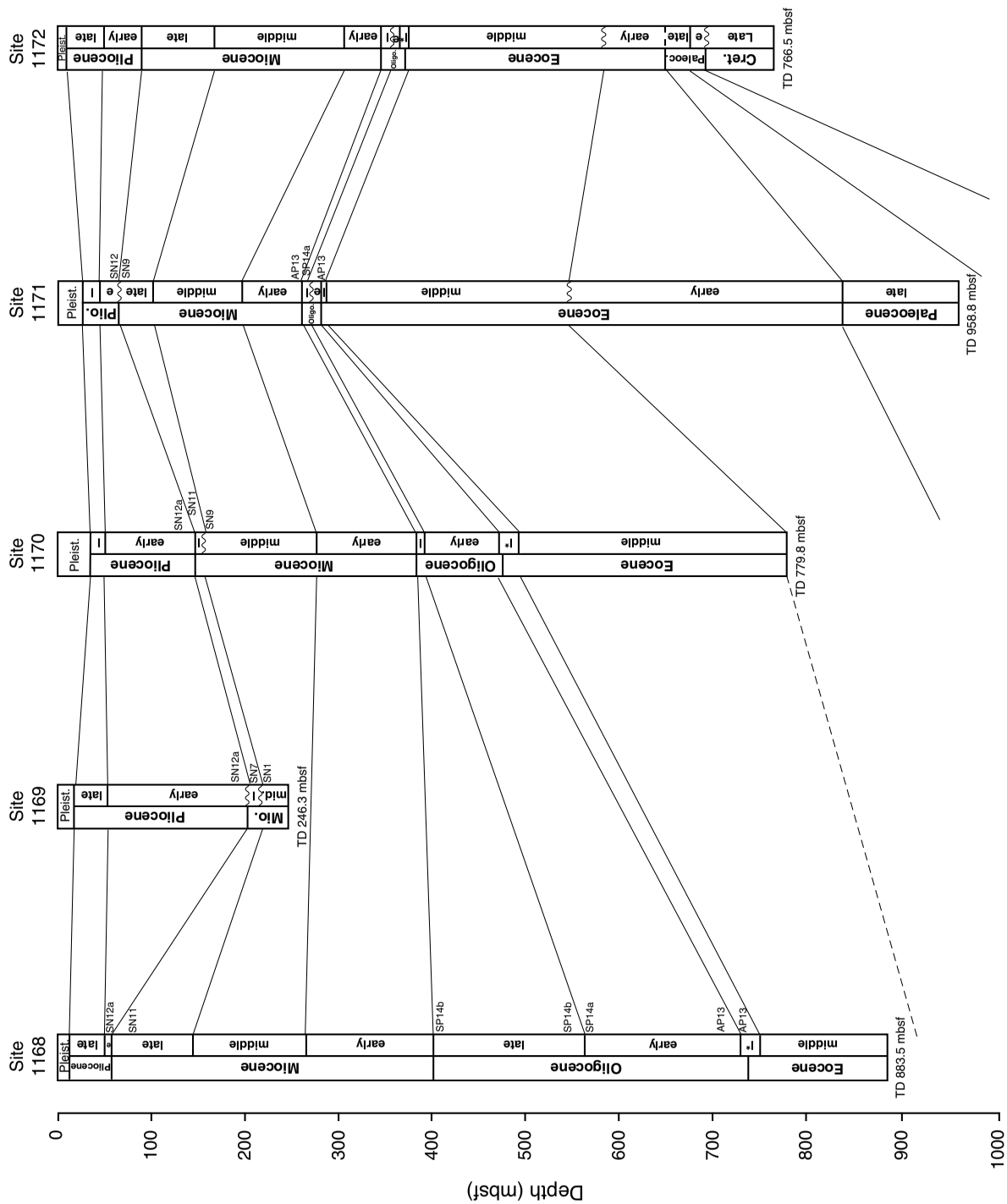
Site 1172
Site 1171
Site 1170
Site 1169
Site 1168
Pleist.
late
early
middle
Pliocene
Miocene
Oligocene
Eocene
Cret.
Paleocene
Plio.
Mio.
Oligo.
TD 766.5 mbsf
TD 958.8 mbsf
TD 779.8 mbsf
TD 246.3 mbsf
TD 883.5 mbsf
SN12
SN9
AP13
SP14a
SN12a
SN11
SN7
SN1
SP14b
Depth (mbsf)
0
100
200
300
400
500
600
700
800
900
1000

Figure 17

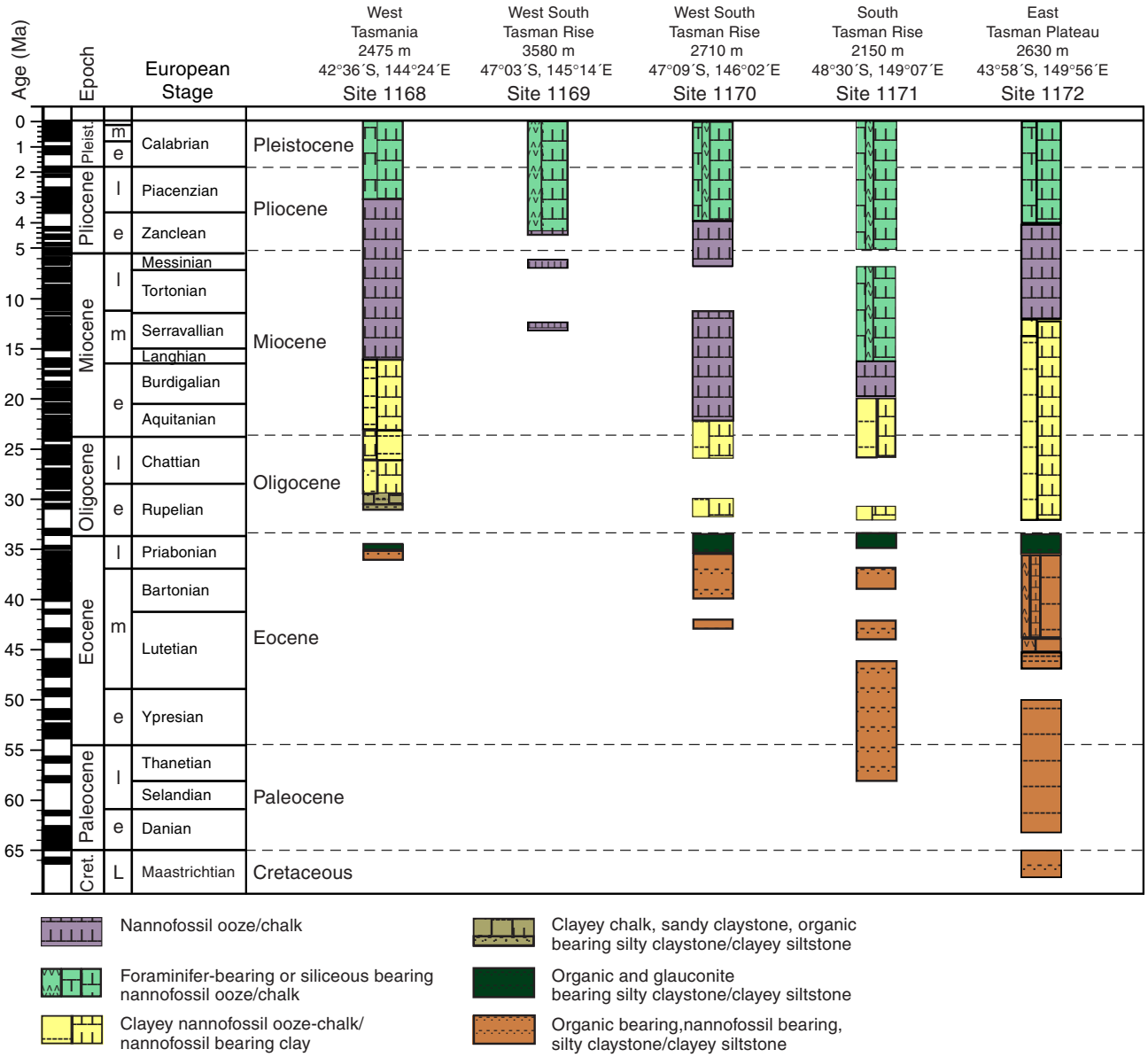
Age (Ma)
Epoch
European Stage
West Tasmania 2475 m 42°36´S, 144°24´E Site 1168
West South Tasman Rise 3580 m 47°03´S, 145°14´E Site 1169
West South Tasman Rise 2710 m 47°09´S, 146°02´E Site 1170
South Tasman Rise 2150 m 48°30´S, 149°07´E Site 1171
East Tasman Plateau 2630 m 43°58´S, 149°56´E Site 1172
Pleistocene
Pliocene
Miocene
Oligocene
Eocene
Paleocene
Cret.
Calabrian
Piacenzian
Zanclean
Messinian
Tortonian
Serravallian
Langhian
Burdigalian
Aquitanian
Chattian
Rupelian
Priabonian
Bartonian
Lutetian
Ypresian
Thanetian
Selandian
Danian
Maastrichtian
Pleistocene
Pliocene
Miocene
Oligocene
Eocene
Paleocene
Cretaceous
Nannofossil ooze/chalk
Foraminifer-bearing or siliceous bearing nannofossil ooze/chalk
Clayey nannofossil ooze-chalk/ nannofossil bearing clay
Clayey chalk, sandy claystone, organic bearing silty claystone/clayey siltstone
Organic and glauconite bearing silty claystone/clayey siltstone
Organic bearing,nannofossil bearing, silty claystone/clayey siltstone

Figure 18

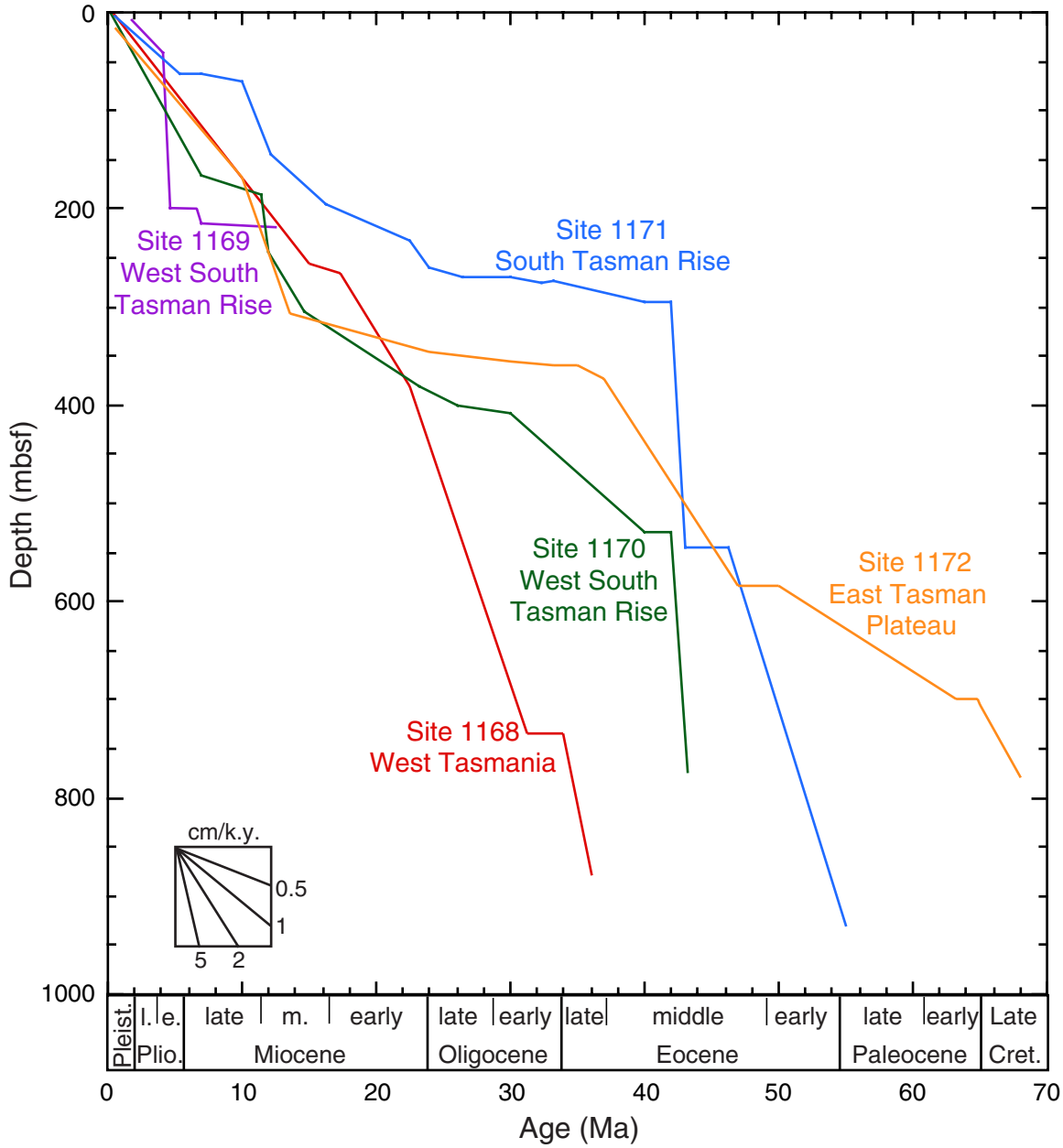
Depth (mbsf)
0
200
400
600
800
1000
Site 1169
West South
Tasman Rise
Site 1171
South Tasman Rise
Site 1170
West South
Tasman Rise
Site 1172
East Tasman
Plateau
Site 1168
West Tasmania
cm/k.y.
0.5
1
2
5
Pleist.
l.
e.
Plio.
late
m.
early
Miocene
late
early
Oligocene
late
middle
early
Eocene
late
early
Paleocene
Late
Cret.
0
10
20
30
40
50
60
70
Age (Ma)

Figure 19

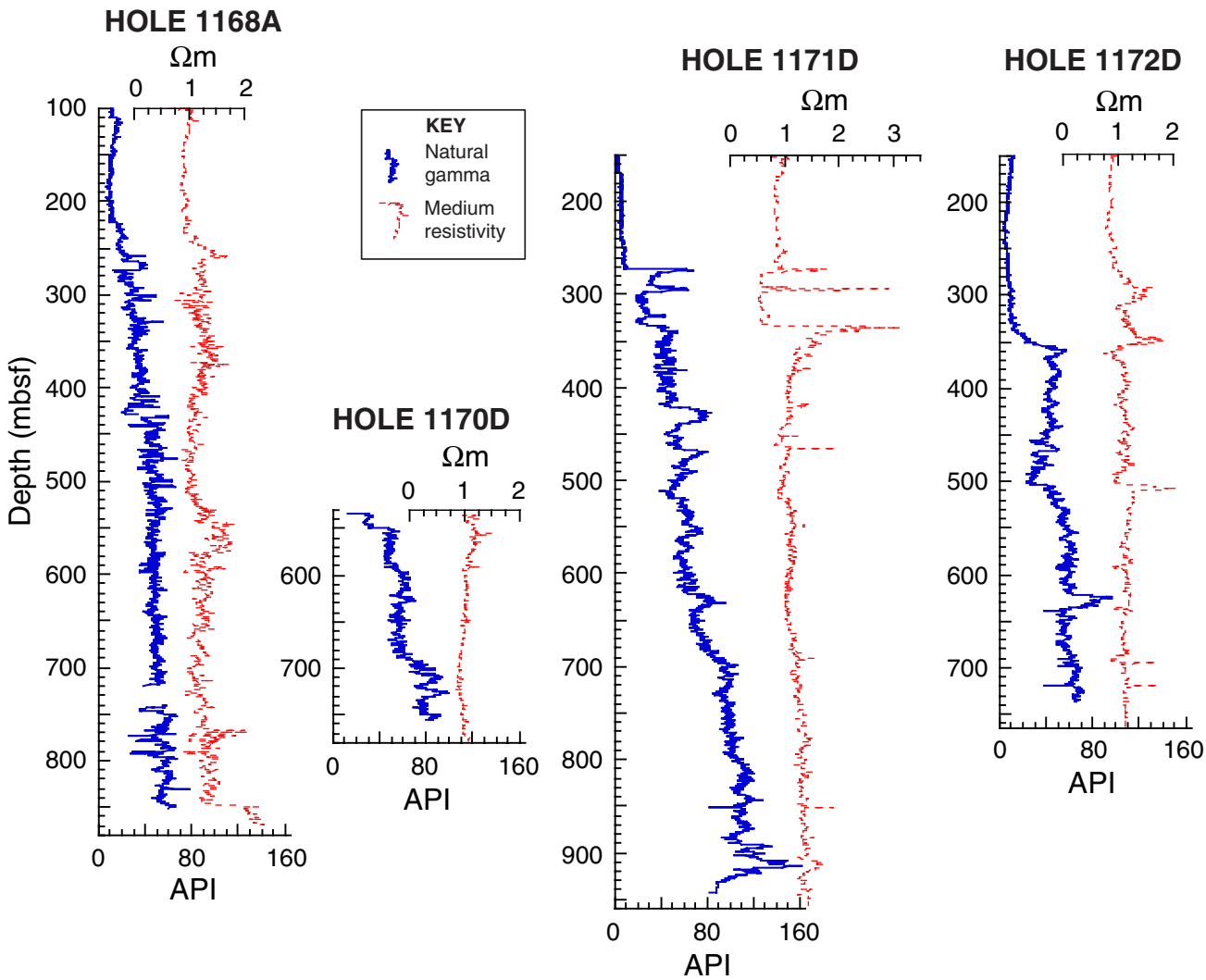
HOLE 1168A
Ωm
0 1 2
100
200
300
400
500
600
700
800
Depth (mbsf)
0 80 160
API
KEY
Natural gamma
Medium resistivity
HOLE 1170D
Ωm
0 1 2
600
700
0 80 160
API
HOLE 1171D
Ωm
0 1 2 3
200
300
400
500
600
700
800
900
0 80 160
API
HOLE 1172D
Ωm
0 1 2
200
300
400
500
600
700
0 80 160
API

Figure 20

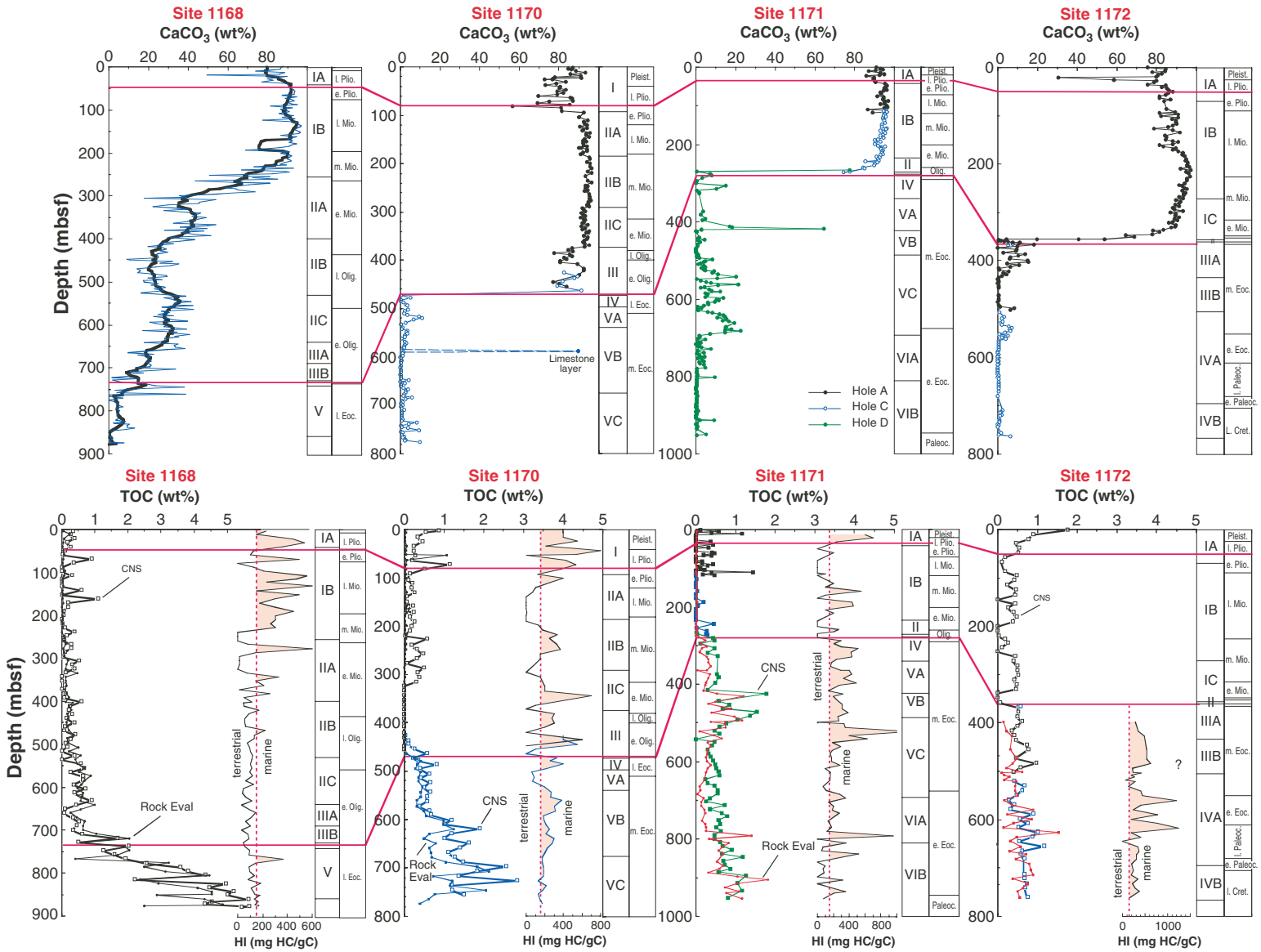
Site 1168
Site 1170
Site 1171
Site 1172
CaCO3 (wt%)
TOC (wt%)
Depth (mbsf)
Limestone layer
Hole A
Hole C
Hole D
CNS
Rock Eval
terrestrial
marine
HI (mg HC/gC)

Figure 21

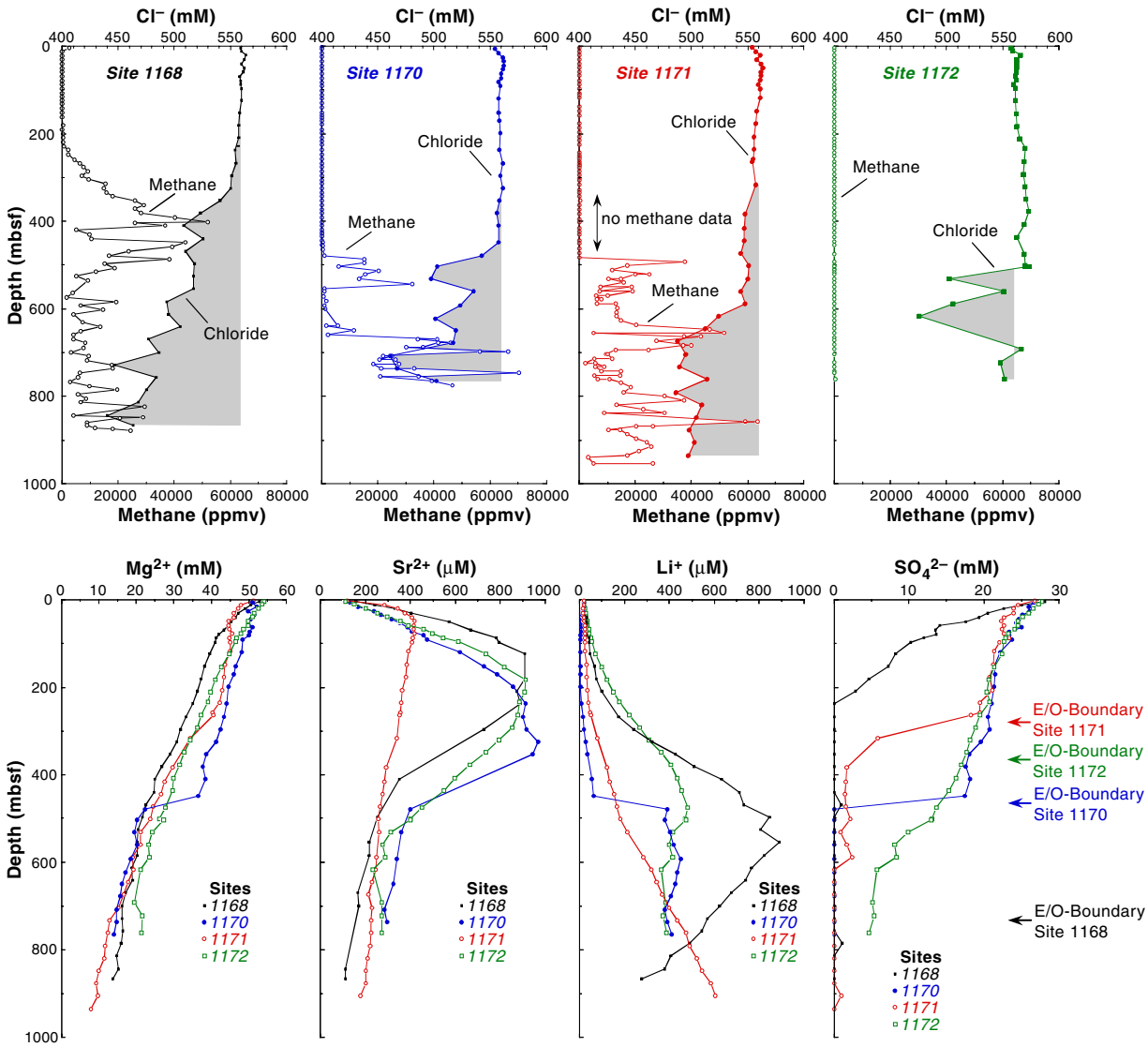
Cl⁻ (mM)
Site 1168
Site 1170
Site 1171
Site 1172
Methane
Chloride
no methane data
Depth (mbsf)
Methane (ppmv)
Mg2+ (mM)
Sr2+ (μM)
Li+ (μM)
SO4 2− (mM)
Sites
1168
1170
1171
1172
E/O-Boundary Site 1171
E/O-Boundary Site 1172
E/O-Boundary Site 1170
E/O-Boundary Site 1168

Figure 22

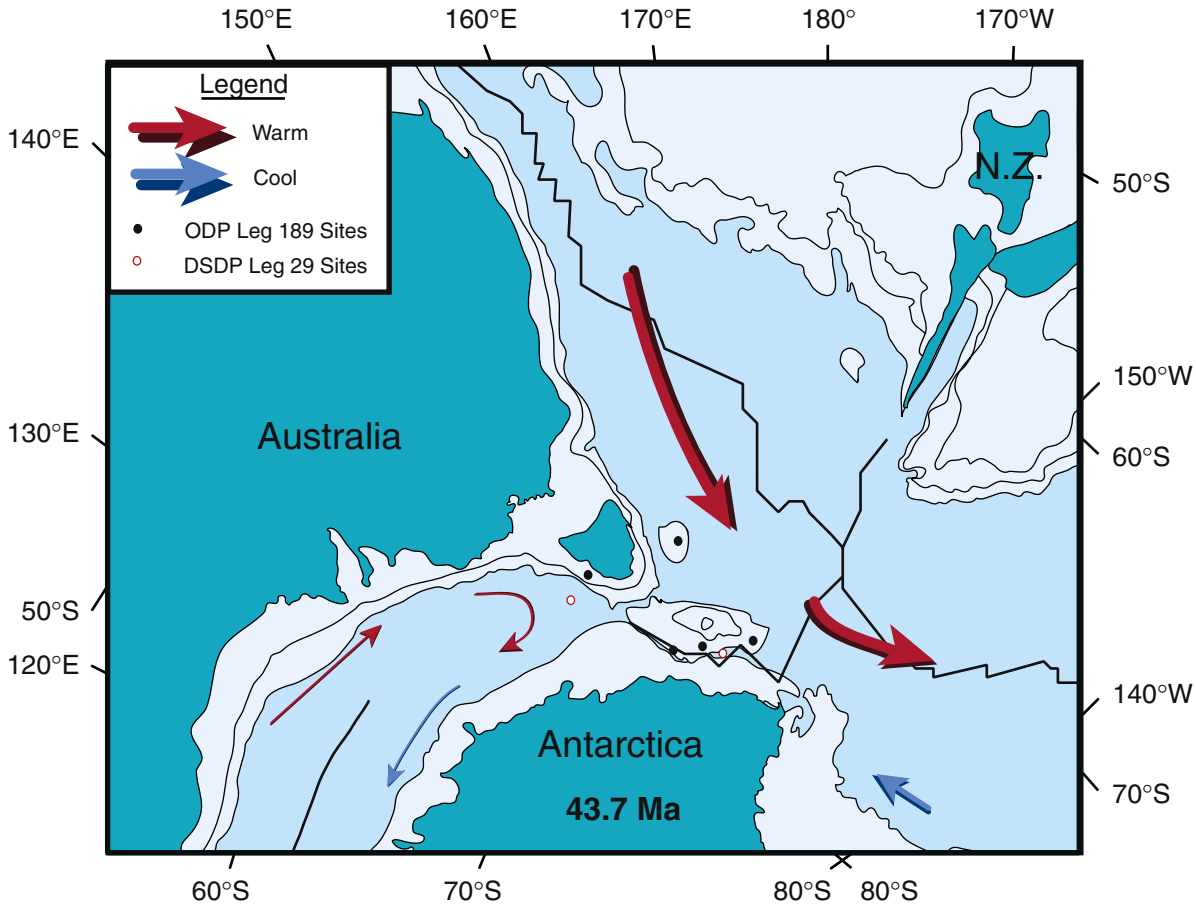
150°E
160°E
170°E
180°
170°W
140°E
130°E
120°E
50°S
60°S
70°S
80°S
80°S
50°S
150°W
60°S
140°W
70°S
Legend
Warm
Cool
ODP Leg 189 Sites
DSDP Leg 29 Sites
Australia
N.Z.
Antarctica
43.7 Ma

Figure 23

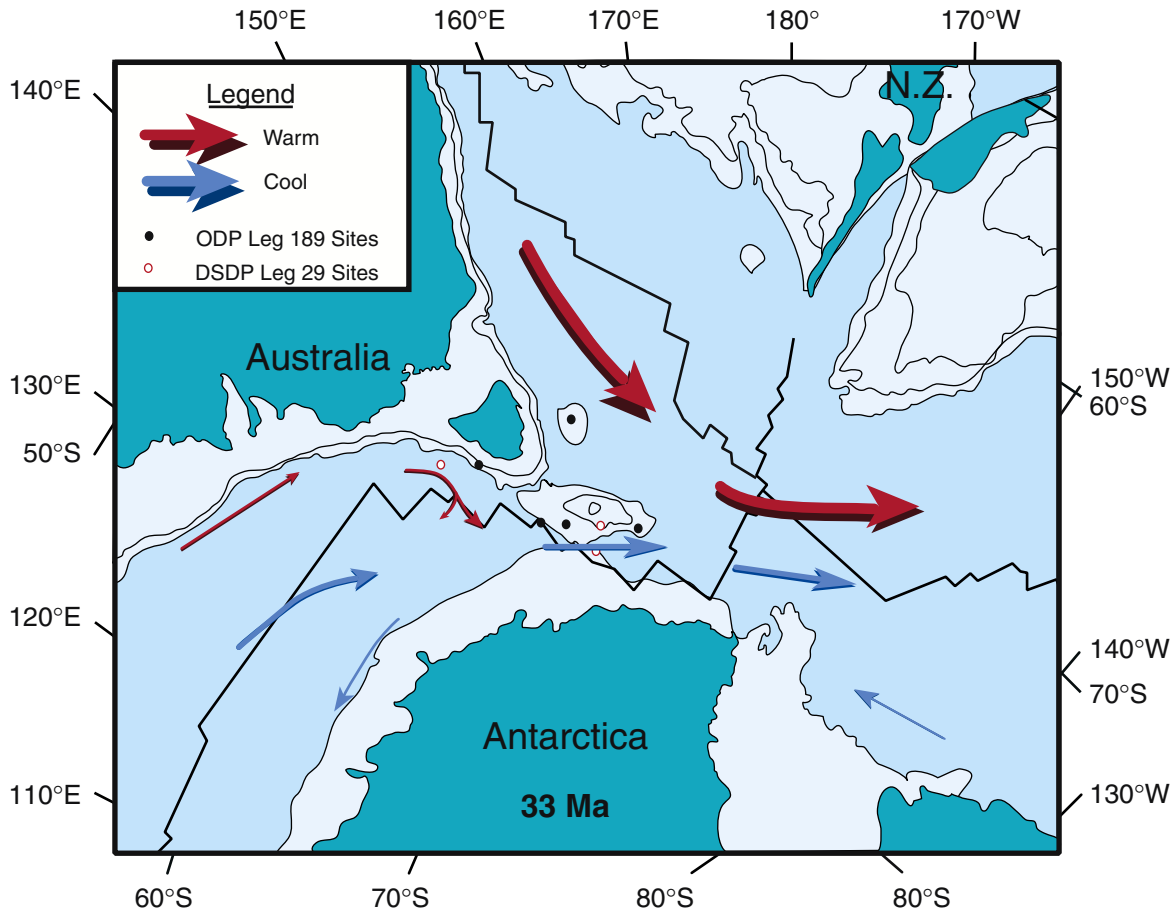
150°E
160°E
170°E
180°
170°W
140°E
130°E
50°S
120°E
110°E
60°S
70°S
80°S
80°S
150°W
60°S
140°W
70°S
130°W
Legend
Warm
Cool
ODP Leg 189 Sites
DSDP Leg 29 Sites
Australia
N.Z.
Antarctica
33 Ma

Figure 24

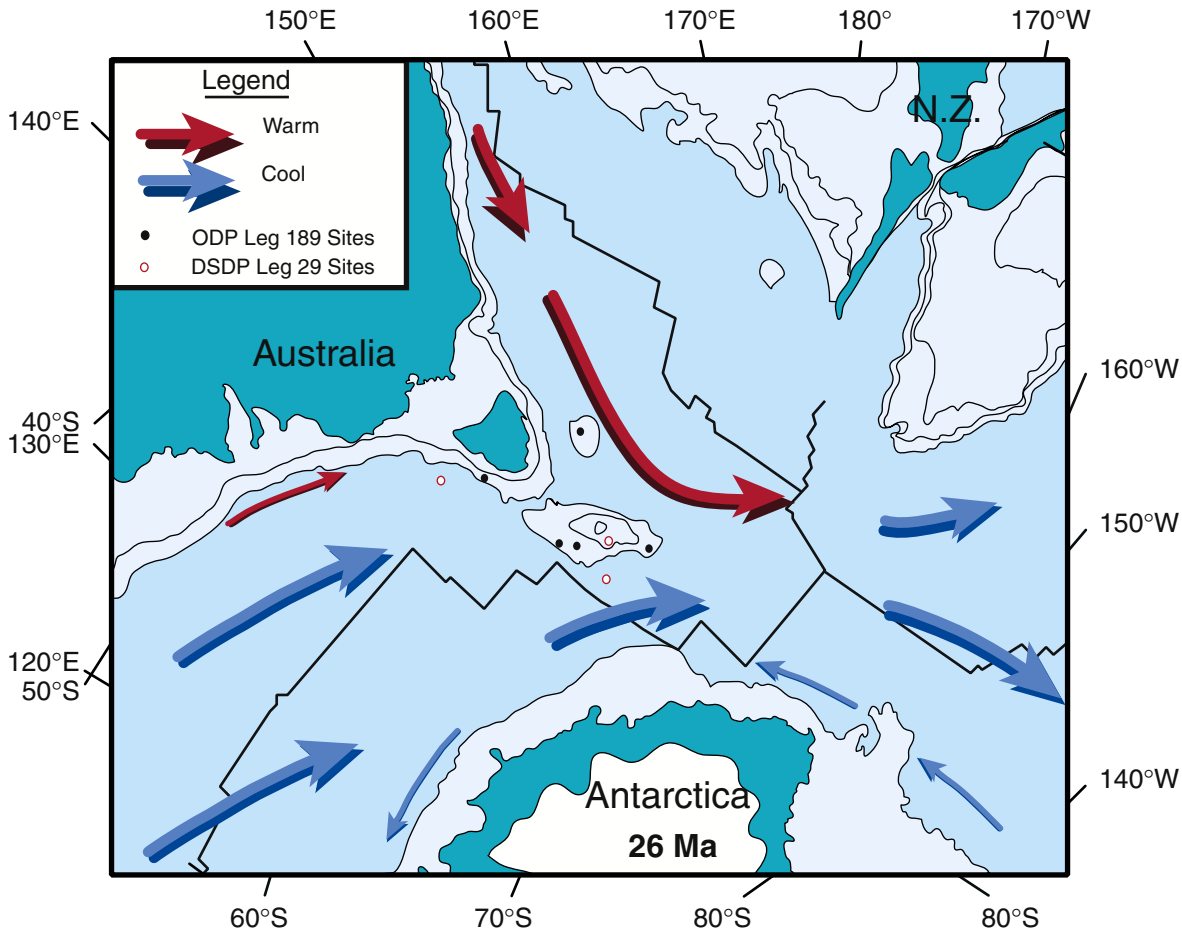
150°E
160°E
170°E
180°
170°W
140°E
Legend
Warm
Cool
ODP Leg 189 Sites
DSDP Leg 29 Sites
N.Z.
Australia
160°W
40°S
130°E
150°W
120°E
50°S
Antarctica
26 Ma
140°W
60°S
70°S
80°S
80°S

Figure 25

OPERATIONS SYNOPSIS[1]

Leg 189 began at 2000 hr on 11 March 2000 when the first line was passed ashore at Macquarie Wharf, Hobart, Tasmania. At 1224 hr on 16 March, after an ~4 day port call, the last line was released from the pier and the ship was maneuvered into the harbor.

Transit, Hobart to Site 1168

The 208-nmi transit to Site 1168 was accomplished at an average speed of 10.6 kt. During this transit there was a moderate amount of rolling caused by a 3- to 4-m westerly swell. Because the vessel pursued a northwest heading to the site, the swell was directly on the port beam and generated rolls as large as 10°. Upon arriving at the coordinates for the site, a beacon was deployed at 0800 hr on 17 March.

Hole 1168A

After the hydrophones and thrusters were extended and the vessel settled on location, the corrected precision depth recorder (PDR) depth referenced to the dual elevator stool (DES) was obtained and indicated 2479.4 m below the rig floor (mbrf). Hole 1168A was spudded with the advanced hydraulic piston corer (APC) at 1715 hr on 17 March. The seafloor depth was calculated from the recovery of the first core and determined to be 2474.2 mbrf, or 2463 mbsl.

Piston coring advanced to 111.8 mbsf (Table 1). Piston cores were oriented starting with Core 3H, and heat-flow measurements were obtained at 45.3, 64.3, 92.8, and 111.8 mbsf. The average recovery of the piston-cored region was 103%. There were two minor incidents involving the wireline while piston coring in Hole 1168A. When vessel heave caused the overshot shear pin to part, it required an extra wireline trip to recover Core 5H. While attempting to recover Core 10H, the wireline came apart at the rope socket. This required one trip in with a wireline fishing tool, which succeeded in recovering the Tensor tool carrying case and core barrel on the first attempt. Subsequent to a full stroke, the core barrel for Core 12H required drilling over to free the hardware from the sediments.

Consequently, we switched to the extended core barrel (XCB) system and the hole was deepened from 111.8 mbsf to refusal depth (883.5 mbsf) (Table 1), which was the depth objective of the previously planned rotary hole. The average recovery of the XCB portion was 94%. During XCB coring, coring operations almost had to be stopped on 19 and 20 March when a complex long period (13 s) swell generated vessel-heave values of 6 m or more. Because of the long period of the swell, the passive heave compensator was able to handle the vertical excursions and coring continued.

Throughout most of the XCB coring, the average rate of penetration (ROP) was 31 m/hr. The ROP slowed dramatically below 848 mbsf. From a depth of 848 mbsf to the bottom of the hole at

[1]The Operations and Engineering personnel aboard the *JOIDES Resolution* during Leg 189 were ODP Operations Manager Ron Grout, ODP Operations Engineer Michael Friedrichs, and Schlumberger Engineer Kerry Swain.

884 mbsf, the ROP gradually decreased from 6.5 to a lethargic 2.9 m/hr. Because of the diminishing returns of continued coring, the hole was terminated and preparations were made for logging.

Hole 1168A was logged with the triple combination (triple combo) tool and the geological high-sensitivity magnetic (GHMT)-sonic tool strings. During the triple-combo tool string run, the bit was positioned at 108 mbsf and was raised to 101 mbsf during logging. The first pass covered 877 to 101 mbsf, and a repeat run was made from 301 to 201 mbsf. The data indicated that hole conditions were poor with an uneven and rugged borehole wall. The borehole width commonly exceeded 19 in, but in places was as narrow as 4 in. Because there were many narrow spots, a wiper trip was conducted before the deployment of the second logging tool suite.

During the GHMT-sonic run, the bit was placed at 110 mbsf and was pulled up to 100 mbsf. The main pass of the logging tool covered 730 to 102 mbsf, and a repeat run was conducted from 376 to 245 mbsf. It was not possible to get the tool string past a bridge at 730 mbsf, and, as a consequence, the bottom 150 m of the hole could not be logged. In view of the scientific importance of the base of the hole and the poor hole conditions, it was decided that a second attempt to log the lower portion of the hole with the GHMT-sonic was more important than running the Formation MicroScanner (FMS). Accordingly, another wiper trip was made and the bit was set at 666 mbsf. Unfortunately, it was still not possible to get any deeper and logging was discontinued. After the logging equipment was demobilized, the bit was pulled back and cleared the seafloor at 2215 hr on 24 March, ending Hole 1168A.

Hole 1168B

The vessel was offset 20 m north of Hole 1168A, and Hole 1168B was spudded with the APC at 0130 hr on 25 March. Based on recovery of the mudline core, the seafloor depth was estimated to be 2463.7 mbsl, or within 0.2 m of the calculated depth of Hole 1168A. Piston coring advanced to 108.4 mbsf with an average recovery of 98%. Cores were oriented beginning with Core 3H. After Core 12H was obtained, the bit was pulled clear of the seafloor at 1215 hr on 25 March, ending Hole 1168B.

Hole 1168C

After the vessel was offset 20 m north of Hole 1168B, Hole 1168C was spudded with the APC at 1330 hr. Piston coring was initiated and advanced to 114.0 mbsf with an average recovery of 96%. Cores were oriented starting with Core 3H. The hole was deepened with the XCB to 290.5 mbsf when the available operational time expired. The average recovery for Hole 1168C was 85%. The average recovery for the entire site was 93%, representing a total of 1192 m of core.

Following the retrieval of the last core barrel, the drill string was recovered and the bottom-hole assembly (BHA) was dismantled in anticipation of the transit to Hobart to transfer two personnel and some light cargo. Concurrent with the recovery of the drill string, the beacon was

successfully retrieved. After the hydrophones and thrusters were retracted and drilling equipment secured, the vessel was under way at 2100 hr on 26 March.

Transit to Site 1169 Via Hobart

The transit from Site 1168 to the Port Huon pilot station for a personnel transfer was accomplished at an average speed of 12.6 kt, which put the vessel at the mouth of the D'Entrecasteaux Channel at 0900 hr, >4 hr ahead of schedule. After reviewing the option of remaining stationary and waiting for the pilot boat to transit to the vessel, we decided to continue directly to the innerpilot station near Hobart, arriving at 1245 hr on 28 March.

The ship rendezvoused with the pilot boat, and three new personnel (two from ODP and one from Overseas Drilling Limited) were transferred on board along with some light cargo. Two personnel, an ODP engineer and a technical representative from Maritime Hydraulics, left the vessel. At 1255 hr, the transfer was completed and the *JOIDES Resolution* altered course and continued to the next site. The vessel proceeded on a southerly course for the 270-nmi transit, which was accomplished at an average speed of 11.3 kt.

Hole 1169A

At 1245 hr on March 28, a beacon was deployed, hydrophones and thrusters were extended, and the vessel settled on location. An APC/XCB BHA was made up and run to near the PDR depth of 3584.4 mbrf.

As the drill string was being deployed, a cold front passed over our location, driving the winds from 28 kt to >55 kt in the space of a few minutes. Accompanying the arrival of the front were very heavy rains and a drop in temperature of 4°C in <15 min. Although the intensity of the winds quickly abated as the direction shifted from the north to the west, the resulting conditions from the passage of the front strongly affected subsequent coring.

Hole 1169A was spudded with the APC at 2245 hr on 28 March. The seafloor depth was calculated from the recovery of the first core and determined to be 3578.9 mbrf, or 3567.9 mbsl. As piston coring was initiated, the weather deteriorated and generated considerable vessel motion that adversely affected the quality of the cores. During coring in this hole, the winds were predominantly from the west and never dropped below 22 kt with gusts frequently measured between 35 and 40 kt. There was also a complex swell from the west and southwest (~5 m amplitude) that would periodically combine and push the vessel heave >6 m.

The weather made for difficult operations with resulting poor quality of the piston cores. During operations, the wireline had to be re-terminated at the rope socket twice because of fraying steel-rope members arising from an excessive bending radius caused by excessive vessel motion. Two additional wireline roundtrips were needed to fish out the core barrel when the wireline eventually parted at the rope socket. On another occasion, coring had to be stopped for several hours while the drill crew disassembled the piston corer to clean out a core liner that

completely failed, likely a result of the extreme hydraulic forces. The wireline speed was also reduced to accommodate the weather-induced motion of the drill string and vessel.

The quality of the cores was poor due to the flow-in and vertical disturbance caused by the dynamics of attempting to piston core in this environment. During piston coring, the heave compensator is not used except for drilling or washing ahead to position the drill bit for the next piston core attempt. When the piston corer is fired, the heave compensator is locked and the bit is forced to follow the vertical motion of the vessel. It was expected that as soon as XCB coring was initiated, the core quality would improve because of the activation of the heave compensator with a resulting decrease in core disturbance. Unfortunately, the main objective for this site was recovery of an upper Neogene section for high-resolution analysis that only undisturbed APC cores could provide.

After the APC coring advanced to a depth of 199 mbsf, we switched to the XCB system in an attempt to minimize core disturbance, despite the fact that only minimum pull-out force was required to free the core barrel from the sediment. Coring concluded when the XCB deepened the hole from 199 mbsf to the depth objective of 247 mbsf. The main goal for this site was high-resolution analysis of the sedimentary record; hence, operations were terminated because of the effect that the sea state was having on core quality. The average recovery of the piston-cored section of the hole was 100%, with overall recovery being 91%.

The drill bit was pulled clear of the seafloor at 0200 hr on 31 March and the drill string was recovered. As the BHA was being disassembled into the component drill collars in preparation for the transit to the next site, the beacon was successfully recovered. Following the retraction of the thrusters and hydrophones and the securing of the drilling equipment, the vessel began the short transit to the next site at 0830 hr on 31 March.

Transit to Site 1170

The transit from Site 1169 to Site 1170 required 3 hr at an average speed of 11.3 kt. Approximately 1 mile from location the vessel slowed, the thrusters were lowered, and a beacon was deployed at 1230 hr on 31 March, initiating operations at the site.

Hole 1170A

After settling on location, an APC/XCB BHA was made up and run close to the estimated depth of 2716.4 mbrf calculated from the PDR. Hole 1170A was spudded with the APC at 2030 hr on 31 March. The seafloor depth of 2715.5 mbrf, or 2704.7 mbsl, was calculated from the amount of recovery of the first core. Piston coring advanced to 163.2 mbsf with an average recovery of 98%. Piston cores were oriented starting with Core 3H, continuing through to Core 18H. Because of the 11-ft vessel heave, no heat flow measurements were attempted.

The XCB system was used to deepen Hole 1170A from 163.2 to 464 mbsf with an average recovery of 73%. The rate of penetration (ROP) slowed to nearly 1 m/hr in a hard nannofossil-limestone interval, which clearly signaled that this was the refusal depth of the XCB system. As

XCB coring was concluding, the growing swell was now pushing the vessel heave over 6 m, which was outside the operating limits of the *JOIDES Resolution.* After the bit was pulled clear of the seafloor at 0545 hr on 3 April, coring operations were suspended for 4.3 hr while we waited for the swell to abate.

Hole 1170B

At 1000 hr on 2 April, the vessel was offset in dynamic positioning mode 20 m north of Hole 1170A. To obtain a stratigraphic overlap with the initial hole of the site, the bit was positioned 3 m shallower before starting Hole 1170B, which was spudded with the APC at 1145 hr on 2 April. The estimated seafloor depth was calculated to be 2715.7 mbrf, or 2704.7 mbsl, from the recovery of the first core. Piston coring advanced to 175.8 mbsf with an average recovery of 102%. Cores were oriented starting with Core 3H. Because of a growing swell that pushed the vessel heave over 4.5 m, the Tensor orientation tool was removed subsequent to the recovery of Core 14H to prevent damage to critical hardware. The bit was pulled clear of the seafloor at 0800 hr on 4 April and the vessel was offset 20 m north of Hole 1170B.

Hole 1170C

At 0945 hr, Hole 1170C was spudded with the APC. The stratigraphic overlap required lowering the bit 6 m from the spud-in depth of Hole 1170B. The seafloor depth estimated from recovery of the first core was 2714.4 mbrf, or 2703.3 mbsl. Piston coring advanced without incident to the depth objective of 180.1 mbsf, with an average recovery of 99.7%. Cores were oriented beginning with Core 3H, and one Adara deployment was made on Core 19H.

Hole 1170D

The ship was offset 20 m north of Hole 1170C, and a rotary core barrel (RCB) BHA was made up and deployed to 2668 mbrf. Hole 1170D was spudded with the RCB at 2000 hr on 4 April and drilled ahead with a center bit to 425 mbsf at an average rate of 55 m/hr. At 0745 hr on 6 April, RCB coring was initiated in Hole 1170D and advanced with increasing recovery (mean = 81%) to the depth objective of 779.8 mbsf. The recovery below 529 mbsf to the bottom of the hole averaged nearly 100%. There were no stability problems encountered while drilling and coring in this hole.

At the conclusion of coring, the contrast in hole conditions between the upper and lower section of the hole was discussed among the relevant personnel. Logging difficulties were expected at a depth of 474–529 mbsf, where indurated limestone horizons were present above a zone of partially consolidated glauconitic sandstones and siltstones. It was agreed that it would be difficult for a logging tool to easily make the transition from the upper 425 m of the hole into the bottom 355 mbsf because of the likelihood that there would be washed out sections overlying a relatively narrow 10- to 12-in-diameter hole into the limestone capped lower section. Hence, it

was decided to log the hole in two stages, with the end of the pipe placed initially at 529 mbsf to log the base of the hole then raised to ~200 mbsf to log the top of the hole.

Following a routine wiper trip and displacement of the hole with a 200-bbl sepiolite solution, the bit was dropped and the end of the drill string was placed at 529 mbsf. At 1730 hr on April 9, the first logging tool was deployed. Three tool-string runs were made with the pipe at 529 mbsf; the triple combo, the GHMT-sonic, and the FMS. The borehole was smooth with a relatively uniform diameter (~11–12 inches), and high-quality data were obtained. All the logs came within 6 m of the bottom of Hole 1170D.

At 1700 hr on April 10, the first part of the logging program was completed and the drill crew made preparations to reposition the end of the pipe at 200 mbsf. After pulling the drill string back from 529 mbsf while encountering increasing drag, the drill string stuck firmly at 468 mbsf. The top drive was picked up and the drill string was subjected to overpulls as large as 200 kilopounds (Kips) in an attempt to free the pipe. After attempts to move the pipe from 1715 to 2130 hr met with no progress, it was decided to sever the drill string just above the BHA.

An explosive charge was made up and deployed on the logging line to 3033 mbrf, which corresponded to the position of the first 5-in drill pipe joint above the BHA. At 0415 hr on April 10, the charge was detonated and severed the pipe. The drill string was then recovered, as were the two beacons. The vessel departed for Site 1171 at noon on 11 April 2000.

Transit to Site 1171

To avoid excessive rolling caused by the southwesterly 5.5-m swell, the captain elected to pursue an east-southeast course that had the ship approach Site 1171 from the northeast. The chosen course added 54 nmi to the transit for a total distance of 202 nmi, which required 18.8 hr. As the ship approached the location, the thrusters and hydrophones were lowered, and a beacon was deployed at 0645 hr on 12 April, initiating Site 1171.

Hole 1171A

An APC/XCB BHA was run to near the PDR depth of 2176.4 mbrf and Hole 1171A was spudded with the APC at 1415 hr on 12 April. The seafloor depth was calculated to be 2159.4 mbrf, or 2148.2 mbsl, based on recovery of the first core. Piston coring advanced to 111.6 mbsf (mean recovery = 98%) where Core 12H could not be retrieved from the sediment with 80 Kips overpull, requiring drilling over the core barrel to release it from the sediments. Piston cores were oriented starting with Core 3H and continued through to Core 12H. Heat-flow measurements were obtained with the Adara cutting shoe at 35.6 mbsf (Core 5H) and 54.6 mbsf (Core 7H).

The XCB system was used to deepen the hole to 124.4 mbsf, with 62% recovery. The original operational plan called for the hole to be cored as deeply as possible with the XCB. Because of unusually calm sea conditions, we decided to stop XCB coring after two cores and to

continue piston coring the remaining two of the three planned APC holes to potentially avoid weather-dependent core disturbance that we had previously encountered.

Hole 1171B

The vessel was offset 20 m north of Hole 1171A. To obtain a stratigraphic overlap with the cores recovered from Hole 1171A, the bit was positioned 3 m shallower, and Hole 1171B was spudded with the APC at 0530 hr on 13 April. The estimated seafloor depth of 2159.2 mbrf (2148 mbsl) was calculated based on recovery of the first core. Piston coring advanced to 108.8 mbsf with an average recovery of 98%, and cores were oriented starting with Core 3H. The bit was pulled clear of the seafloor at 1545 hr on 13 April, ending Hole 1171B.

Hole 1171C

The vessel was offset 20 m to the east, and Hole 1171C was spudded with the APC at 1630 hr. To maintain appropriate stratigraphic overlap with the two previous holes, the bit was lowered 6 m from the spud-in depth of Hole 1171B. The seafloor depth was estimated to be 2159.0 mbrf, or 2147.8 mbsl. Piston coring advanced without incident to the depth objective of 104.5 mbsf, with an average recovery of 101%. Cores were oriented beginning with Core 3H and one Adara deployment was made at 38.0 mbsf (Core 5H).

The XCB system was used to deepen Hole 1171C from 104.5 to 274.8 mbsf, where a glauconitic sandstone was encountered. When the ROP slowed to 1.5 m/hr, the refusal depth of the XCB system was declared and coring terminated. The average recovery of the XCB portion of this hole was 82%, with a total average recovery of 89% for Hole 1171C.

Hole 1171D

Following the recovery of the last core from Hole 1171C, the drill string was recovered, a RCB BHA was made up, and the ship was offset 20 m east of Hole 1171C. Hole 1171D was spudded at 0400 hr on 15 April and drilled ahead with a center bit to 100 mbsf. The center bit was recovered by wireline and the Davis-Villinger Temperature Probe (DVTP) deployed to obtain a temperature measurement at this depth. Following the recovery of the DVTP, the center bit was dropped again and drilling resumed to the depth objective of 247.6 mbsf. The average ROP for the drilled interval was 62 m/hr, excluding the time expended on the DVTP measurement. At 1235 hr on 15 April, RCB coring was initiated and advanced with increasing recovery to the depth objective of 958.8 mbsf. The average recovery for this hole was 74%, with an average ROP of 17 m/hr for the 711-m cored interval. There were no stability problems encountered while drilling and coring in this hole.

Following an 11-hr wiper trip and hole preparation that included the release of the bit at the bottom of the hole, the pipe was raised to the logging depth of 162.2 mbsf. Three tool string runs were planned for this hole; the triple combo, the GHMT-sonic, and the FMS. The first logging run with the triple combo reached the target depth of 958.8 mbsf, and excellent quality data were

collected from the entire section of open hole. While running in with the second log, the GHMT-sonic, the tool string bridged out at ~291 mbsf, near the transition from nannofossil chalk to Eocene glauconitic sandstones. Apparently while running in with this logging suite, power was lost to the GHMT-sonic tool when the unit became caught on this bridge. The tool string was returned to the rig floor, where ~600 m of damaged logging cable was removed and the logging line was re-terminated.

In an attempt to clear the bridge in the formation, the drill string was lowered with the objective of clearing all hole obstructions to ~300 mbsf. Perhaps as a result of the 4- to 5.5-m heave, the open end of the BHA became plugged with sediment after traversing <1 stand of pipe at 190 mbsf. The drill string was worked free with 150,000 lb of additional tension after working the drill string for 45 min. Because the bottom of the pipe was plugged and we thought that the drill string had apparently meandered into the side of the borehole, no further logging could be undertaken.

While we retrieved the drill string, the primary beacon was recovered. The alternate beacon was also successfully released; however, the flasher apparently did not activate upon surfacing and the beacon drifted off into the dark and could not be located. The drilling equipment was secured by 0645 hr on 22 April as the ship departed for the next site. The errant beacon was observed on the surface as the vessel left location, but when the ship came about to recover the unit, it could not be found in the 4.5-m swell.

Transit to Site 1172

Site 1172, the final site of the leg, is located 275-nmi north of Site 1171 in 2622 m of water Approximately 1 mile from location, the ship slowed, the thrusters were lowered, and a beacon was deployed at 0915 hr on 23 April, initiating Site 1172.

Hole 1172A

An APC/XCB BHA was made up and run to near the depth indicated by the PDR (2637.4 mbrf). Hole 1172A was spudded with the APC at 1630 hr on 23 April. The seafloor depth was calculated from the recovery of the first core as 2633.2 mbrf, or 2621.9 mbsl. Piston coring advanced to 224.8 mbsf where Core 24H could not be retrieved from the sediment with 80,000 lb of overpull, requiring a drillover to release the core barrel. Piston cores were oriented starting with Core 3H and continued through Core 24H. Because of the ~4 m heave, heat-flow measurements were deferred until the next hole in anticipation of improving conditions. The average recovery in Hole 1172A was 102%; however, the excessive heave resulted in many of the shallower piston cores being dominated by flow-in, in particular Cores 5H through 10H and Cores 15H and 19H.

The XCB system was used to deepen the hole to 522.6 mbsf, with 85% average recovery. XCB coring was terminated because of the slow ROP (7 m/hr) and poor recovery (8%) of the last two cores. The overall average recovery for Hole 1172A was 93%.

Hole 1172B

The ship offset 20 m north of Hole 1172A, and Hole 1172B was spudded with the APC at 1050 hr on 26 April. To obtain an appropriate stratigraphic overlap with the Hole 1172A, the bit was positioned 3 m shallower at spud-in. The estimated seafloor depth of 2633.6 mbrf (2622 mbsl) was calculated from the recovery of the first core. Piston coring advanced to 202.4 mbsf (average recovery = 102%), where 75,000 lb was required to free the core barrel (Core 22H) from the sediment. Cores were oriented starting with Core 3H and three Adara heat-flow measurements were obtained at 40.9 (Core 5H), 59.9 (Core 7H), and 88.4 mbsf (Core 10H).

Hole 1172C

The vessel was offset 20 m north of Hole 1172B, and Hole 1172C was spudded with the APC at 1130 hr on 27 April. To maintain stratigraphic overlap with the previous two holes, the bit was positioned 6 m deeper than at Hole 1172B for spud-in. The seafloor depth was estimated to be 2633.0 mbrf (2621.7 mbsl).

Piston coring advanced to 171.0 mbsf, where APC refusal was encountered. The core barrel for Core 18H required drilling over when 75,000 lb of overpull could not free the core barrel from the sediment. The average recovery was 101% and cores were oriented beginning with Core 3H.

Hole 1172D

Following the recovery of the last core from Hole 1172C, the drill string was recovered and a RCB BHA was assembled. Before spudding the fourth hole of the site, the vessel was offset 20 m north of Hole 1172C. Hole 1172D was spudded with the RCB at 1630 hr on 28 April and drilled ahead with a center bit in place to 343.6 mbsf with an average penetration rate of 57 m/hr. The interval from 343.6 to 372.4 mbsf was rotary cored (Cores 1R through 3R) with an average recovery of 68%; however, the first core did not recovery any material, probably because of excessive hydraulics. The average recovery for the second and third core was 103%.

Following the recovery of the third core barrel, a wash barrel was dropped and was drilled ahead from 372.4 to 497.4 mbsf with an average ROP of 27 m/hr. Continuous rotary coring was initiated at 1500 hr on 29 April in Hole 1172D and extended until 2215 hr on 1 May, when operational coring time expired. The final depth of Hole 1172D was 766.5 mbsf, with an average recovery of 80%. Following a 12-hr wiper trip and hole preparation, which included the release of the bit at the bottom of the hole, the end of the pipe was placed at 160 mbsf for logging. In the first logging run, the triple combo tool string reached a depth of 762 mbsf and the pipe was pulled to 150 mbsf while logging up to accomplish overlap with the shipboard splice. However, excessive heave caused the wireline heave compensator (WHC) to stroke out repeatedly (six times) during the logging pass. Despite the heave, the data obtained were of good quality, noting some borehole rugosity but no extensive areas of washout. Sea conditions continued to deteriorate as logging progressed (heave of ~6 m), and the WHC was abandoned during the

GHMT-sonic run after stroking out six times within 10 min of activation. The GHMT-sonic also reached target depth, and good sonic and magnetic data were obtained up to the base of the pipe. The FMS was then rigged up in hopes that heave would subside to within the effective range of the WHC. The conditions did not improve within the allotted time, and the FMS run was abandoned.

After the logging equipment was rigged down, the drill string was recovered and the BHA dismantled in preparation for the voyage to Sydney, Australia. Both beacons were successfully recalled and recovered. After the drilling equipment was secured, the vessel departed for Sydney at 2100 hr on 3 May.

Transit from Site 1172 to Sydney

The 620-nmi transit from Site 1172 to Sydney was accomplished in 59.7 hr in good weather at the maximum speed possible (average = 10.4 kt). The ship docked and the first line was ashore at 1025 hr, May 6, ending Leg 189.